Aalborg Universitet

Transport and Fate of Volatile Organic Chemical in Soils

influence of soil physical properties

Petersen, Lis Wollesen

Publication date:
1998

Document Version
Publisher's PDF, also known as Version of record

Link to publication from Aalborg University

Citation for published version (APA):
Petersen, L. W. (1998). *Transport and Fate of Volatile Organic Chemical in Soils: influence of soil physical properties* . Institut for Vand, Jord og Miljøteknik, Aalborg Universitet.

General rights
Copyright and moral rights for the publications made accessible in the public portal are retained by the authors and/or other copyright owners and it is a condition of accessing publications that users recognise and abide by the legal requirements associated with these rights.

- Users may download and print one copy of any publication from the public portal for the purpose of private study or research.
- You may not further distribute the material or use it for any profit-making activity or commercial gain
- You may freely distribute the URL identifying the publication in the public portal -

Take down policy
If you believe that this document breaches copyright please contact us at vbn@aub.aau.dk providing details, and we will remove access to the work immediately and investigate your claim.

Downloaded from vbn.aau.dk on: January 09, 2025

TRANSPORT AND FATE OF VOLATILE ORGANIC CHEMICALS IN SOILS: INFLUENCE OF SOIL PHYSICAL PROPERTIES

LIS WOLLESEN PETERSEN

Environmental Engineering Laboratory
Aalborg University
Ph.D. Dissertation, 1994

TRANSPORT AND FATE OF VOLATILE ORGANIC CHEMICALS IN SOILS: INFLUENCE OF SOIL PHYSICAL PROPERTIES

LIS WOLLESEN PETERSEN

Environmental Engineering Laboratory
Aalborg University
Ph.D. Dissertation, 1994

The Environmental Engineering Laboratory Ph.D. Dissertation Series:

1. PER HALKJÆR NIELSEN. 1988. Svovlbrintedannelse i biofilm fra spildevandsledninger (Hydrogen sulfide formation in biofilm in sewers).
2. PER MØLDRUP. 1990 (minor updating 1993). New methods for modeling transport of water and solutes in soils.
3. SØREN OLE PETERSEN. 1991. Nedbrydning af flydende organisk affald i jord - med særligt henblik på anaerobe processer (Decomposition of liquid organic wastes in soil - with emphasis on anaerobic processes).
4. JACOB HØYGAARD BRUUS. 1992. Filterability of wastewater sludge flocs.
5. JIMMY ROLAND CHRISTENSEN. 1992. A systematic approach to characterization of sludge conditioning and dewatering.
6. PETER BORGEN SØRENSEN. 1992. Unified modeling of filtration and expression of biological sludge.
7. KAMMA RAUNKJÆR. 1993. Characterization and transformation of wastewater organic matter in sewer systems.
8. NIELS AAGAARD JENSEN. 1994. Air-water oxygen transfer in gravity sewers.
9. HANNE RASMUSSEN. 1994. Anaerobic processes in activated sludge with an impact on floc structure and dewaterability.
10. BO FRØLUND. 1994. Qualitative and quantitative characterization of activated sludge exopolymers.
11. LIS WOLLESEN PETERSEN. 1994. Transport and fate of volatile organic chemicals in soils: Influence of soil physical properties.
12. MIKKEL L. AGERBÆK. 1994. Occurrence of streaming potentials in sludge dewatering.
13. CHARLOTTE W. KRUSE. 1994. Factors regulating atmospheric methane consumption in soils.
14. RIKKE PALMGREN. 1996. Quantification of bacterial extracellular polymers in activated sludge - Using *P.putida* as model organism.
15. BIRGITTE L. SØRENSEN. 1996. Filtration of activated sludge.
16. HANNE LØKKEGAARD BJERRE. 1996. Transformation of wastewater in an open sewer: The Emscher River, Germany.
17. TORBEN OLESEN. 1996. Nitrogen diffusion and transformations in and around soil/organic manure hot-spots.
18. TJALFE G. POULSEN. 1997. Predicting soil-air and soil-water transport properties during soil vapor extraction.

Printed in Denmark by
Centertrykkeriet, Aalborg University, February 1998
ISBN 87-90033-07-8
ISSN 0909-6159

Cover design: Hanne Rimmen

Preface

The present work including the enclosed six articles is hereby submitted in partial fulfillment of the requirements for the Doctor of Philosophy (Ph.D.) degree.

The experimental work has been carried out partly at the University of California at Davis, Soils and Biogeochemistry, Department of Land, Air, and Water Resources during my stay in 1991/1992 and visit in Nov. 1993, and partly at Research Centre Foulum, The Danish Institute of Plant and Soil Science, Department of Soils Science where I have stayed from January 1993 until now. I am matriculated as a Ph.D. student since August 1991 at Aalborg University, Environmental Engineering Laboratory, Department of Civil Engineering. The studies have been funded in part by the U.S. EPA (R819658) Center for Ecological Health Research at UC Davis, the Danish Ministry of Agriculture, the Danish Research Academy, and the Danish Ministry of the Environment. Although the information in this document has been funded in part by the United States Environmental Protection Agency, it may not necessarily reflect the views of the Agency and no official endorsement should be inferred.

I want to gratefully thank my supervisors Dr. Per Møldrup, Aalborg University, Professor Dennis E. Rolston, University of California at Davis, and Dr. Ole Hørbye Jacobsen, The Danish Institute of Plant and Soil Science for their tremendous help, guidance, and pats on my shoulder. Also I want to express my warmest thanks to Laboratory Assistant Dianne T. Louie who with her warm heart and wonderful personality made my stay in Davis even better, to all the other guys in Rolston's Lab and at the Department of Soil Science, Foulum who have always been ready with a helping hand, to Jens for surviving without a computer for half a year, to Claus and Leonard for mental caring, to Yassar for everything, and to my parents for all their love. Also thanks to Lizzy and Anne for careful preparation of figures and Anne for being the best secretary in this world.

Foulum, August 1994

Lis Wollesen Petersen

Summary

Recently much attention has been paid to the behavior of volatile organic chemicals (VOCs) in the environment. This is due to the fact that the environmental pollution with these hazardous chemicals has drastically increased during the last decades. The present study is limited to consider the transport and fate of VOCs in the gaseous phase, thus contributing to the overall understanding of VOCs behavior in soil, which eventually will facilitate future cleanup.

The diffusion and adsorption of VOCs were studied in several laboratory experiments on different homogeneous soils. The effects of differences in soil-texture, and soil-water content on adsorption, manifested in the vapor/solid partition coefficient, K_D', were investigated in batch experiments for trichloroethylene (TCE) and toluene using the EPICS (Equilibrium Partitioning in Closed Systems) method. For low relative vapor pressures it was found that K_D'-values for wet soils (> four molecular layers of water) were consistent with values predicted by Henry's constant (K_H) and the aqueous/solid partition coefficient, K_D. Also under wet conditions K_D' was linearly related to soil-water content, w. In dry soils (< four molecular layers of water) sorption increased by up to several orders of magnitude, and K_D' became highly non-linearly related to soil-water content. A one parameter, exponential model was developed, which described well the log K_D'-w curve in the non-linear region. Use of this model can reduce the number of experiments necessary to obtain the K_D'-w relationship for a given soil. The model can be incorporated into existing numerical VOC transport models.

For the whole range of vapor pressures the applicability of the multicomponent BET (Brunauer-Emmett-Teller) model to describe adsorption of VOC vapors in the presence of water on soils was investigated. Adsorption isotherms were obtained by using both the EPICS method (for low vapor pressures) and a High Vacuum Technique (for higher vapor pressures). For relative humidities (RH) corresponding to less than one molecular layer of water coverage and at low vapor pressures the model underpredicted the adsorbed amounts of VOC in binary mixtures in which only water and one VOC was present. At RHs corresponding to between one and two molecular layers of water coverage, model predictions compared well with experimental data. At RHs corresponding to about two layers of water, the model overpredicted the adsorbed amounts.

Diffusion, with simultaneous adsorption, of TCE, toluene and $freon_{12}$ was measured on packed soil cores over a range of constant soil-water contents. Vapor retardation factors, calculated from vapor partition coefficients, along with the measured diffusion allowed a calculation of diffusion coefficients, D_P, for the three chemicals. D_P/D_0 (diffusion coefficient in soil divided by diffusion coefficient in free air) values for the VOCs, TCE and toluene, agreed very well with values for the non-reactive tracer $freon_{12}$ for higher soil-water contents. Only values obtained for air-dry soil were under-predicted. Hence in most cases considering transient diffusion of VOC gases, it is reasonable to use simple equilibrium partition theory to account for the adsorption. The experimental work for determination of effective diffusion of reactive tracers can be limited to the determination of D_P/D_0-ε relations (ε is the volumetric soil-air content) for a non-reactive tracer and measurements of partition coefficients for the reactive tracers.

Diffusion, adsorption and emissions of TCE gas were also measured in column experiments with fluctuating soil-water contents. Decrease in soil-water contents resulted in an increase in the soil adsorption capacity up to several orders of magnitude. Both increase and decrease in soil-water content had an effect on the volatilization flux, but not as significant as expected. This could be explained by the fact that water vapor constantly was transported upwards from more wet soil layers. Another reason could be a constant very high flux of gaseous VOCs that was applied from the bottom of the soil column. This flux constantly maintained all adsorption sites occupied. The volatilization flux was highly influenced by changes in temperature.

The time-domain reflectometry (TDR) technique was used to determine the changes in soil-water content in the column experiments mentioned above. Small TDR-probes which could be placed close to each other and close to the soil-surface were developed. The effect of different diameters, spacings and lengths of probe rods was examined. The volume of soil that influences the measurement was found to be highly dependent on the spacing of the rods and not so much on the rod diameter. For rod spacings of 1, 2, and 5 cm, measurements could accurately be made as close to the soil surface as 1, 1.5, and 2 cm, respectively. The data was used to successfully validate a newly proposed model by Knight et al. (1994) which describe the spatial sensitivity of TDR.

Dansk resumé (Danish summary)

I de senere år er man blevet mere og mere interesseret i, hvorledes flygtige organiske kemikalier (VOCer) opfører sig efter de er blevet udledt i vort miljø. Dette er begrundet i, at forureningen med disse farlige stoffer drastisk er steget gennem de sidste årtier. Det foreliggende studium er afgrænset til at omhandle transport og jordfysiske reaktioner af VOCer i gasfasen. Dette vil forhåbentlig kunne bidrage til den overordnede forståelse af VOCers opførsel i jord, og dermed være med til at lette de fremtidige oprensningsforanstaltninger.

Diffusion og adsorption af VOCer blev studeret i adskillige laboratorieforsøg på forskellige homogene jorde. Adsorptionens (udtrykt ved ligevægtskonstanter, K_D') afhængighed af ændringer i jordtekstur og vandindhold blev undersøgt i forskellige "batch"-eksperimenter for trichlorethylen (TCE) og toluen, vha EPICS (Equilibrium Partitioning in Closed Systems) metoden. For lave damptryk kunne det konkluderes, at K_D'-værdier for våde jorde (> fire molekylelag vand) stemte overens med værdier bestemt vha Henry's konstant (K_H) og vand/stof ligevægtskonstanten, K_D. Ligeledes i våd jord viste det sig, at der var en lineær sammenhæng mellem K_D' og jordens vandindhold, w. I tør jord (< fire molekylelag vand) steg adsorptionen med op til flere størrelsesordner og sammenhængen mellem K_D' og w fik en kraftig ikke-lineær karakter. Der blev udviklet en en-parameter model, som var i stand til at beskrive log K_D'-w kurven i det ikke-lineære område. Brug af denne model vil kunne reducere antallet af eksperimenter, som er nødvendige for at kunne fastlægge sammenhængen mellem K_D' og w for en given jord. Modellen foreslåes indbygget i eksisterende numeriske VOC transportmodeller.

Den multikomponente BET (Brunauer-Emmett-Teller) models evne til at beskrive adsorption af VOC gasser med samtidig tilstedeværelse af vand blev undersøgt for hele området af damptryk. Adsorptionsisothermerne blev bestemt vha EPICS metoden (for lave damptryk) og en Høj Vacuum Teknik (for høje damptryk). Ved lave relative fugtigheder (RH) svarende til mindre end eet lags dækning med vandmolekyler og samtidig lave damptryk, underestimerede modellen de adsorberede mængder af VOC for binære blandinger, hvor udelukkende vand og et enkelt VOC var tilstede. Ved RHer svarende til mellem eet og to lags dækning med vandmolekyler, stemte modelsimuleringerne overens med målt data. Ved RHer svarende til omkring to lags dækning med vandmolekyler overestimerede modellen de adsorberede

mængder.

Diffusion og samtidig adsorption af TCE, toluen og freon$_{12}$ blev målt på pakkede jordsøjler ved forskellige konstante vandindhold. Tilbageholdelsesfaktorer for gas (beregnet vha gas-ligevægtskonstanter), sammen med den målte diffusion muliggjorde en beregning af diffusionkoefficienter, D_P, for de tre kemikalier. Værdier af D_P/D_0 (diffusionskoefficient i jord divideret med diffusionskoefficient i fri luft) for TCE og toluen, stemte for højere vandindhold godt overens med værdier bestemt for den ikke-reaktive "tracer" freon$_{12}$. Kun værdier for lufttørt jord var underestimerede. Man kan derfor i langt de fleste tilfælde af transient diffusion af VOC gasser, anvende simpel ligevægtskoefficientsteori til at tage højde for adsorptionen. Ligeledes kan det eksperimentielle arbejde forbundet med beskrivelsen af diffusionen af reaktive "tracere" begrænses til en bestemmelse af D_P/D_0-ε forholdet (ε er jordens volumetriske luftindhold) for en ikke-reaktiv "tracer" suppleret med målinger af ligevægtskonstanter for de reaktive tracere.

Diffusion, adsorption og emission af TCE gas blev også målt i kolonneforsøg med fluktuerende vandindhold. Fald i jordens vandindhold resulterede i en stigning i jordens adsorptionskapacitet på op til flere størrelsesordner. Både stigning og fald i jordens vandindhold havde en effekt på fordampningsfluksen, men denne var dog ikke så signifikant som forventet. Dette kunne delvis forklares ved, at der var en konstant opadrettet vanddamptransport fra dybereliggende våde jordlag. En anden grund kunne være en konstant høj fluks af VOC-gasser nedefra, som forårsagede, at der hele tiden var VOC-molekyler i overflod til at besætte tilstedeværende adsorptionspladser. Fordampningsfluksen var i høj grad afhængig af ændringer i temperaturen.

Time-domain reflectometry (TDR) teknikken blev brugt til at bestemme ændringerne i jordens vandindhold i søjleforsøgene nævnt ovenfor. Der blev udviklet små mini TDR-prober som kunne placeres tæt på hinanden og ligeledes tæt på overfladen. Effekten af forskellige diametre, afstande og længder af probebenene blev undersøgt. Det kunne konkluderes, at størrelsen af det jordvolumen, som influerede på målingen, var i høj grad afhængig af afstanden mellem probebenene og ikke videre afhængig af valget af diameteren. For afstande mellem probebenene på 1, 2 og 5 cm kunne en måling foretages nøjagtigt i afstande fra jordoverfladen på henholdsvis 1, 1.5 og 2 cm. Måleresultaterne blev med succes anvendt til at validere en ny model udviklet af Knight et al. (1994) som beskriver størrelsen af målevolumen for TDR.

Table of contents

Page

Preface 1

Summary 3

Dansk resumé (Danish summary) 5

List of supporting articles 10

1. Introduction 11

2. Diffusion of gaseous volatile organic compounds 17

3. Adsorption of gaseous volatile organic compounds 23

4. Emissions of gaseous volatile organic compounds 39

5. Concluding remarks 45

6. Related future perspectives 47

7. References 49

List of supporting articles:

I. Petersen, L.W., D.E. Rolston, P. Møldrup, and T. Yamaguchi. 1994. Volatile Organic Vapor Diffusion and Adsorption in Soils. J. Environ. Qual. 23:799-805

II. Petersen, L.W., P. Møldrup, Y.H. EL-Farhan, O.H. Jacobsen, and D.E. Rolston. 1995. The Effect of Moisture and Soil Texture on the Adsorption of Organic Vapors. J. Environ. Qual. 24:752-759

III. Petersen, L.W., Y.H. El-Farhan, P. Møldrup, D.E. Rolston, and T. Yamaguchi. 1996. Transient Diffusion, Adsorption, and Emission of Volatile Organic Vapors in Soils with Fluctuating Low Water Contents. J. Environ. Qual. 25:1054-1063

IV. Amali, S., L.W. Petersen, D.E. Rolston, and P. Møldrup. 1994. Modeling Multicomponent Volatile Organic and Water Vapor Adsorption on Soils. J. Hazard. Mat. 36:89-108

V. Petersen, L.W., A. Thomsen, P. Møldrup, O.H. Jacobsen, and D.E. Rolston. 1995. High-Resolution Time Domain Reflectometry: Sensitivity Dependency on Probe-Design. Soil Science 159:149-154

VI Yamaguchi, T., P. Møldrup, D.E. Rolston, and L.W. Petersen. 1994. A Semi-Analytical Solution for One-Dimensional Solute transport in Soils. Soil Science 158:14-21

In this thesis the publications will be referred to by their Roman numerals.

1. Introduction

Over the past two decades the chemical contamination of our environment and its effects on human life have created a fast growing concern at all levels in our society. The problem has arisen due to the last 100 years of industrial development during which the soil has been used as a disposal medium, often using the philosophy of: "Out of sight, out of mind". But cliches do not always hold true. In the United States alone \$10 billion is currently being spent annually on environmental cleanup and at this rate, cleanup will last well into the next century (~ 75 years) costing approximately \$750 billion (Bredehoeft, 1994). Likewise in Europe (including Denmark) we see the effects of years of inconsiderate handling of chemicals, resulting in numerous cleanup projects. Figure 1 shows a map of known polluted sites and registered deposit sites in the county of Viborg, Denmark (where Research Centre Foulum is located).

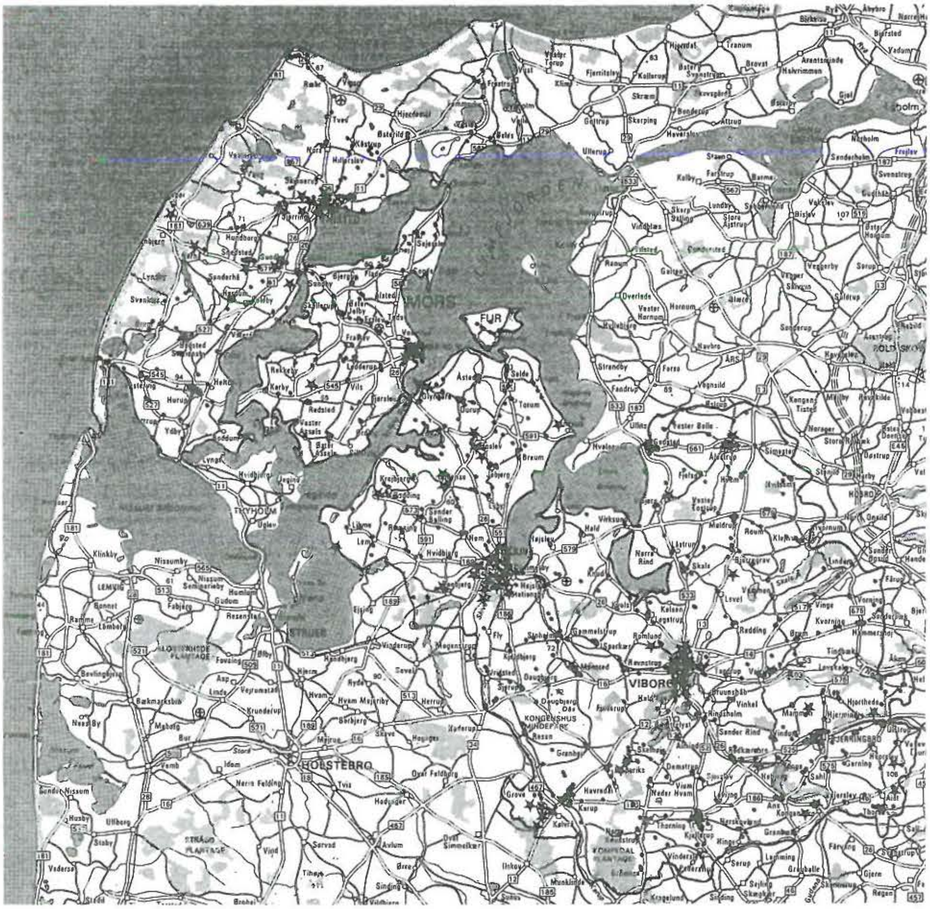

Fig. 1. Contaminated sites in the county of Viborg Denmark (Viborg Amtsråd, 1993). Red dots represent contaminated sites and stars represent registered waste deposit sites.

There is no reason to believe that the number of known sites here or anywhere will not increase significantly during the next decade. This is, among other things, due to the fact that groundwater movement is very slow, thus it often takes decades before society becomes aware that contamination exists. Keeping in mind the third world, where industrial development has only just begun, the intensity of future pollution problems might be severely increased.

The most common groundwater contaminants in the United States are volatile organic compounds, VOCs, (Culver et al., 1991) and recently chemicals from this group were also found in drinking water at several places in Denmark (e.g., Helweg, 1994). The principal documented cases of VOC soil and groundwater contamination result from leaks or spills at manufacturing plants, leakage at chemical waste disposal sites, and leakage from gas stations. At the same time many household products, such as oil-based paints, drain cleaners, spot and paint removers, fabric protectors etc. contain VOCs. This along with e.g. filling of gasoline, visiting dry cleaners, inhalation of contaminated ambient air (especially in traffic, near filling stations or in houses where VOCs have entered from the soil), and ingestion of contaminated drinking water create the potential for a significant human background exposure (Barbee, 1994) (see Fig. 2).

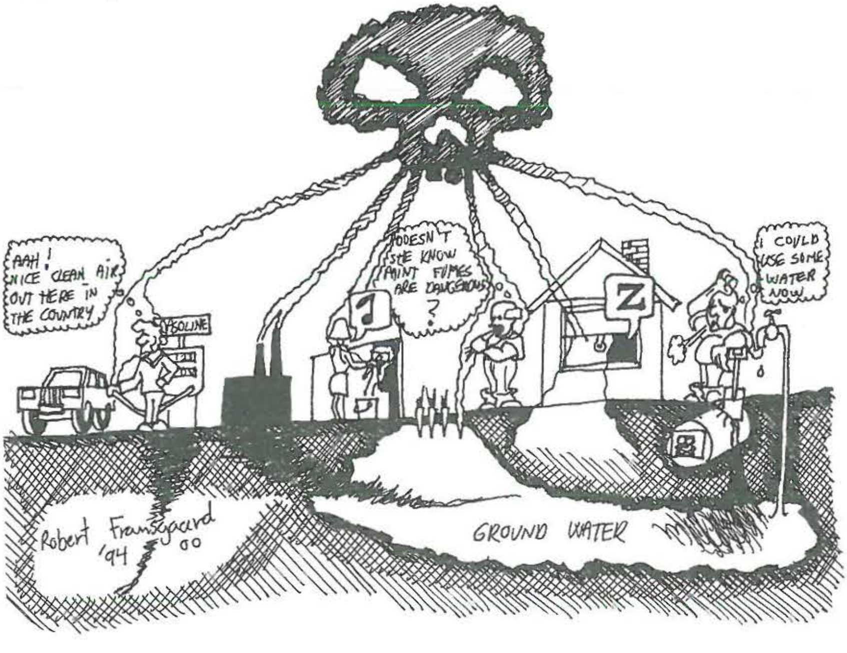
AAH! NICE CLEAN AIR OUT HERE IN THE COUNTRY
GASOLINE
DOESN'T SHE KNOW PAINT FUMES ARE DANGEROUS ?
Z
I COULD USE SOME WATER NOW
GROUND WATER
Robert Fransgaard '94

Fig. 2. There are numerous sources resulting in human exposure to VOCs.

The potential for chronic low-level and short-term high level exposure is a more than sufficient reason to develop a thorough understanding of the environmental fate and toxicological effects of VOCs to minimize human exposures and health risks posed by these chemicals.

Among the most common VOCs in the environment belong toluene and in particular trichloroethylene, TCE (see Fig. 3).

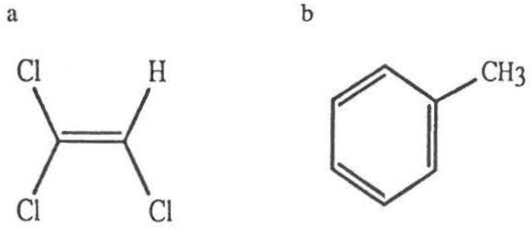

Fig. 3. a: TCE (C_2HCl_3) *is an unsaturated, chlorinated, aliphatic compound with a low molecular weight (131.4 g/mol). At room temperature it is a volatile, non-viscous liquid with a higher density (1.46 g/ml) than water. It is moderately soluble in water (1100 mg/l at 25°C) and has a high vapor pressure (69 mmHg at 25°C). b: Toluene* (C_7H_8) *is an aromatic compound that consists of a benzene ring in which a single methyl group has been introduced. It has a low molecular weight (92.13 g/mol), and is at room temperature a volatile, non-viscous liquid with a lower density (0.6669 g/ml) than water. The solubility in water is low (534.8 mg/l at 25°C) and the vapor pressure is relatively high (28.4 mmHg at 25°C). (Howard, 1990).*

Chronic or repeated exposure to TCE and toluene can cause severe health problems, e.g., nausea, vomiting, abdominal cramps, sleepiness, swelling, loss of coordination, double vision, anorexia, blindness, muscle pains, liver damage, kidney damage, brain damage, and coma. Reproductive effects have been reported in animals. At high level exposure death may occur from respiratory arrest. TCE and toluene are classified as "probably carcinogenic to humans". (Fisher Scientific, 1991; CEPA, 1992; and CEPA,1993).

After TCE and toluene enter the soil medium several factors influence the transport, accumulation, and fate of these chemicals. Because of their nature, they tend to be rather mobile in the subsurface. In the vadose zone they can move either dissolved in the soil-water or much more importantly, due to their low molecular weight, low water solubility, and high vapor pressure, volatilize and move by diffusion in the gaseous phase. Since the diffusion in air is 10^3 to 10^4 times faster than diffusion in water, these chemicals volatile character drastically increases their overall spreading. This is leading to an accelerated movement towards the groundwater and likewise to the atmosphere where gases can migrate in to houses and office buildings and cause the risk of human inhalation. After entering the groundwater they can move as dissolved constituents or dense (TCE) or light (toluene) non-aqueous phase liquids (DNAPLs or LNAPLs, respectively). Since they are uncharged, non-polar molecules and subsurface soils or aquifer materials typically have very low organic carbon contents, the dissolved amounts do not adsorb strongly, but are on the contrary quite mobile.

Toluene and TCE are biodegradable in soils under specific conditions (e.g., Claus and Walker, 1964; Nelson et al., 1987; Armstrong et al., 1991; Ensley, 1991; Fan and Scow, 1993). After having spread to the subsurface environment where microbial activity is low this might, however, be a very slow process. Also at high concentrations, e.g. in the vicinity of a contamination plume, the chemicals are toxic to the microbial population. Microbial degradation can end up creating intermediate products, which are even more hazardous to humans (e.g. in case of TCE: vinyl chloride) than TCE and toluene itself.

During gaseous movement through the soil TCE and toluene will simultaneously adsorb onto the soil minerals. Because of the non-polar characteristics of these chemicals, water-vapor will very strongly compete for adsorption sites. In addition VOCs also compete among themselves; this phenomenon is labelled competitive adsorption. Adsorbed chemicals in the soil compartment will cause an extended period of release and existence of VOCs in the environment.

The objectives of the present work is to contribute to the overall understanding of the movement and environmental fate of VOCs by determining some of the effects of changes in soil physical properties like soil texture and soil-water content on the diffusion, adsorption, and emissions of gaseous volatile compounds in and from soils. And, based on this, to develop model concepts, which by incorporation into existing numerical VOC transport models can improve predicting the spreading of gaseous VOCs in the soil environment.

Included in the objectives are development/implementation of soil physical measurement methods, which are necessary for the above analysis, e.g. non-destructive measurements of soil-water content with high resolution time domain reflectometry (**Article V**) and measurements of specific surface area (**Articles I and II**)

2. Diffusion of gaseous volatile organic compounds

Because of their high vapor pressure, VOCs almost instantly partition into the gas-phase. Thus the gaseous movement, highly dominated by diffusion, plays an important role in the overall spreading of a given contamination.

The diffusion of gases in soils can be described by Fick's first law (Eq. [1]), which states that the rate of transfer of material by diffusion is directly proportional to the concentration gradient or rate of concentration change with respect to distance (e.g., Rolston,1986)

$$\frac{F}{At} = f = -D_P \left(\frac{\partial C}{\partial x}\right) \qquad [1]$$

where F is the amount of gas diffusing (g gas), A is the cross-sectional area of the soil (cm^2 soil), t is time (s), f is the gas flux density (g gas cm^{-2} soil s^{-1}), C is concentration in the gaseous phase (g gas cm^{-3} soil air), x is distance (cm soil), and D_P is the soil-gas diffusivity (cm^3 gas cm^{-1} soil s^{-1}). For unsteady diffusion in soils Eq. [1] is introduced into the equation of continuity leading to Fick's second law. Assuming D_P is a constant and therefore independent of C and t we get (e.g., Rolston, 1986)

$$\varepsilon \frac{\partial C}{\partial t} = D_P \frac{\partial^2 C}{\partial x^2} \qquad [2]$$

where ε is the volumetric soil-air content (cm^3 air cm^{-3} soil).

Several sink terms must be introduced into Eq. [2] in order to correctly describe the transport since VOCs interact with the soil. Those sink-terms represent adsorption onto soil organic matter and soil minerals, dissolution into soil-water, and biological and chemical degradation. The two first mentioned will be addressed later, while the biological and chemical degradation will not be addressed further in this study.

The value of D_P is substantially lower than the diffusivity in bulk air, D_0 (cm^3 gas cm^{-1} air s^{-1}), since only a smaller fraction of the soil volume is occupied with continuous air-filled pores, which at the same time have a tortuous character. D_P/D_0 has been related empirically and theoretically to ε by numerous authors (e.g., Penman, 1940a,b; van Bavel, 1952; Currie, 1970; Millington and Quirk, 1961; Troeh et al, 1982; Currie, 1984; Sallam et al., 1984; Shimamura, 1992). None of the proposed relationships have, however, shown to be universal applicable for different soil types. Different laboratory and field methods for determination of D_P are described in Rolston (1986) and Glauz and Rolston (1989). Table 1 shows a comparison of measured values of D_P/D_0 for diffusion of freon$_{12}$ (a non-reactive tracer) in Yolo silt loam and calculated values using four different models. The calculated values are given relatively to the measured values.

*Table 1. Relative D_P/D_0-values (i.e., compared to D_P/D_0 measured for freon$_{12}$) for Yolo silt loam, predicted from four different models: Troeh et al., 1982: $D_P/D_0=((\varepsilon-u)/(1-u))^v$, where u and v are fitting parameters equal to 0.12 and 1.23 for Yolo silt loam, respectively (**Article I**), Penman, 1940: $D_P/D_0=0.66\varepsilon$, Millington and Quirk, 1961: $D_P/D_0=\varepsilon^{10/3}/n^2$, where n is porosity, and Currie, 1970: $D_P/D_0=\varepsilon^4/n^{2.5}$. For easy comparison, the measured D_P/D_0 values are set equal to 100%. From Petersen and Møldrup (1993).*

	D_P/D_0				
	Measured	--------Predicted--------			
ε	Freon$_{12}$	Troeh et al.	Penman	M-Q	Currie
cm^3/cm^3	%	%	%	%	%
0.1225	100	7	930	45	16
0.1692	100	110	429	45	20
0.1810	100	110	351	45	21
0.2752	100	101	156	50	30
0.3792	100	99	112	69	51
0.4189	100	97	101	94	77

In general the Penman model over-estimates the measured values, whereas both the Millington-Quirk(M-Q) and in particular the Currie model under-estimate the values. Note that for increasing values of ε the accuracy also increases. The Troeh et al. model is a fitting model and therefore agree well with the measured values, except at the lowest ε value (**Article I**). The parameter u usually has a value larger than zero, which indicates that D_P reaches zero while there still is some air-filled porespace in the soil. Very wet soils, for example, have a volumetric air-content that will be in the form of isolated air pockets. Therefore D_P reaches zero at $\varepsilon > 0$ because those air pockets are disconnected and the channels of diffusion therefore blocked (**Article I**).

The Millington-Quirk equation has been widely used in the literature when modelling solute transport in soils, including VOC transport (e.g., Jury et al., 1983; Jury et al., 1990; Culver et al., 1991; Møldrup and Hansen, 1993; Møldrup et al., 1994; Lindhardt, 1994). Lindhart (1994) suggests that the found discrepancies between modelled and measured (in laboratory experiments) emissions of *o*-xylene may be partly related to the description of the tortuosity. It can be concluded that in situations where diffusion in the gaseous phase plays a dominant role for the overall transport the relationship between D_P/D_0 for the actual soils should be determined experimentally (**Article I**).

Like mentioned above VOCs do not behave as non-reactive tracers like freon_{12}. If adsorption onto the soil solids and dissolution into the soil-water are taken into account, Eq. [2] becomes

$$\varepsilon \frac{\partial C}{\partial t} = D_P \frac{\partial^2 C}{\partial x^2} - \frac{\partial S_W}{\partial t} - \frac{\partial S_S}{\partial t} \qquad [3]$$

where S_W is amount of VOC-gas dissolved in soil-water (g VOC cm^{-3} soil), and S_S is amount of VOC-gas adsorbed onto soil solids (g VOC cm^{-3} soil). Assuming that the dissolution of VOC in soil-water can be described by Henry's Law the relation between gas phase and solution phase concentrations is

$$S_W = \frac{C\,\theta}{K_H} \qquad [4]$$

where K_H is Henry's Constant (cm^3 H_2O cm^{-3} air), and θ is the volumetric soil-water content (cm^3 H_2O cm^{-3} soil). Similar, assuming that adsorption to soil solids happens from the aqueous phase and can be described by the equilibrium aqueous/solid partition coefficient, K_D (cm^3 g^{-1}), the relation between aqueous and sorbed phase concentrations is

$$S_S = K_D \frac{C}{K_H} \rho_b \qquad [5]$$

where ρ_b is the soil bulk density (g soil cm^{-3} soil). Taking the derivatives of S_W and S_S with respect to time and substituting Eqs. [4] and [5] into Eq. [3] gives

$$R\varepsilon \frac{\partial C}{\partial t} = D_P \frac{\partial^2 C}{\partial x^2} \qquad [6]$$

where R is the retardation factor and is given by

$$R = 1 + \frac{\theta}{\varepsilon K_H} + \frac{\rho_b K_D}{\varepsilon K_H} \qquad [7]$$

When the soil becomes so dry that Henry's Law is no longer valid and partition can not be described using K_D, the solid/vapor partition coefficient K_D' (cm^3 g^{-1}) is introduced where

$$S_S + S_W = K_D^{\prime} \, C \, \rho_b \qquad [8]$$

Using the same procedure as above the retardation factor for this case can be described as

$$R = 1 + \frac{K_D^{\prime} \, \rho_b}{\varepsilon} \qquad [9]$$

Figure 4 shows results of diffusion experiments with TCE and toluene in which Eq. [6] has been used along with Eqs. [7] and [9] to determine the respective D_P values for these two chemicals. Since D_P/D_0 values for different types of gases are virtually identical at a specific soil-air content the fact that D_P/D_0 values for the reactive tracers, TCE and toluene, are identical to the values for the non-reactive tracer, $freon_{12}$, suggests that the dissolution/adsorption processes can be adequately described by including simple retardation factors as those given in Eqs. [7] and [9]. Only at the highest soil-air content this approach does not hold, which might be explained by faster diffusion at this air-content, and thus, lack of equilibrium. Also, K_D' values for dry soils are very high and extremely dependent on very small changes in water content, which can result in uncertainty in the K_D'-value used to calculate D_P (**Article I**). The K_D' dependency on soil water content will be discussed further in Chapter 3.

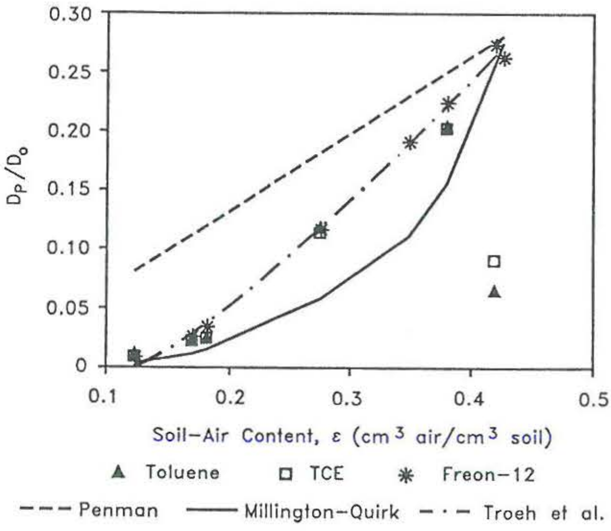

*Fig. 4. Change in D_P/D_0 with volumetric soil-air content for freon$_{12}$, trichloroethylene, and toluene (**Article I**).*

Figure 5 shows an example of results from a diffusion experiment on Ødum sandy loam which is compared to numerical simulations where Eq. [6] and [7] have been used (**Article III**). The introduction of a retardation factor (Eq. [7]) clearly retards the propagation of the concentration front. The diffusion and simultaneous adsorption can as shown be very well simulated by using the simple retardation concept. For all concentrations the simulated and measured concentrations agree very well.

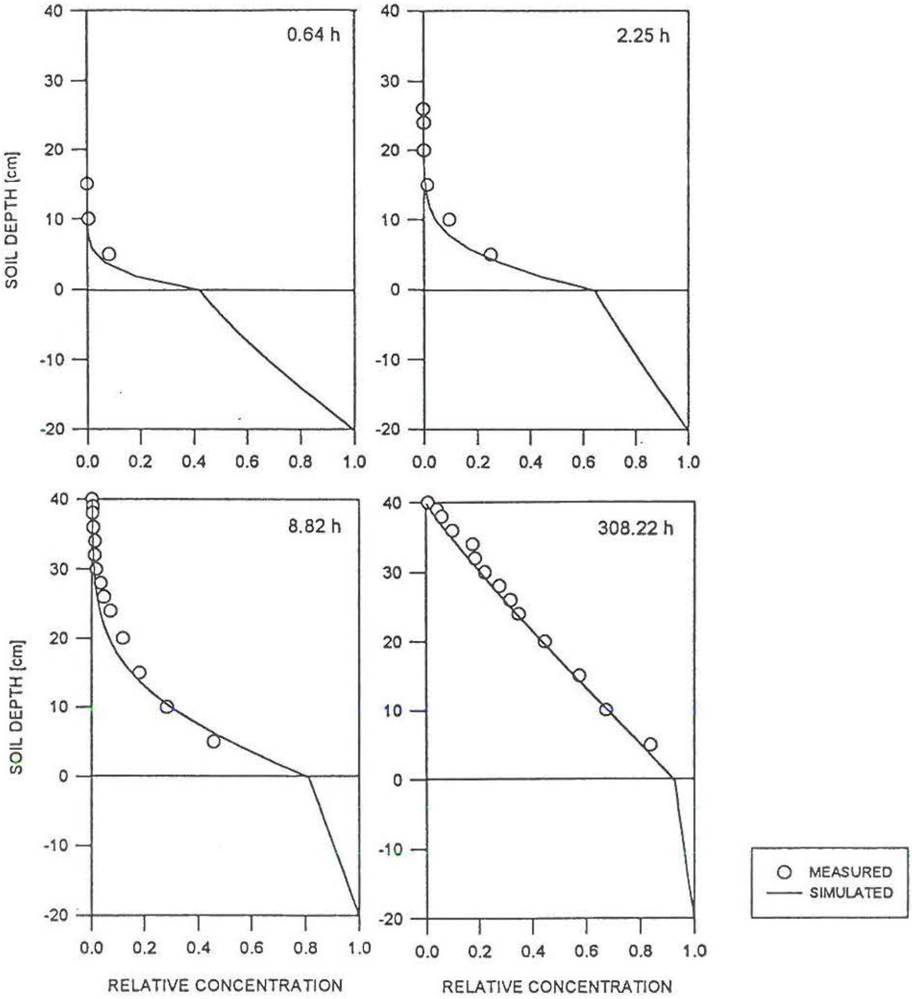

*Fig. 5. Measured and simulated concentration profiles for Ødum sandy loam at four different times after start of the transport process. Relative concentrations are calculated as the measured concentration in a specific depths divided by the concentration at the VOC source (here at depth -20 cm). The depths -20 to 0 (below the horizontal line) represent a chamber with VOC gases in which diffusion takes place in air (**Article III**).*

Therefore for all relative vapor pressures it is reasonable to use the simple equilibrium partition concept. Thus, it would be convenient to use this concept incorporated into simple, numerical models (**Article III**) and semi-analytical models (like the one presented in **Article VI**) to simulate VOC transport and fate.

3. Adsorption of gaseous volatile organic compounds

Adsorption is the process through which a net accumulation of a substance occurs at the common boundary of two contiguous phases. It is a surface phenomenon that takes place because of (and often changes) the forces active in the surface boundaries, which result in characteristic boundary energies. Adsorption can be divided into two broad classes: Physical and chemical adsorption.

Physical adsorption is relatively nonspecific and takes place because of weak forces of attraction or van der Waals forces between molecules (same type of relatively nonspecific intermolecular forces that are responsible for the condensation of a vapor to a liquid). The adsorbed molecules are not fixed to a specific site on the adsorbent surface, but can move around i.e., diffusion in the adsorbed phase is possible. The adsorbed gasses may condense and thereby form several superimposed layers on the adsorbent surface. The equilibrium of physical adsorption is attained very fast and is a reversible process. Physical adsorption is usually only important for gases below their critical temperature, i.e., vapors.

Chemical adsorption can be either fast or slow and can occur both above and below the critical temperature of the adsorbate. It happens as a result of strong forces that are comparable to those leading to the formation of chemical compounds. It differs qualitatively from physical adsorption since chemical specificity is higher and the energy of adsorption is large enough to suggest that full chemical bonding has occurred. Normally the adsorbed material forms only one molecular layer on the surface and molecules are not "free" to move from one site to another. Gas that is chemisorbed may be difficult to remove (not reversible), and desorption can be accompanied by chemical changes (e.g. heating of the adsorbent might be necessary to remove the adsorbate).

Volatile organic compounds like TCE and toluene consist of non-polar molecules. Even though much of the molecular framework of soil organic matter also is electrically uncharged the non-ionic structure can nevertheless still react strongly with the uncharged part of the VOC by van der Waals interactions. The induced van der Waals interaction is the result of correlations between fluctuating polarizations created in the electron configurations of two nearby non-polar molecules. Even though the time-averaged polarization induced in each molecule is zero (remember it is non-polar), the correlations between the two induced polarizations do not average to zero. Therefore a net attractive interaction is produced between the two molecules at very small intermolecular distances (Sposito, 1989).

When a molecule has been adsorbed its motion is restricted to two dimensions. Thus gas adsorption processes are accompanied by a decrease in entropy, ΔS. Since also free energy, ΔG, is decreased, the enthalphy (or heat of adsorption), ΔH, must be negative (Shaw, 1991) because

$$\Delta G = \Delta H - T\Delta S \qquad [10]$$

where T is temperature. Hence the adsorption of gases and vapors on solids is always an exothermic process. The amount of gas adsorbed therefore increases with decreasing temperature. The heats of *physical* adsorption of gases are usually similar to their heats of condensations (Shaw, 1991). Ong and Lion (1991a) found values of ΔH for TCE as high as -10 and -20 Kcal/mol for oven-dried sorbates (aluminum oxide, iron oxide, kaolinite, and montmorillonite). Since this is in the range of the heats of condensation, this indicate that the sorption of TCE is indeed a physical sorption process. I.e., the molecules are adsorbed with the van der Waals mechanism.

Different methods for determining solid/vapor adsorption isotherms for VOCs are described and used in **Articles I, II, III, IV**. Brunauer (1945) suggested that there are five different shapes of isotherms as illustrated in Fig. 6.

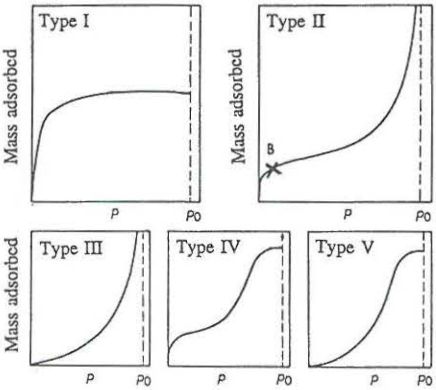

Fig. 6. The five different types of adsorption isotherms (after Brunauer, 1945). P and P_0 are vapor pressure and saturated vapor pressure, respectively.

Multi-layer adsorption

Figures 7a-d show measured adsorption isotherms for TCE single-component (no other VOCs or water vapor present) adsorption onto four different oven-dry soils (**Article IV**, and Petersen (1994) unpublished data). They all have a Type II shape. The Type II isotherms are in general frequently encountered and represent multi-layer physical adsorption. The "kneepoint" (point B) in Fig. 6 on the Type II isotherm is normally recognized as representing the formation of an adsorbed monolayer.

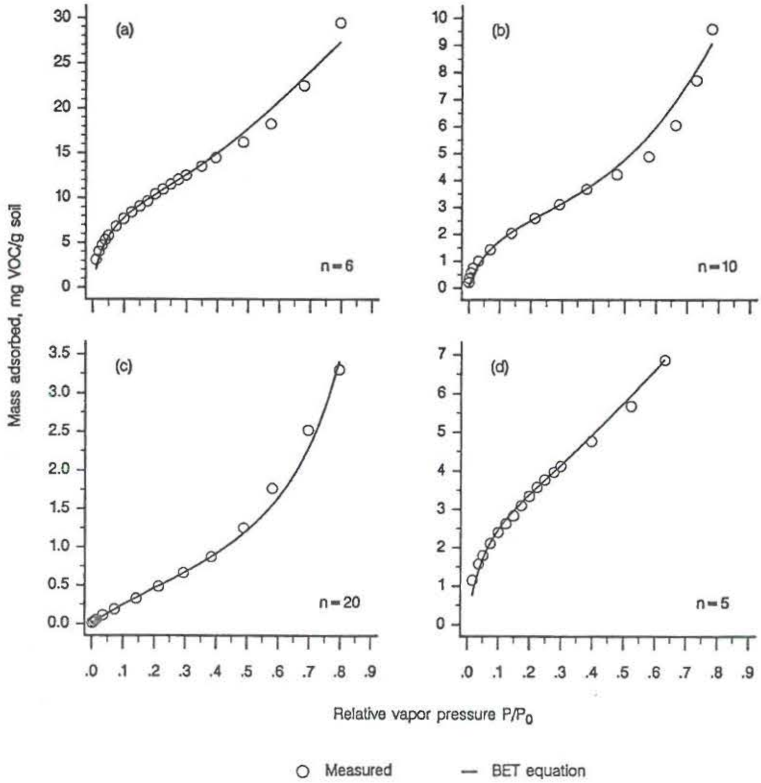

*Fig. 7a-d. TCE adsorption isotherms for a. Yolo silt loam, b: Ødum sandy loam, c: Lundgaard coarse sand, and d: An aquifer material (**Article IV**, and Petersen (1994) unpublished data).*

For high concentrations (i.e., high vapor pressures) typically very close to a concentration plume ("hot-spot"), multi-layer adsorption will occur. In those cases the adsorption capacity of the soil when both water (water vapor) and VOC are present can be estimated from the multi-component BET equation, Eq. [11]. The isotherms shown in Fig. 7a-d can be used along with the single-component BET equation (**Article IV**) to determine the monolayer capacity W^m, and the two constants B and n, which all are parts of the multi-component BET equation for adsorption of species *i* from a vapor mixture containing *s* species (**Article IV**),

$$W_i = \frac{W_i^m E_0 X_i}{(1-E)+E_0(1-E^n)} \left[\frac{B_i(1-E^n)}{E_0} + \sum_{k=2}^{n} E^{k-2}(1-E^{n-k+1}) \right] \qquad [11]$$

where $E_0 = \sum_{i=1}^{s} x_i B_i$, $E = \sum_{i=1}^{s} X_i$, W_i is sorbed mass of species *i* per soil mass, W_i^m is the monolayer capacity (mass of species *i* required to form a monolayer coverage on adsorbent surface per soil mass), X_i is relative vapor pressure (P/P_0), B_i is related to the molar heat of adsorption of the adsorbate on bare mineral surface, and *n* is an integer signifying the maximum possible number of layers *i* on the adsorbent surface for single component systems. When $n=1$ Eq. [11] yields the Langmuir equation, which is also represented by the Type I isotherm (Fig. 6) and which is restricted to monolayer adsorption.

The maximum number of adsorption layers, *n*, is an important parameter in correctly describing multicomponent adsorption. At low VOC relative vapor pressures, the amount adsorbed is irrespective of the value of *n* and a simplified equation based on $n=\infty$ can be used. At higher relative vapor pressures, the choice of $n=\infty$ leads to overestimation of adsorption and a finite *n* should be used (**Article IV**).

When using Eq. [11] for modelling purposes the values W_i for the VOC of interest can be introduced into Eq. [2] as a sink term which will then be dependent on the concentration of both water vapor and other VOC species in the soil. Equation [11] can successfully be used to model VOC adsorption on soils over the range of water content corresponding to between one and two molecular layers. It under-predicts the adsorption amount at lower water contents and low VOC relative vapor pressures. At higher water contents it lacks a suitable vapor solution theory so that the measured adsorption isotherms have to be employed. However, the amount of over-prediction may be small enough to render its use for modelling purposes worthwhile (**Article IV**).

Adsorption described by linear partitioning

The simplest method for modelling the effect of gaseous VOC adsorption on VOC transport is to assume that the VOC partitions linearly to equilibrium between the adsorbed and gaseous phases. This is then incorporated into the diffusion equation, Eq. [2], by introducing the retardation factor, R, like described in Chapter 2. Traditionally R has been predicted by using Eq. [7], which state that the partitioning can be described by employing Henry's Law for dissolution

$$C_{gas} = K_H \, C_{liquid} \qquad [12]$$

and the aqueous/solid partition coefficient K_D (e.g., Jury, 1983; Jury, 1990; Mendoza and McAlary, 1990; Mendoza and Frind, 1990; Møldrup et al., 1994). Recently research has been conducted which, though, question the validity of applying K_D and Henry's Law to predict the vapor phase sorption (e.g., Chiou and Shoup, 1985; Peterson et al., 1988; Ong and Lion, 1990a,b; Culver et al., 1991; Ong et al., 1992; **Articles I, II, III**). The solid/vapor partition coefficient, K_D' has been introduced and has been shown to be highly dependent on the soil-water content. Figure 8 shows an example of this dependency for two different soil types (**Articles I and II**).

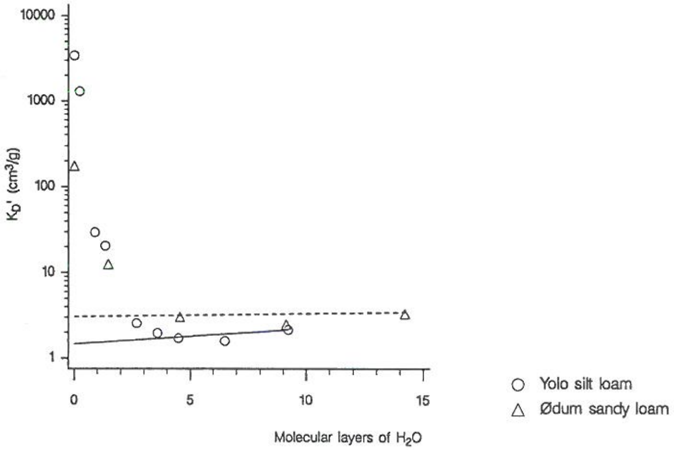

*Fig. 8. Curves relating K_D'-values to change in soil-water content here expressed as number of molecular layers of water adsorbed on the total specific soil surface. Note that for soil-water contents higher than four molecular layers K_D'-values fall on the lines indicating the validity of applying Henry's Law and the aqueous/solid partition coefficient, K_D, (**Article I, II**). For soil-water contents lower than four molecular layers K_D' is highly underestimated if predicted from K_H and K_D.*

For soil-water contents higher than what is equivalent to four molecular layers coverage of water (w_4) the Henry's Law and K_D assumption is valid, and K_D' can be described by

$$K_D' = \frac{K_D}{K_H} + \frac{w}{K_H \phi \rho} \qquad [13]$$

where ϕ is the aqueous activity coefficient (≈ 1), and ρ is the density of water (=1 g/cm^3). (Ong and Lion, 1991a,b; **Articles I,II**). (Note: Inserting Eq. [13] into Eq. [9] yields Eq. [7]). For soil-water contents lower than four molecular layers this approach is clearly in error cf. Fig. 8. At oven-dry conditions K_D' is up to several orders of magnitude higher than at w_4. Thus when modelling transport of gaseous VOCs in dry soil layers, K_D's extremely high dependency on soil-water content should be taken into account.

To describe the shape of the curves in Fig. 8 from oven-dry conditions through to four molecular layers of water ("non-Henry range") a one-parameter, exponential model for log K_D' as a function of soil-water content, w (g H_2O g^{-1} soil) was suggested, Eq. [14] (**Article II**)

$$A = (A_0 - \beta)\, e^{-\alpha w} + \beta \qquad 0 \leq w \leq w_4 \qquad [14]$$

where A=log K_D'(w), A_0=logK_D'(w=0), w is water content by weight, w_4 is the water content at four molecular layers of water, β is a fitting parameter, and α is a function of β. To observe the criteria $A=A_0$ for w=0, and A=(logK_D'($w=w_4$))=A_4 for $w=w_4$, α as a function of β is given by Eq. [15],

$$\alpha = \frac{\ln\left(\frac{A_4 - \beta}{A_0 - \beta}\right)}{w_4} \qquad [15]$$

where α is conceptualized as a measure of the exchange rate of adsorbed VOC molecules by water molecules (**Article II**). The two-part model for VOC vapor adsorption (K_D'-w) where Eq. [13] and Eq. [14] are valid for soil-water contents higher and lower than four molecular layers, respectively, is illustrated in Fig. 9.

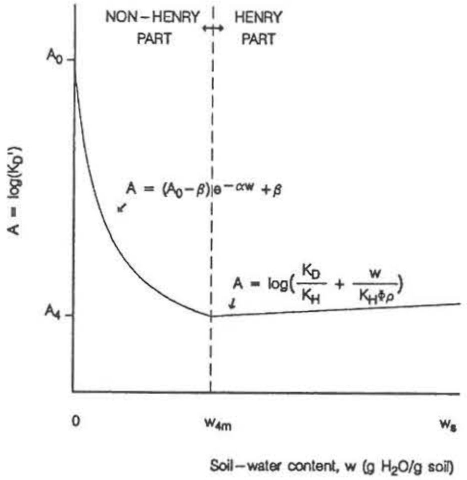

*Fig. 9. Two-part model concept for VOC vapor adsorption as a function of soil-water content. The parameter w_s is the saturated soil-water content (**Article II**).*

The K_D'-w curve can therefore be determined by relatively few experiments: 1. Determination of total specific surface area to determine the soil-water content equivalent to four molecular layers of water. 2. Determination of K_D, which along with Eq. [13] describe the curve for w higher than or equal to four molecular layers of water. 3. Determination of K_D' at oven-dry conditions, and 4. Determination of K_D' at one or more soil-water contents between oven-dry and four molecular layers of water (**Article II**).

Often K_D is determined by applying the widely used empirical equation K_D=f_{OC} K_{OC}, where f_{OC} is the fraction of organic carbon in the soil, and K_{OC} is the organic carbon partition coefficient. By using K_{OC} values of 138 cm^3/g and 98 cm^3/g for TCE and toluene, respectively (Jury et al., 1990) this equation over-predicts K_D values measured on Yolo silt loam (**Article I**) with 150% for TCE and 18% for toluene. For a variety of sorbents, Schwarzenbach and Westall (1981) found, that K_D-values for non-polar organic compounds could be estimated from Eq. [16]

$$\log K_D = 0.72\ \log K_{OW} + \log f_{OC} + 0.49 \qquad [16]$$

where K_{OW} is the octanol-water partition coefficient. By using K_{OW} values of 2.42 and 2.73 for TCE and toluene, respectively (Howard, 1990), Eq. [16] over-predicts the K_D values with more than 200% for both chemicals. Accurate K_D values should therefore be determined experimentally (**Article I**).

Inclusion of the model concept (Eqs. [14] and [15]) for water contents lower than w_4 and the Henry's Law approach for water contents higher than w_4 into conventional VOC transport models seems promising for analyzing the effects of VOC vapor adsorption upon VOC transport.

Effects of soil-texture and specific soil surface area

Besides soil-water content, soil texture plays an important role considering the adsorption capacities of soils, i.e., the magnitude of K_D and K_D'. Under wet conditions, at which the adsorption capacity can be described by using K_D, the amount adsorbed is highly dependent on the organic matter content of the soil. Figure 10 illustrates this dependency, which has a highly linear fashion.

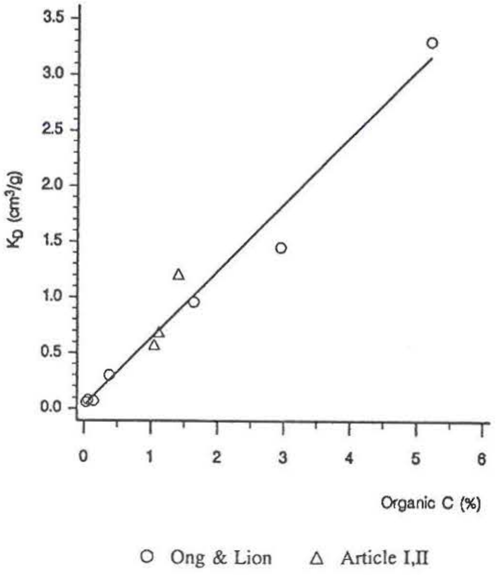

*Fig. 10. Relationship between K_D and % organic carbon. K_D values reported by Ong and Lion (1991b) are included (**Article II**).*

For dry soils, on the contrary, the mineral fraction of the soil is taking over, since adsorption sites directly on the adsorbent will be free for VOC adsorption. Since the mineral fraction of a soil generally contributes significantly towards the total specific surface area, SA (cm^3/g) (Foth, 1978), this is a factor which can indicate the extent of adsorption sites in the soil. Methods for measuring this parameter has been described and used in (Cihacek and Bremner, 1979; Carter et al., 1986; ; Petersen and Jacobsen, 1994; **Articles I, II, IV**). For oven-dry sorbents K_D' has been found to be highly dependent on SA (Ong and Lion, 1991b). The important role of the mineral fraction in the adsorption of gases under oven-dry conditions is consistent with results of other researchers (e.g., Newman, 1987; Rhue et al., 1988; Ong and Lion, 1991b). Figure 11 shows a plot of K_D' at oven-dry conditions vs. SA.

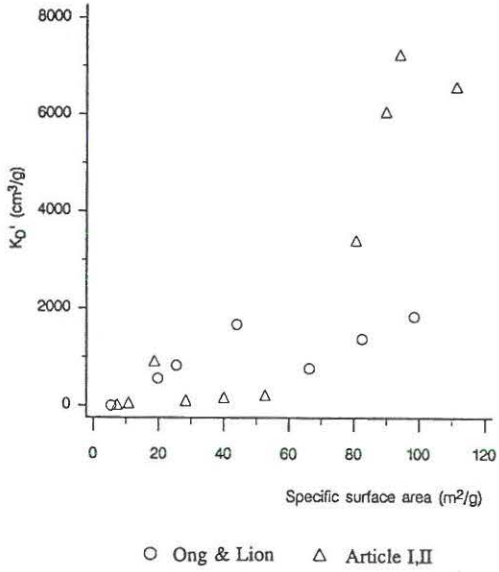

*Fig. 11. Relationship between K_D'-values at oven-dry conditions and total specific surface area. K_D'-values reported by Ong and Lion (1991b) are included (**Article II**).*

There is no significant relationship between the two factors. This might partly be explained by the fact that mainly the external surface area of soil particles contribute to the adsorption capacity of VOC gases (**Article IV**), whereas SA determined above is total surface area. It is therefore recommended that K_D' values for oven-dry conditions be determined experimentally and not by use of empirical equations (**Article II**).

The coefficient α, given by Eq. [15], which is conceptualized as a measure of the exchange rate of adsorbed VOC molecules by water molecules, has been found to be highly dependent on the specific surface area of the soil (**Article II**). Figure 12 shows this dependency for four different soil types (**Article II**). With knowledge of the specific surface area of a soil of interest, α can possibly be determined from the regression equation shown in Fig. 12, thereby reducing the number of experiments necessary for determining the K_D'-w curves.

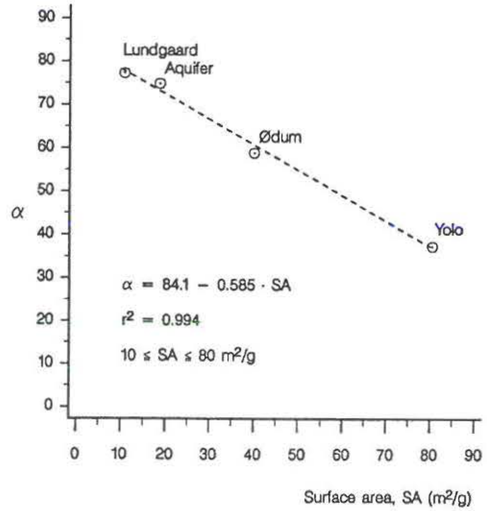

*Fig. 12. Relationship between α and specific surface area (**Article II**).*

The decrease in the curves in Fig. 8 with an increase in soil-water content is really not as much dependent on an actual increase in the amount of water present as the increase in water-film thickness (or layers of adsorbed water molecules). The water-film thickness dictates how strongly the attractive force (from the sorbent) acts on a VOC molecule i.e., the larger the distance between sorbent and molecule the weaker the force. Asymptotically far from the surface the force (potential) decreases as Z^{-3} where Z is the distance of the molecule from the surface (Kreuzer and Gortel, 1986). This decrease is illustrated in Fig. 13a.

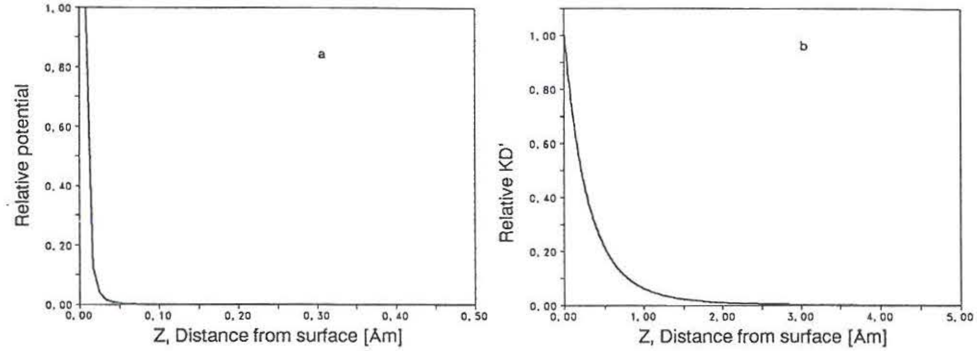

*Fig. 13a-b. a: The surface potential of physiosorption decrease with Z^{-3}. b: Decrease in K_D' for Yolo silt loam (**Article II**) as a function of distance from the sorbent surface. The soil-water contents corresponding to specific K_D'-values are transformed to distances from the surface by first transferring soil-water content to molecular layers and secondly assuming that the diameter of a water molecule approximately is given by $1.854 \cdot 10^{-10}$m.*

Keeping the shape of the curve illustrated in Fig. 13a in mind it can explain some of the tendencies discovered in the curvature of the graphs shown in Fig. 8, and described mathematically by Eqs. [14] and [15]. An example of the K_D'-Z curves for Yolo silt loam is illustrated in Fig. 13b in a non-logarithmical way. The reason why the actual decrease is "stretched" (Fig. 13b) compared to theory (Fig. 13a) can partly be explained by the adsorptive characteristics of the adsorbed water molecules, which is not included in Fig. 13a. An adsorbed water molecule does not only add to the distance between the sorbent and the molecule, but does, in it self, slightly increase the adsorption capacity.

The magnitude of the specific surface area of a soil is to a large extent dependent on the amount of clay in the soil, and the type of clay mineral. The smaller the particles the higher the surface area. Figure 14 shows the relation between specific surface area and clay size fraction for 29 soils (Petersen and Jacobsen, 1994, **Article II**)

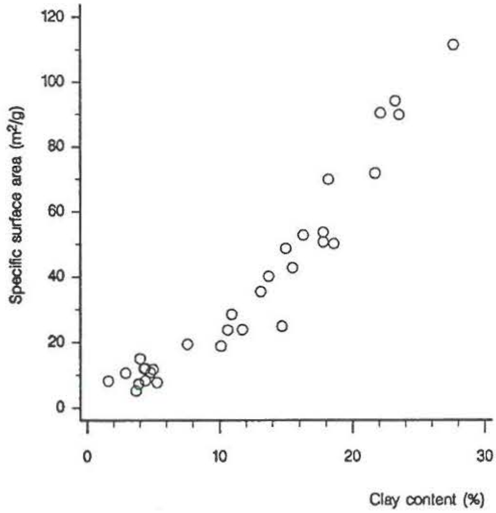

*Fig. 14. Relationship between total specific surface area and clay content (**Article II**).*

It is obvious that the clay size fraction plays a dominant role in the specific surface area. The scatter of the data may partly be explained by differences in the type of clay minerals in the soils since Danish soils contain a variety of different clay minerals and by the fact, that the percentage of clay mineral by weight can be more or less than the percentage of particles of clay size (< 2 um). The surface area of both the silt and sand fractions is reflected in the curve not intersecting 0 at 0% clay content. However, the contribution made by these fractions to the overall surface area seems fairly small.

It is evident that the surface area, and therefore clay content will play an important role in the adsorption of water molecules and in how readily they are desorbed during a drying period. Figure 15 and 16 show the relationship between specific surface area and the soil-water content at -15 bar and -0.1 bar pressure potential, respectively.

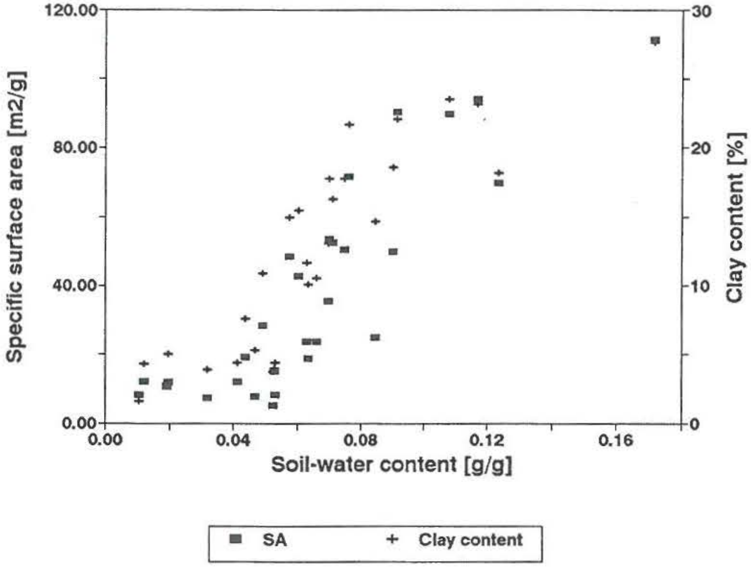

Fig. 15. Soil-water content present at -15 bar pressure potential (the so-called wilting point) as a function of specific surface area and clay content. (Petersen, 1994 unpublished data).

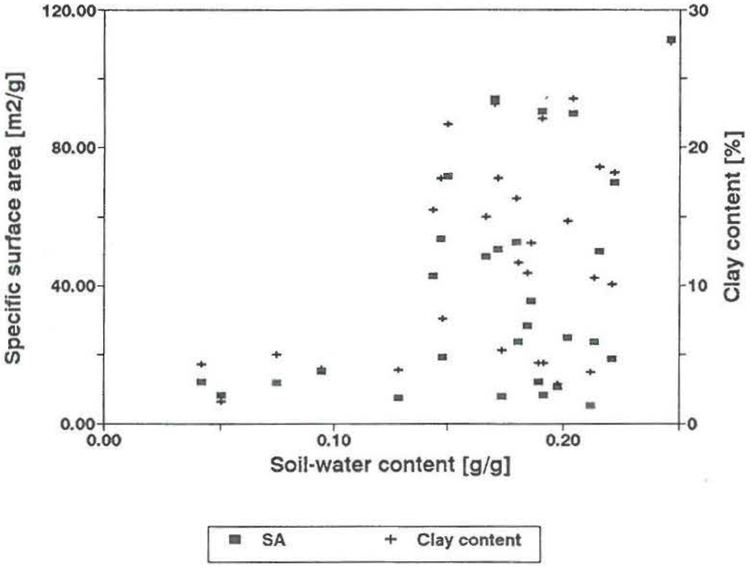

Fig. 16. Soil-water content present at -0.1 bar pressure potential as a function of specific surface area and clay content (Petersen, 1994 unpublished data).

Figure 15 shows the same tendency as described above for VOC vapor, namely for dry soils specific surface area, and thereby the mineral fraction, plays a dominant role for the adsorption capacity (here adsorption of water). For the more wet soils illustrated in Figure 16, the specific surface area does not play a significant role for the adsorption.

Transferring the soil-water contents at -15 bars pressure potential into molecular layers of water and plotting it versus specific surface area (Fig. 17) it is interesting to notice that the majority of points are located between 4 and 8 molecular layers of water. Only the very coarse-textured soils are outside of this range. An explanation may be that small, water-filled pores dominate for coarse-textured soils, rather than an average water-film thickness for the other finer textured soils.

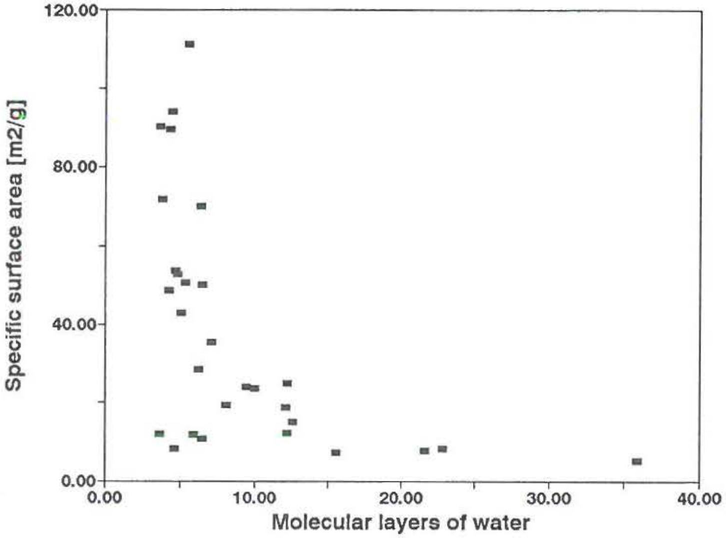

Fig. 17. Relationship between specific surface area and molecular layers of water (Petersen, 1994 unpublished data).

Thus, there seems to be a connection between the soil-water content at the wilting point and the soil-water content above which Henry's Law and the aqueous/solid partition coefficient can be applied. It might be that below this point water molecules stop acting as free water since they are highly adsorbed. Due to the negative charge of the soil surface and the polar nature of a water molecule, water molecules tend to coat the surfaces of the soil particles. Distinctly different than free mobile water, this bound water will be alinged in a well-structured pattern. In fact, bound or hygroscopic water is held so tightly that much of it is considered non-liquid. Henry's constant for bulk water does not apply when the activity of the water has been drastically changed due to binding on a surface. Conceptually, one can consider bound water to be part of the soil. (Shoemaker et al., 1990).

Since water retention data are often available, the soil water-content present at the wilting point can be used as an indication (rule of thumb) for whether adsorption can be described the traditional way by applying Henry's Law and the aqueous/solid partition coefficient or whether non-Henrian adsorption onto the mineral fraction should be taken into account

4. Emissions of gaseous volatile organic compounds

Emission of VOCs into the atmosphere, due to e.g., volatilization and VOC laden soil particles carried by wind action, is a major pathway influencing the fate of these compounds. Emissions take place from industrial sites, hazardous waste treatment and disposal facilities, above shallow groundwater plumes and anywhere the contamination might have spread due to the transport in the soil or migration in groundwater. This can cause human exposure at the contaminated sites and also downwind from them. The VOC emissions are highly dependent on the transport and especially the gaseous diffusion in the vadose zone.

Volatilization as used here is defined as the loss of chemicals from surfaces in the vapor phase, i.e., vaporization followed by movement into the atmosphere (Spencer et al., 1982). Volatilization of VOCs is rather complicated and difficult to predict because of the many factors affecting their adsorption, movement, and persistence as discussed in the previous chapters. Volatilization from soil involves desorption from the soil particles, movement to the soil surface, and vaporization into the atmosphere.

When water is not evaporating, the volatilization rate depends upon rate of movement of the VOC through the soil compartment towards the soil surface by diffusion. The rate at which VOCs move away from the surface is also diffusion controlled. The chemical escapes to the atmosphere by molecular diffusion in the gaseous phase through a stagnant air-layer at the soil surface. The volatilization flux away from a surface by diffusion will be proportional to the diffusion coefficient in air, D_0, and to the concentration of the chemical at the soil surface. If the concentration of VOC in the atmosphere is assumed negligible the volatilization flux, q (μg VOC cm^{-2} min^{-1}), is given by Eq. [17] (e.g., Jury et al., 1990; Møldrup et al., 1994)

$$q = D_0 \frac{C_0}{d} \qquad [17]$$

where C_0 is the concentration of VOC at the soil surface [g cm^{-3}], and d is the thickness of the stagnant boundary layer [cm].

Figure 18 shows an example of measured and simulated volatilization from a soil (Yolo silt loam) from which water is not evaporating (**Article III**) In the simulations adsorption is taken into account by introducing the retardation factor as described in Chapter 2.

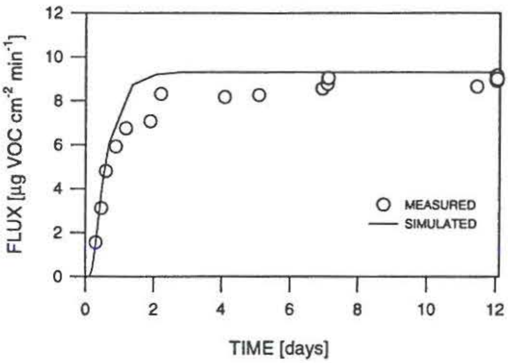

*Fig. 18. Measured and simulated volatilization flux for Yolo silt loam without evaporating water. A thickness of the stagnant boundary layer (d) of 0.475 has been used as suggested by Jury (1983), (**Article III**).*

As illustrated, measured and simulated volatilization fluxes agree very well. The results of the simulations are independent on the value of d. The magnitude of d depends on factors like air flow rate and air turbulence.

Temperature influences volatilization rates mainly through its effect on vapor pressure. Temperature may also influence volatility through its effect on movement of the chemical to the surface by diffusion or mass flow in the evaporating water or through its effect on the soil-water adsorption-desorption equilibrium. Increases in temperature are usually associated with increases in volatilization rate (Spencer et al.,1982). Figure 19 illustrates the effect of change in temperature on the volatilization flux for Yolo silt loam.

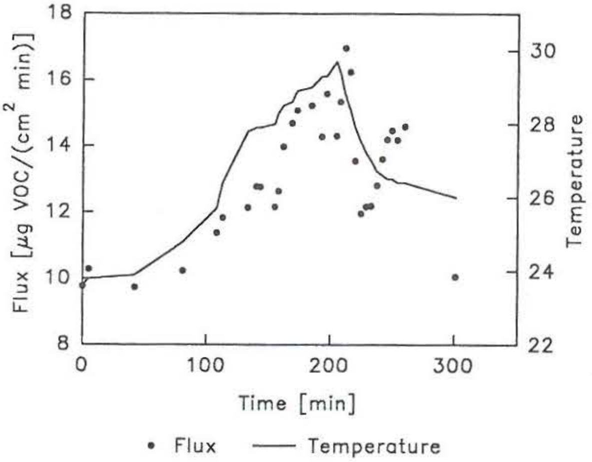

Fig. 19. Change in volatilization flux as a function of temperature for Yolo silt loam (Petersen, 1994 unpublished data).

As can be seen, the size of the volatilization flux clearly increases with increasing temperature. The effect of changing temperature on D_P can be described by Eq. [18] (e.g., Shonnard and Bell, 1993)

$$D_P(T_2) = D_P(T_1)\left(\frac{T_2}{T_1}\right)^n \qquad [18]$$

where T is temperature in degrees Kelvin, and the suggested range of *n* has been found to be within 2.0 at low temperatures and 1.65 at high temperatures (Bird et al., 1960). The increase in D_P determined by Eq. [18] for the increase in temperature given in Fig. 19 can not explain the increase in volatilization flux in Fig. 19. Instead factors like increased vapor pressure and increased desorption (decreased adsorption) must be taken into account).

Due to the extreme dependency of soil mineral adsorption capacity on changes in soil-water content (Fig. 8) the rate of volatilization must be highly dependent on fluctuations in soil surface water contents. One will expect a diurnal cycle: During day time sun-shine and dry wind (low relative humidity) may severely dry the upper-most part of the soil compartment, which will restrict emissions of VOCs to the atmosphere due to an highly increased adsorption capacity. Increase in temperature will have an opposite effect, though, since adsorption decreases with increasing temperature, cf. Chapter 1. During night time with dewfall and increased relative humidity of the air, the polar water molecules will cause desorption of VOC molecules and thus increased volatilization. Figure 20 illustrates the changes in adsorption capacity due to changes in soil-water content in a soil profile, which was dried and rewetted from above by sweeping the soil surface with air having a relative humidity of 0% and 100%, respectively.

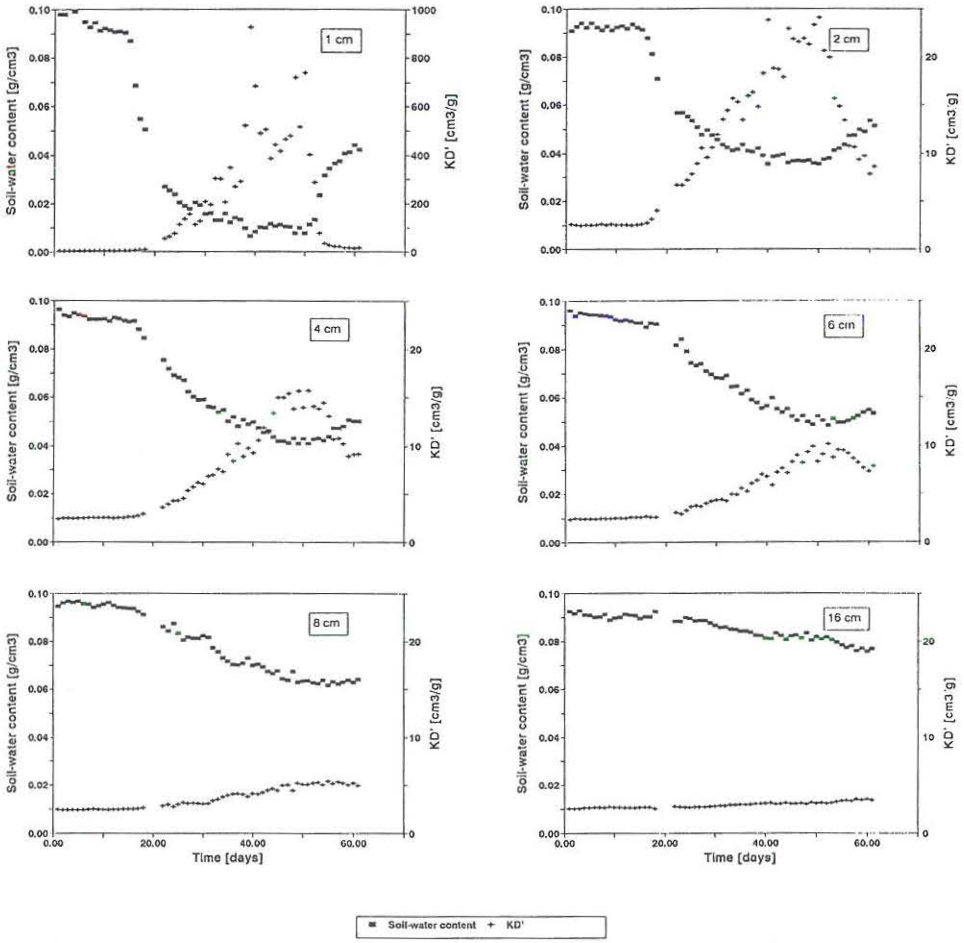

*Fig. 20. Change in soil-water content and K_D' for Yolo silt loam in six depths as a function of time. Drying and wetting were obtained by sweeping a dry or wet air-stream across the soil surface (**Article III**). Note the different y-axis values.*

The change in K_D' is determined by applying Eqs. [14]-[15] (**Articles II and III**). The increase in adsorption capacity is extremely pronounced in the top one centimeter of the soil. The lowest soil-water content obtained is equivalent to 0.22 molecular layers of water, which is well within the non-Henry range (cf. Chapter 2). If the soil simultaneously had been influenced by increased temperature and thus all water molecules was removed (even chemically bonded water) K_D' would have increased to 3401 cm^3/g (**Article I**) for this soil. One would expect this phenomenon to highly restrict the volatilization from the soil compartment and into the atmosphere. Hence even a few millimeters of soil could store big amounts of adsorbed VOC gas, which would be released as soon as water molecules were re-introduced to the surface. Figure 21 shows the response in volatilization flux due to the decrease in soil-water content shown in Fig. 20, and hence increase in adsorption capacity. Also the response to the later increase in soil-water content (wetting) is shown.

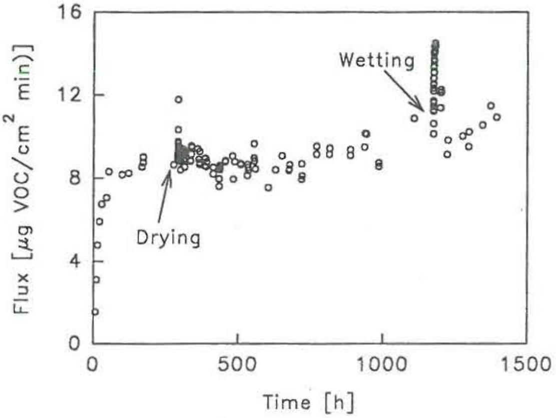

*Fig. 21. Response in volatilization flux for Yolo silt loam due to drying and wetting with a sweep air-stream across the soil surface (**Article III**). From start of the experiment and until drying was initiated the relative humidity of the sweep-air was 100%. During the drying and wetting periods RH in the sweep-air was maintained at 0% and 100%, respectively.*

As seen, the decreased soil-water content does not seem to have the expected effect of decreasing the volatilization fluxes. Immediately after the drying is initiated, the volatilization flux increased in a rapid peak. This phenomena may be explained by the fact that the water which immediately start to evaporate contains dissolved VOC. This leads to a sudden increase in VOC concentration in the liquid phase which, by Henry's partitioning, will result in a corresponding increase in VOC concentration in the gas phase.

Despite the large decrease in soil-water content and consequently the increase in adsorption capacity during the drying period, the soil mineral adsorption does not seem to restrict the volatilization flux. This could be explained by the fact that the constant very high flux of gaseous VOCs that, for this specific case (**Article III**) was applied from the bottom of the soil column, constantly maintained all adsorption sites occupied. Evidently, the increase in the adsorption capacity is gradual enough that it does not decrease the volatilization flux significantly. Even though K_D' is increasing, so is the flux, q (since the air-filled porosity and thefore D_P is increasing). Hence, it seems that the relative increase in q is more than enough to overwhelm the gradual increase in the adsorption capacity. Overall, the flux keeps gradually increasing. The situation is analogous for example to a leaky container of VOC, buried relatively close to the soil surface. This is, however, in contrast to situations where the source of contamination is deep under the soil surface and concentrations at the surface are quite low. For these conditions, the top few mm of soil, in periods when the soil-water content is low and adsorption capacity is high, may still temporarily restrict the volatilization flux of VOCs to the atmosphere (**Article III**). When re-wetting is initiated, the volatilization flux again increase drastically, which is expected since the adsorption capacity increases greatly during drying. This behavior is a reflection of water molecules out competing the VOC molecules sorbed on the soil particle surfaces.

In general further studies, both experimental and modeling, are essential in order to completely describe the effects of fluctuating RH on the volatilization rates. The simultaneous effects of diurnal changes in RH and temperature should be considered, both in laboratory setups and under field conditions, at which the impact from the sun could have an important effect.

5. Concluding remarks

During an environmental investigation of a contaminated site, the authorities often must estimate whether a soil compartment contaminated with volatile organic compounds (VOCs) will influence the outdoor and indoor environment, and hence cause human health risks. I.e., whether a given soil contamination results in an unacceptable degree of chemical volatilization. Calculations are often based on knowledge of chemical concentrations in the soil or groundwater and some physical and chemical properties of the chemicals and the soil (Miljøstyrelsen, 1992). Results of these calculations are also the basis for the selection of a feasible cleaning or encapsulation method, e.g. soil-venting or protecting clay layers.

During the calculations of a potential contamination risk it is important to keep in mind that soil characteristics like relationships between the soil diffusivity and the volumetric soil-air content and between VOC partition coefficients and soil-water content should be carefully considered. This study showed that empirical expressions or simplified equations often can lead to wrong estimates of these transport dominating factors.

When planning a reasonable program for measurements of chemical concentrations and chemical volatilization fluxes at a contaminated site, it must be kept in mind that measurements at a specific time only represent a snapshot. Based on the findings in the present work a snapshot at the "wrong" time can easily lead to erroneous conclusions. It was shown in batch experiments, that the adsorption capacity of a soil is extremely dependent on soil-water content. At very low soil-water contents the adsorption capacity increased with several orders of magnitude compared to moist soils. A control measurement of concentrations and volatilization flux during the daytime, where sunshine causes severe drying of the soil-surface, might therefore result in different conclusions compared to measurements performed during nighttime with dewfall or on a rainy day. In transient transport experiments the effects of successive drying and wetting showed that this resulted in pronounced responses in the volatilization flux. These responses should be taken into account in the estimations of risk, but at the same time the risk could be over-estimated if conclusions are based on measurements performed solely at a time where those fluctuations took place.

In conclusion measurements should be repeated over a carefully planned period of time including both daytime and nighttime. Additionally, VOC concentration and flux measurements must be accompanied by measurements of soil-water content, temperature, and soil organic matter content. As shown in this study a continuous and non-destructive determination of soil-water content even in the uppermost centimeter of the soil, which highly influences the VOC adsorption capacity, could relatively easy be performed by high resolution time domain reflectometry.

6. Related future perspectives

The present work has answered some of the questions related to gaseous VOC transport. At the same time it has opened up for new ideas and inspired to continuous work in related areas, of which some will be mentioned below.

- To do drying/wetting emission column experiments in which chemicals have been incorporated into the soil compartment. Thus ensuring that the induced changes in adsorption sites are not overwhelmed by the flux of VOC from a constant liquid source. Meanwhile a heated drying method could be applied facilitating the removal of chemically bound water

- Perform field studies in which relative humidity and temperature fluctuate naturally and simultaneously and investigate the effects on the volatilization loss of VOCs and surface applied pesticides

- Investigate the importance of adsorption kinetics for unsteady transport of VOCs and pesticides

- Develop a numerical model taking into account competitive adsorption, adsorption kinetics, immiscibility, and water-vapor transport and validate against experimental column data

- Develop semi-analytical solutions based on simple equilibrium partition theory for rapidly screening the relative fate of a large number of VOC compounds

- Investigate the importance of transport of VOCs or pesticides adsorbed onto colloids through macropores or through surface runoff (erosion), thus taking into account soil structure

7. References

Armstrong, A.Q., R.E. Hodson, H-M Hwang, and D.L. Lewis. 1991. Environmental Factors Affecting Toluene Degradation in Ground Water at a Hazardous Waste Site. Environ. Toxicol. Chem. 10:147-158.

Barbee, G.C. 1994. Fate of Chlorinated Aliphatic Hydrocarbons in the Vadose Zone and Ground Water. GWMR. Winter:129-140.

Bird, B.R., W.E. Stewart, E.N. Lightfoot. transport Phenomena, 1st ed.; John Wiley & sons: New york, 1960; pp 511 and 594.

Bredehoeft, J.D. 1994. Hazardous Waste Remediation: A 21st Century Problem. GWMR. Winter:95-100.

Brunauer, S. 1945. The Adsorption of Gases and Vapors, Vol. 1. Princeton University Press, Princeton, NJ.

Carter, D.L., M.M. Mortland, and W.D. Kemper. 1986. Specific Surface. p. 413-423. *In* A. Klute, (ed.). Methods of Soil Analysis. Part 1. 2nd ed., Physical and Mineralogical Methods, Agron. Monogr. 9. ASA and SSSA, Madison, WI.

CEPA, 1992. Toluene. Priority Substances List Assessment Report No. 4. Ministry of Supply and Services. Ottawa, Canada.

CEPA, 1993. Trichloroethylene. Priority Substances List Assessment Report. Ministry of Supply and Services. Ottawa, Canada.

Chiou C.T., and T.D. Shoup. 1985. Soil Sorption of Organic Vapors and Effects of Humidity on Sorptive Mechanism and Capacity. Environ. Sci. Technol. 19:1196-1200.

Cihacek, L.J., and J.M. Bremner 1979. A Simplified Ethylene Glycol Monoethyl Ether Procedure for Assessment of Soil Surface Area. Soil Sci. Soc. Am. J. 43:821-822.

Claus, D., and N. Walker. 1964. The decomposition of Toluene by soil Bacteria. J. Gen. Microbiol. 36:107-122.

Culver, T.B., C.A. Shoemaker, and L.W. Lion. 1991. Impact of Vapor Sorption on the Subsurface Transport of Volatile Organic Compounds: A Numerical Model and Analysis. Water Resour. Res. 27:2259-2270.

Currie, J.A. 1970. Movement of Gases in Soil Respiration. *In* Sorption and Transport Processes in Soil. Rothamsted Experimental Station monograph No. 37. Rothamsted, London. 152-169.

Currie, J.A. 1984. Gas Diffusion through Soil Crumbs: The Effects of Compaction and Wetting. J. Soil Sci. 35:1-10.

Ensley, B.D. 1991. Biochemical Diversity of Trichloroethylene Metabolism. Annu. Rev. Microbiol. 45:283-299.

Fan, S., and K.M. Scow. 1993. Biodegradation of Trichloroethylene and Toluene by Indigenous Microbial Populations in Soil. Appl. Environ. Microbiol. 59:1911-1918.

Fisher Scientific. 1991. Material Safety Data Sheet. Fisher Scientific, Fair Lawn NJ.

Foth, H.D. 1978. Fundamentals of Soil Science. 6th edition. Wiley. New York.

Glauz, R.D., and D.E. Rolston. 1989. Optimal Design of Two-Chamber, Gas Diffusion Cells. Soil Sci. Soc. Am. J. 53:1619-1624.

Helweg, A. 1994. Mange Kilder til Grundvandsforurening med Bekæmpelsesmidler. Vandteknik. 3:110-117.

Howard, P.H. (ed.) 1990. Handbook of Environmental Fate and Exposure Data for Organic Chemicals, Volumen II: Solvents. 3rd. ed. Lewis Publ. Chealsea, MI.

Jury, W.A., W.F. Spencer, and W.J. Farmer. 1983. Behavior Assessment Model for Trace Organics in Soil: I. Model Description. J. Environ. Qual. 12:558-564.

Jury, W.A., D. Russo, G. Streile, and H. E. Abd. 1990. Evaluation of Volatilization by Organic Chemicals Residing Below the Soil Surface. Water Resour. Res. 26:13-20.

Knight, J.H., I. White, and S.J. Zegelin. 1994. Sampling Volume of TDR Probes Used for Water Content Monitoring. Symposium and Workshop on Time Domain Reflectometry, North Western University, Evanston, Illinois, Sept. 8-9, 1994.

Kreuzer, H.J., and Z.W. Gortel. 1986. Physisorption Kinetics. Springer-Verlag, Berlin Heidelberg, Germany.

Lindhart, B. 1994. Volatilisation of Aromatic Hydrocarbons from Coal Tar Contaminated Soil. Ph.D. Dissertation, Institute of Environmental Science and Engineering, Technical University of Denmark.

Mendoza, C.A., and T.A. McAlary. 1990. Modeling of Ground-Water Contamination Caused by Organic Solvent Vapors. Ground Water. 28:199-206.

Mendoza, C.A., and E.O. Frind. 1990. Advective-Dispersive Transport of Dense Organic Vapors in the Unsaturated Zone. 1. Model Development. Water Resour. Res. 26:379-387.

Miljøstyrelsen. 1992. Generel Branchevejledning for Forurenede Grunde. Vejledning nr. 3. Miljøministeriet, København.

Millington, R.J., and Quirk. 1961. Permeability of Porous Solids. Trans. Faraday Soc. 57:1200-1207.

Møldrup, P., and J.Aa. Hansen. 1993. Beregning af Flygtige Organiske Kemikalier's Fordampning under Ikke-Stationære Forhold ved Anvendelse af PC-Modellen RIOCATS. Indlæg ved ATV-møde om "Vurdering af ude- og indeklimaet på grunde forurenet med flygtige organiske kemikalier", 4.11.1993.

Møldrup, P., T.G. Poulsen, D.E. Rolston, T. Yamaguchi, and J.Aa. Hansen. 1994. Integrated Flux Model for Unsteady Transport of Trace Organic Chemicals in Soils. Soil Science. 157:137-152.

Nelson, M.J.K., S.O. Montgomery, W.R. Mahaffey, and P.H. Pritchard. 1987. Biodegradation of Trichloroethylene and Involvement of an Aromatic Biodegradative Pathway. Appl. Environ. Microbiol. 53:949-954.

Newman, A.C.D. 1987. The Interaction of Water with Clay Mineral Surface. *In* Chemistry of Clays and Clay Minerals (Edited by Newman A.C.D.). pp 235.274. Mineralogical Society monograph No. 6. Longman Sci. and Tech., England.

Ong, S.K., and L.W. Lion. 1991a. Mechanisms for Trichloroethylene Vapor Sorption onto Soil Minerals. J. Environ. Qual. 20:180-188.

Ong, S.K., and L.W. Lion. 1991b. Effects of Soil Properties and Moisture on the Sorption of Trichloroethylene Vapor. Water Res. 25:29-36.

Ong, S.K., T.B. Culver, L.W. Lion, and C.A. Shoemaker. 1992. Effects of Soil Moisture and Physical-Chemical Properties of Organic Pollutants on Vapor-Phase Transport in the Vadose Zone. J. Contam. Hydrol. 11:273-290.

Penman, H.L. 1940a. Gas and Vapour Movements in the Soil: I. The Diffusion of Vapours through Porous Solids. J. Agric. Sci. 30:437-462.

Penman, H.L. 1940b. Gas and Vapour Movements in the Soil: II. The Diffusion of Carbon Dioxide through Porous Solids. J. Agric. Sci. 30:570-581.

Petersen, L.W., and P. Møldrup. 1993. Diffusion af Trichloroethylen og Toluen i Lerjord ved Forskellige Luftindhold. Indlæg ved ATV-møde om "Vurdering af ude- og indeklimaet på grunde forurenet med flygtige organiske kemikalier", 4.11.1993.

Petersen, L.W., and O.H. Jacobsen. 1994. Specific Soil Surface Area for Soils from the Danish State Experimental Stations. In preparation.

Peterson, M.S., L.W. Lion, and C.A. Shoemaker. 1988. Influence of Vapor-Phase Sorption and Diffusion on the Fate of Trichloroethylene in an Unsaturated Aquifer System. Environ. Sci. Technol. 22:571-578.

Rhue, R.D., P.S.C. Rao, and R.E. Smith. 1988. Vapor Phase Adsorption of Alkylbenzenes and Water on Soils and Clays. Chemosphere 17:727-741.

Rolston, D.E. 1986. Gas Diffusivity. p. 1089-1102. *In* A. Klute (ed.). Methods of Soil Analysis. Part 1. (2nd ed.). Physical and Mineralogical Methods. Agron. Monogr. no. 9. ASA and SSSA, Madison, WI.

Sallam, A., W.A. Jury, and J. Letey. 1984. Measurements of Gas Diffusion Coefficients under Relatively Low Air-Filled Porosity. Soil Sci. Soc. Am. J. 48:3-6.

Schwarzenbach, R.P., and J. Westall. 1981. Transport of Nonpolar Organic Compounds from Surface Water to Groundwater: Laboratory Sorption Studies. Environ. Sci. Technol. 15:1360-1367.

Shaw, D.J., 1991. Introduction to Colloid & Surface Chemistry. Butterwroth-Heinemann Ltd. Oxford.

Shimamura, K. 1992. Gas Diffusion through Compacted Sands. Soil Sci. 153:274-279.

Shoemaker, C.A., T.B. Culver, L.W. Lion, and M.G. Peterson. 1990. Analytical models of the impact of two-phase sorption on subsurface transport of volatile chemicals. Water Resour. Res, 26:745-758.

Shonnard, D.R., and R.L. Bell. 1993. Benzene Emissions from a Contaminated Air-Dry Soil with Fluctuations of Soil Temperature or Relative Humidity. Environ. Sci. Technol. 27:2909-2913.

Spencer, W.F., and M.M. Cliath. 1973. Pesticide Valatilization as Related to Water Loss from Soil. J. Environ. Qual. 2:284-289.

Spencer, W.F., W.J. Farmer, W.A. Jury. 1982. Review: Behavior of Organic Chemicals at Soil, Air, Water Interfaces as Related to Predicting the Transport and Volatilization of Organic Pollutants.

Sposito, G. 1989. The Chemistry of Soils. Oxford University Press, Inc. New York.

Troeh, F.R., J.D. Jabro, and D. Kirkham. 1982. Gaseous Diffusion Equations for Porous Materials. Geoderma 27:239-253.

van Bavel, C.H.M. 1952. Gaseous Diffusion and Porosity in Porous Media. Soil Sci. 73:91-104.

Viborg Amtsråd, 1993. Regionplan 1994-2006 for Viborg Amt. Olesen Offset, Viborg.

Article I.

Reprinted from the *Journal of Environmental Quality*
Vol. 23, no. 4, July-August 1994, Copyright © 1994, ASA, CSSA, SSSA
677 South Segoe Road, Madison, WI 53711 USA

Volatile Organic Vapor Diffusion and Adsorption in Soils

L. W. Petersen,* D. E. Rolston, P. Moldrup, and T. Yamaguchi

ABSTRACT

Knowledge of the relationship between D_P/D_0 (diffusion coefficient in soil divided by diffusion coefficient in free air) and the volumetric soil-air content, ε, is important when modeling gaseous movement of volatile organic compounds (VOCs) in soils. The effective diffusion (i.e., diffusion and retardation) of trichloroethylene (TCE), toluene and freon in Yolo silt loam (fine-silty, mixed, nonacid, thermic Typic Xerorthent) were measured in a two-chamber diffusion apparatus. The experiments were conducted on packed soil cores over a range of water contents. Vapor retardation factors were calculated from soil parameters and equilibrium partition coefficients. Partition coefficients were measured in batch experiments. It was found that for water contents higher than four molecular layers of water surface coverage, solid/vapor partition coefficients, K_D', were consistent with values predicted by Henry's Law constants (K_H), and aqueous/solid partition coefficients, K_D. For less than four molecular layers of water, sorption increased by orders of magnitude. The vapor retardation factors, along with the measured effective diffusion, allowed a calculation of diffusion coefficients (D_P) for the investigated species by using the analytical solution to diffusion in a two-chamber apparatus. Values of the ratio D_P/D_0 were generally higher than the values predicted by the Millington-Quirk equation, and lower than the values predicted by the Penman equation. Compared with the nonreactive tracer freon, D_P/D_0 values for TCE and toluene agreed very well for higher water contents. Values obtained for air-dry soil, however, were under-predicted. The experimental work for determination of the effective diffusion of reactive tracers can, therefore, for sufficiently high water contents be limited to the determination of D_P/D_0-ε relations for a nonreactive tracer and measurement of K_D, K_D', and K_H values for the reactive tracers.

GASEOUS TRANSPORT, especially gaseous diffusion, plays an important role in the movement of VOCs in soils. Since VOCs readily partition to the gas-phase from a liquid spill, the overall spreading of the contamination is increased, because the diffusion in air is 10^3 to 10^4 times faster than diffusion in water.

Due to the importance of diffusion in the gaseous phase, several investigators have attempted to find a relationship between the ratio of the diffusion coefficient in soil to the diffusion coefficients in free air, D_P/D_0, and the volumetric soil-air content, ε (e.g., Penman, 1940a,b; van Bavel, 1952; Millington and Quirk, 1961; Troeh et al., 1982; Currie, 1984; Sallam et al., 1984; Shimamura, 1992). This previous work shows that no single relationship between D_P/D_0 and ε is universally applicable for different soil types. A specific relation must therefore, if possible, be obtained experimentally for the soil of interest.

It is generally assumed that the ratio of D_P/D_0 is independent of the nature of the diffusing gases. Shimamura (1992) investigated this for three different nonreactive tracers (N_2, CH_4, and H_2) and found good agreement. Theoretically, it will therefore be sufficient to determine the D_P/D_0-ε relationship for one gas and use that to determine the behavior of other gases knowing only their respective diffusion coefficients in free air.

Adsorption is another important abiotic process that influences the fate and transport of VOCs in soils. This process is highly dependent on the amount of moisture present in the soil (Chiou and Shoup, 1985; Valsaraj and Thibodeaux, 1988; Rao et al., 1989; Rhue et al., 1989; Thibodeaux et al., 1991; Ong and Lion, 1991a,b), since polar water molecules are strong competitors for adsorption sites relative to nonpolar organic compounds.

Experimental determination of diffusion coefficients for adsorptive tracers is considerably more complex than for nonreactive tracers since the decrease in concentrations due to adsorption needs to be quantified.

The objective of this work was to examine whether or not it is sufficient to establish the D_P/D_0-ε relationship for a nonreactive tracer like freon-12 and use that to determine the effective diffusion of reactive tracers, like TCE and toluene, using equilibrium partition coefficients to quantify the adsorption.

THEORY

Unsteady diffusion of gas in soils can be described by the following equation,

$$\varepsilon R\left(\frac{\partial C}{\partial t}\right) = D_P\left(\frac{\partial^2 C}{\partial x^2}\right) \quad [1]$$

where ε is the volumetric soil-air content (cm^3 air/cm^3 soil), C is the gas concentration (g gas/cm^3 soil), D_P is the soil-gas diffusivity (cm^3 air/cm soil s), t is time (s), x is distance (cm), and R is the retardation factor. Where Henry's Law is applicable, R can be determined using Henry's constant, K_H, which governs the equilibrium distribution of the VOC between aqueous and vapor phase, together with the aqueous/solid partition coefficient, K_D (cm^3/g), for sorption of dissolved VOCs onto soil particles, i.e.,

$$R = 1 + \frac{\theta}{\varepsilon K_H} + \frac{\rho_b K_D}{\varepsilon K_H} \quad [2]$$

where θ is the volumetric soil-water content (cm^3 H_2O/cm^3 soil), and ρ_b is the bulk density (g soil/cm^3 soil). For low water contents where Henry's Law and Eq. [2] are not valid, Eq. [3] can be used;

$$R = 1 + \frac{K_D'\rho_b}{\varepsilon} \quad [3]$$

L.W. Petersen and P. Moldrup, Environmental Engineering Laboratory, Dep. of Civil Engineering, Aalborg Univ., Sohngaardsholmsvej 57, DK-9000 Aalborg, Denmark; D.E. Rolston, Soils and Biogeochemistry, Dep. of Land, Air, and Water Resources, Univ. of California, Davis, CA 95616; and T. Yamaguchi, Dep. of Civil and Environmental Engineering, Faculty of Engineering, Hiroshima Univ., 1-4-1 Kagamiyama, Higashi-Hiroshima, 724, Japan. Received 5 Apr. 1993. *Corresponding author (lwp@dina.foulum.min.dk).

Published in J. Environ. Qual. 23:799-805 (1994).

Abbreviations: VOC, volatile organic compounds; TCE, trichloroethylene, EGME, ethylene glycol monoethyl ether; EC, electrical conductivity; CEC, cation-exchange capacity; FID, flame ionization detector; EPICS, equilibrium partitioning in closed systems.

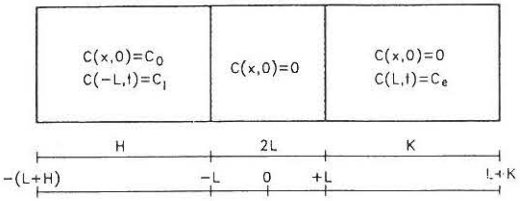

Fig. 1. Initial and boundary conditions for two-chamber diffusion apparatus.

where K'_D is the solid/vapor partition coefficient (cm^3/g) and R is equal to 1 for a nonreactive tracer.

Initial and boundary conditions for the two-chamber diffusion apparatus used in this work are illustrated schematically in Fig. 1. It is assumed that the gas within the air chambers is perfectly mixed at all times due to the much larger diffusivity in air than in soil. Sallam et al. (1984) provided evidence that this assumption is valid. In this study it was experimentally confirmed that concentrations of gas samples taken from two sampling ports placed at each end of the inlet chamber (Fig. 2) were equal. The boundary condition at the left soil boundary, $x = -L$ (Fig. 1), is

$$C_i = C_0 + (D_P/H) \int_0^t (\partial C/\partial x)_{x=-L} dt \quad [4]$$

and the boundary condition at $x = L$ is

$$C_e = -(D_P/K) \int_0^t (\partial C/\partial x)_{x=L} dt \quad [5]$$

where C_i and C_e are inlet and exit chamber concentrations, C_0 is the initial concentration (g/cm^3), and H and K are the effective length of the inlet and exit chambers (Fig. 1) (Glauz and Rolston, 1989).

The analytical solution to diffusion in a two-chamber diffusion apparatus at the left soil boundary in contact with the inlet chamber is (Glauz and Rolston, 1989)

$$C/C_0 = \frac{1}{1 + \frac{1}{\gamma} + \frac{2}{\beta}} + \sum_{n=1}^{\infty} [-A(\alpha_n)/B(\alpha_n)]\exp(-\alpha_n^2\tau) \quad [6]$$

where

$$\gamma = \frac{H}{K} \quad \beta = \frac{H}{L\varepsilon R} \quad \tau = \frac{D_P t}{\varepsilon R L^2} \quad [7]$$

$$A(\alpha_n) = -\frac{\gamma}{\beta^2} - \frac{\alpha^2}{\gamma} \quad [8]$$

$$B(\alpha_n) = \alpha_n^4(\beta/\gamma) + \alpha_n^2\left[\frac{1}{\gamma\beta} + \frac{\gamma}{\beta} + \frac{1}{2\gamma} + \frac{1}{2}\right] + \frac{\gamma}{\beta^3} + \frac{\gamma}{2\beta^2} + \frac{1}{2\beta^2} \quad [9]$$

and α_n are the roots of

$$\tan 2\alpha = \frac{\alpha\beta(1 + \gamma)}{\alpha^2\beta^2 - \gamma} \quad [10]$$

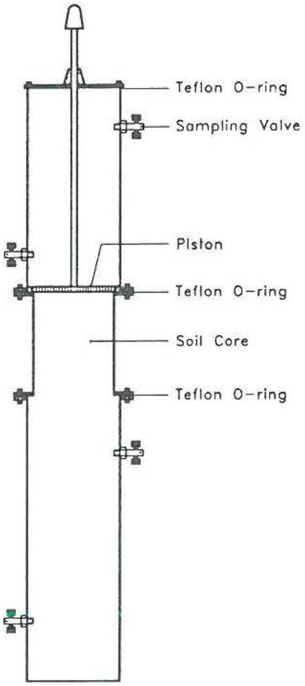

Fig. 2. Illustration of two-chamber diffusion apparatus. The apparatus was placed horizontally during experiments.

If sampling from the exit chamber is desired, Eq. [8] must be substituted by

$$A(\alpha_n) = [\alpha_n^4 + (\gamma^2/\beta^4) + (1 + \gamma^2)(\alpha_n^2/\beta^2)]^{1/2} \quad [11]$$

The D_P values, corresponding to a measured relative concentration and time, were determined from Eq. [6] to [10]. Time, t, was fixed at the measured time, and D_P iteratively changed until the measured relative concentration was obtained.

The aqueous/solid partition coefficient, K_D, can be determined as the slope obtained from plotting the left hand side of Eq. [12] against $M/(V_{LS} + \lambda K_H V_{GS})$ (Peterson et al., 1988). Equation [12] arises from combining mass balance equations for bottles with sorbent, gas phase, and liquid phase and bottles containing only gas phase and liquid to give

$$\frac{C_{GB}(\lambda K_H V_{GB} + V_{LB})}{C_{GS}(\lambda K_H V_{GS} + V_{LS})} = K_D \frac{M}{V_{LS} + \lambda K_H V_{GS}} + 1 \quad [12]$$

where V_{LB} and V_{GB} are liquid and gas volumes in a bottle without sorbent (cm^3), V_{LS} and V_{GS} are liquid and gas volumes in bottles with sorbent, C_{GB} and C_{GS} are headspace concentration in bottles without and with sorbent (g/cm^3), M is mass of sorbent (g), and λ is the activity coefficient for VOC in 0.1 M NaCl. Sodium chloride is used because it adequately swamps out any ionic influences attributed to the sorbent (Gabarini and Lion, 1985). The values of λ and K_H must be determined separately. The values obtained by Garbarini and Lion (1985) and experimentally confirmed in this study for TCE are $K_H = 0.397$ and $\lambda = 1.06$ and for toluene are $K_H = 0.261$ and $\lambda = 1.05$.

For linear isotherms, the solid/vapor partition coefficient, K'_D is the slope obtained from plotting the left hand side of Eq. [13] against M/V_S (Ong and Lion, 1991a,b). Equation [13] arises from equating mass balance equations for bottles with sorbent to bottles without sorbent

$$\frac{V_B C_B}{V_S C_S} - 1 = K'_D \frac{M}{V_S} \qquad [13]$$

where V_B and C_B are the gas volume and concentration in bottles without sorbent, and V_S and C_S are the gas volume and concentration in bottles with sorbent. The Langmuir equation was used to fit data from nonlinear isotherms,

$$W = \frac{C_B V_B - C_S V_S}{M} = \frac{W^m k C_S}{1 + k C_S} \qquad [14]$$

where W is amount adsorbed per mass of soil (g VOC/g soil), W^m is the monolayer capacity (g VOC/g soil), k is a constant related to the binding energy, and K_D' is given by $W^m k$ and is applicable to the linear region of the isotherm.

MATERIALS AND METHODS

The soil used in the experiments was a Yolo silt loam. It was collected from the top 20 cm of an agricultural field on the campus of the University of California, Davis. The soil was air dried, passed through a 2-mm sieve (no. 10), and mixed thoroughly to obtain a homogeneous mixture. Some characteristics of the soil are given in Table 1. Total surface area was determined by the ethylene glycol monoethyl ether (EGME) method (Heilman et al., 1965; Carter et al., 1986). Pretreatments to remove organic matter and saturation with Ca^{2+} were omitted (Cihacek and Bremner, 1979). The organic C content of the soil was analyzed by a modified Walkley and Black method (Nelson and Sommers, 1982). The pH was measured on saturated paste by pH meter, while electrical conductivity (EC) was measured on saturation extracts using a conductivity meter. Cation-exchange capacities (CEC) were determined by saturation with Ba acetate. Particle size analysis to determine sand, silt, and clay fractions was performed by hydrometer (Gee and Bauder, 1986). The soil-water content corresponding to four molecular layers of water was calculated using the total surface area determined by the EGME method, assuming that a water molecule occupies an area of 10.8×10^{-20} m^2 (Livingston, 1949).

For diffusion coefficient determinations, a two-chamber diffusion apparatus was used (Glauz and Rolston, 1989). Stainless steel and Teflon were used to build the apparatus to prevent the VOCs from adsorbing on or diffusing through the walls of the chambers. The apparatus, consisting of two air-filled chambers separated by a packed soil column, is illustrated in Fig. 2.

The effective length of the inlet and exit chambers was H = 25.5 cm and K = 41.3 cm (actual length = 20 cm and 30 cm), respectively. Effective length corresponds to the volume of the chamber divided by the surface area of the soil core. The length of the soil column used was either 10 or 20 cm, depending on water content, and the diameter was 7.67 cm. The optimum size of the chambers were determined using the error analysis given in Glauz and Rolston (1989).

Table 1. Characteristics of the soil (Yolo silt loam) used in the diffusion and adsorption experiments.

Surface area, m^2/g	80.6
Organic C, %	1.05
pH	7.9
Electrical conductivity, milli-mhos/cm	0.77
Cation-exchange capacity, meq/100g	21.1
Sand, %	33
Silt, %	49
Clay, %	18
Four molecular layers of water (g water/g soil)	0.089

Initially, the piston was closed, separating the inlet chamber from the soil chamber. Gas was introduced to the inlet chamber and allowed to equilibrate to an initial concentration, C_0, determined by gas chromatography. The piston was pulled back and diffusion through the soil column initiated. A volume of air equal to the volume of the retracted piston rod was introduced to the chamber to avoid pressure differences between the two end chambers. Gas samples were taken at several successive times from the inlet chamber. The D_P was calculated at each sampling time and then averaged across the sampling period. The coefficient of variation for D_P never exceeded 15% and was in general on the order of 2 to 4%.

When sampling, 1 mL of gas was removed with a gas-tight syringe (Hamilton 1001, Hamilton Company, Reno, NV) and analyzed on a Hewlett Packard 5890A gas chromatograph equipped with a flame ionization detector (FID). For TCE and toluene analysis, the packed gas chromatograph column was a 3.04 m (10 ft) 20% SP-2100, 0.1% Carbowax 1500, on 100/120 mesh Supelcoport (Supelco Inc., Bellefonte, PA), operated isothermally at 140 °C. For freon-12 analysis, the column used was a 6 ft Haysept Q on 80/100 mesh (Alltech, San Jose, CA), operated isothermally at 140 °C. Zerograde helium was used as the carrier gas.

For the higher water contents stainless steel cylinders were packed with air-dry soil. Additional 10-cm columns were attached to each end of the soil cores prior to packing. The middle part, which was expected to have the most homogeneous packing, was used in the experiment. The cores were carefully sprayed with water to obtain the desired volumetric water and air contents. The cores were allowed to equilibrate for 2 to 3 wk. The uniformity of this packing technique was tested using gamma attenuation. Also water content of soil in the cylinder and end pieces was determined gravimetrically and showed no differences. For the lower water contents the soil was sprayed with water before packing, and additional end pieces were attached during packing. Water contents ranged from 0.04 cm^3 H_2O/cm^3 soil to 0.36 cm^3 H_2O/cm^3 soil, and air contents ranged from 0.12 cm^3 air/cm^3 soil to 0.42 cm^3 air/cm^3 soil. During the experiments, the apparatus was placed horizontally and rotated frequently to avoid differences in water content inside the soil column.

Since toluene and TCE are biodegradable (e.g., Claus and Walker, 1964; Nelson et al., 1987; Armstrong et al., 1991; Ensley, 1991), packed soil cores with water contents higher than air-dry soil were irradiated to prevent microbial activity (McLaren et al., 1962; Eno and Popenoe, 1964). Radiation was chosen as the sterilization method because it offers a possibility for minimizing changes in the soil since neither heat nor chemicals are involved. Any possible changes due to radiation are mostly associated with the organic matter content of the soil (Eno and Popenoe, 1964); a soil like Yolo silt loam (fraction of organic C, f_{OC} = 0.0105) will therefore not be altered nearly as much as a highly organic soil. Preparation of experiments with sterile soil were performed in a laminar flowhood to avoid airborne contamination. Water content and bulk density were determined after each diffusion experiment by oven drying the soil for 24 h at 105 °C. The soil air content was calculated from porosity and water content. Experiments were carried out at room temperature ($\approx$25 °C).

The diffusion coefficients in free air were calculated using the Fuller correlation (Fuller et al., 1966). The D_0 values obtained for freon-12, TCE, and toluene were 0.0763 cm^2/s, 0.0835 cm^2/s, and 0.0805 cm^2/s, respectively.

The headspace technique, equilibrium partitioning in closed systems (EPICS) (e.g., Peterson et al., 1988; Ong and Lion, 1991a,b) was used for determining partition coefficients. The method can briefly be described as a mass balance technique that involves measurement of an equilibrium headspace vapor concentration in sealed glass bottles by gas chromatography. A system with known gas volume and mass of sorbent is compared with a control that contains no sorbent. Sorbent masses ranged from 0.2 to 60 g. The amount of sorbent was increased for increasing water contents. For each adsorption isotherm, seven different sorbent masses were used with three replicates for each mass. The sorbent was introduced to glass bottles with a volume of 60 or 250 mL. The bottles were wrapped with paper to prevent photodecomposition of the VOCs and sealed with Teflon Mininert valves (Dynatech, Baton Rouge, LA). Two and a half milliliters of air were withdrawn from and 2.5 mL of saturated VOC vapor was introduced to each bottle. Saturated vapors were taken from the headspace of a 5 L flask containing 1 L of liquid VOC (certified toluene and TCE were obtained from Fisher Scientific, Fair Lawn, NJ). All bottles were rotated for 24 to 36 h at 25 °C to reach equilibrium. Preliminary work showed that equilibrium was reached after this period of time. One milliliter of headspace was removed for concentration analysis.

The K_D values were determined from adsorption isotherms of a water saturated system. Adsorption isotherms, used to calculate K_D' values, were determined for ten different water contents ranging from 0 to 21 g H_2O/g soil. Water contents less than air-dry ($\approx 68\%$ relative humidity) were obtained by mixing specific amounts of oven dry and air dry soils. Water contents higher than air dry were obtained by spraying air dry soil with a predetermined mass of water.

RESULTS AND DISCUSSION

Sorption

Figure 3 shows adsorption isotherms obtained with the EPICS method using Eq. [13]. Linear isotherms were characteristic for soil-water contents higher than or equal to 0.02 g H_2O/g soil, i.e., from soil water contents slightly less than air dry soil. This is in agreement with what other investigators have found for hydrated sorbents (Chiou and Shoup, 1985; Rao et al., 1989; Rhue et al., 1989; Ong and Lion, 1991a,b). An increase in moisture content results in a drastic decrease in K'_D values for both gases (Fig. 3). For Yolo silt loam, air dry soil corresponds to between one and two molecular layer of water coverage. A strong dipole interaction between the water molecules and the polar surface of the soil particles may account for the inhibition of nonpolar VOC vapor adsorption (Rao et al., 1989), especially since VOC molecules are thought to be adsorbed with relatively weak van der Walls forces. Partition coefficients were, without exception, higher for toluene than for TCE at the same water content. This was expected even though the monolayer capacity for TCE on Yolo silt loam is higher than that for toluene (Amali et al., 1994; W^m values for TCE and toluene on Yolo silt loam were 9.7 and 5.3, respectively). For the same relative vapor pressure (vapor pressure divided by saturated vapor pressure, P/P_0) of TCE and toluene, a larger mass of TCE will be adsorbed per gram of soil; however, K'_D is a function of concentration,

$$C_{SOIL} = K'_D \, C_{VAPOR} \qquad [15]$$

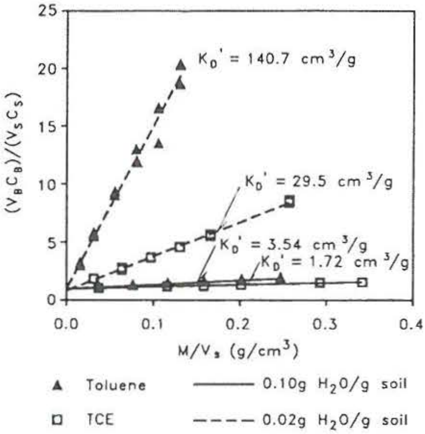

Fig. 3. Adsorption isotherms for trichloroethylene and toluene on Yolo silt loam at a soil-water content of 0.02 and 0.10 g H_2O/g soil. Equation [11] is used and the K'_D values are determined as the slope of the isotherms.

Hence, relative vapor pressures must be converted to concentrations. For the same concentration of TCE and toluene, P/P_0 for toluene is much higher than that for TCE. Thus, a larger mass of toluene adsorbs per gram of soil, resulting in a higher K'_D value.

The adsorption of freon-12 was also checked using the EPICS method. The determined K'_D-values were very low and within the error of the method. Therefore, the adsorption of freon-12 was assumed negligible.

Figure 4 summarizes the change in toluene and TCE vapor phase partition coefficients with water content. From oven dry conditions to 0.09 g H_2O/g soil ($\approx 100\%$ relative humidity), K'_D values decreased by several orders of magnitude. For toluene, K'_D decreased from 21645 cm^3/g to 3.54 cm^3/g and for TCE from 3401 cm^3/g to 1.71 cm^3/g. For water contents higher than 0.09 g H_2O/g soil (≈ 4 molecular layers of H_2O), K'_D values increase due to VOC dissolution into soil water. This phenomenon is represented by the solid lines in Fig. 4. The lines arise from the following equation (Ong and Lion, 1991a,b) assuming that water surface sorption and condensation are negligible,

$$K'_D = \frac{K_D}{K_H} + \frac{W}{K_H \, \varphi \, \rho} \qquad [16]$$

where W is the water content by weight (g H_2O/g soil), φ is the aqueous activity coefficient (= 1), and ρ is the density of water (= 1 g/cm^3). The points where measured K'_D values fall on the line indicate the applicability of Henry's Law.

Aqueous/solid partition coefficients, K_D, used in the above equation were determined by the EPICS method and Eq. [12]. The K_D values were 0.58 cm^3/g and 0.87 cm^3/g

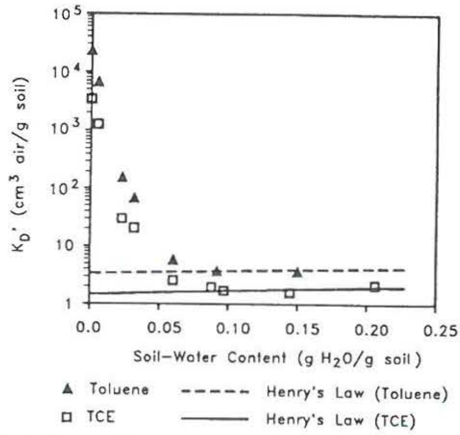

Fig. 4. Change in trichloroethylene and toluene vapor phase partition coefficients with soil-water content.

for TCE and toluene, respectively. Both values are significantly smaller than values predicted by the widely used empirical equation $K_D = f_{OC}\,K_{OC}$. By using the K_{OC} values of 138 and 98 cm^3/g for TCE and toluene, respectively (Jury et al., 1990), this equation over-predicts the K_D value with 150% for TCE and 18% for toluene. For a variety of sorbents, Schwarzenbach and Westall (1981) found that K_D-values for nonpolar organic compounds could be estimated from Eq. [17].

$$\log K_D = 0.72 \times \log K_{OW} + \log f_{OC} + 0.49 \quad [17]$$

where K_{OW} is the octanol-water partition coefficient. By using log K_{OW} values of 2.42 and 2.73 for TCE and toluene, respectively (Howard, 1989), Eq. [17] over-predicts the K_D values with >200% for both chemicals. Accurate K_D values should therefore be determined experimentally.

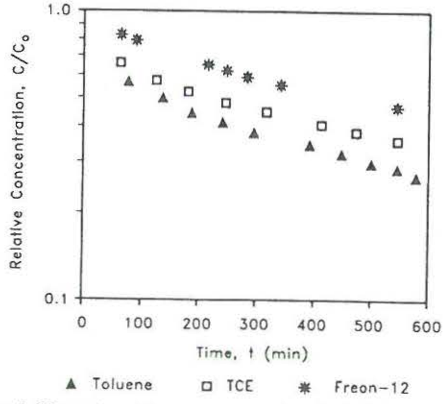

Fig. 5. Change in relative gas concentrations in the inlet chamber of the two-chamber diffusion apparatus with time. $\varepsilon = 0.28$ cm^3 air/cm^3 soil.

Diffusion

Figure 5 shows examples of the decrease in relative concentrations for freon-12, TCE, and toluene with time, as measured in the inlet-chamber of the diffusion apparatus. Each packed soil column was run with all three gases. When changing to another gas, excess gas from the previous run was flushed out. Thus, only changes between the diffusion coefficients in air and the retardation factors changed between runs with different gases. Examination of D_0-values alone reveals that C/C_0 for TCE would be expected to decrease slightly faster than for toluene, which would decrease slightly faster than freon-12. However, due to partitioning, the order is different as shown in Fig. 5. As previously mentioned, partition coefficients for toluene were higher than those for TCE; the decrease in VOC concentration are, therefore, highly dependent on the retardation of vapors. Generally, for all experiments, when plotting $\log(C/C_0)$ as a function of time, the relative concentration decreased in a nearly linear fashion.

Using Eq. [6] to [10], it was investigated whether the faster decrease in C/C_0 for toluene and TCE compared with freon-12 could be accounted for by the equilibrium partition coefficients measured by the EPICS method. Retardation factors (Eq. [2], [3]) were calculated based on equilibrium partition coefficients and introduced into Eq. [6] to [10]. Calculated D_P values for the three gases divided by their respective D_0 values should be identical at a specific volumetric air-content, if in fact equilibrium partition coefficients can be used. Figure 6 compares D_P/D_0 values for freon-12, TCE, and toluene across a range of volumetric air contents. The D_P/D_0 values for TCE and toluene agree very well with values for freon-12. This indicates, that diffusion is slow enough to allow adsorption sites to be filled and, hence, to allow equilibrium to be reached. Differences between the values can be ex-

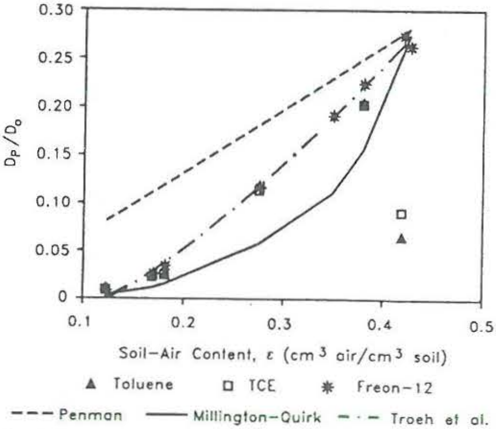

Fig. 6. Change in D_P/D_0 with volumetric soil-air content for freon-12, trichloroethylene, and toluene. The Penman model is given by $D_P/D_0 = 0.66\,\varepsilon$, the Millington-Quirk model by $D_P/D_0 = \varepsilon^{10/3}/f^2$ where f is porosity, and the Troeh et al. (1982) model by $D_P/D_0 = ((\varepsilon - u)/(1 - u))^v$, where u and v are fitting parameters.

plained by experimental errors and uncertainties in the calculation of D_0. The only exception is for the highest air content, which corresponds to air dry soil (water content of 0.03 g H_2O/g soil). The reason for the deviation may be explained by faster diffusion at this air content, and thus, lack of equilibrium. Also, K_D' values for dry soils are very high and extremely dependent on very small changes in water content, which can result in uncertainty in the K_D'. We have investigated this low end of water content, since top soils in arid areas can dry out to water contents as low and lower than this during the summer period.

The measured D_P/D_0 data were compared with three models. The Penman model ($D_P/D_0 = 0.66 \times \varepsilon$) greatly overestimates, and the Millington-Quirk model ($D_P/D_0 = \varepsilon^{10/3}/f^2$, where f is porosity) underestimates the measured data. At low air contents, the Millington-Quirk model is fairly accurate. This is in agreement with what Sallam et al. (1984) found for low air-filled porosities. The data are best fitted with the model introduced by Troeh et al. (1982),

$$\frac{D_P}{D_0} = \left(\frac{\varepsilon - u}{1 - u}\right)^v \qquad [18]$$

where u and v are fitting parameters.

The parameter u usually has a value larger than zero, which indicates that D_P reaches zero while there still is some air-filled porespace in the soil (Troeh et al., 1982). Very wet soils, for example, have a small volumetric air-content that will be in the form of isolated air pockets. D_P reaches zero because those air pockets are disconnected and the channels of diffusion therefore blocked. The ε-value where zero diffusion occurs is not universal, but for several soils it has been found to be between 0.1 and 0.2 (Wesseling and Van Wijk, 1957). The parameter v controls the curvature of the line representing the equation on a graph. Troeh et al. (1982) stated that $0 \leq u \leq 1$, $u \leq \varepsilon \leq 1$, and $1 \leq v \leq 2$. For our measured data, $u = 0.12$ and $v = 1.23$ with an R^2 of 0.997. The values for u and v are within the above limits and in agreement with what Troeh et al. (1982) found for various experimental data, over a range of soil types. For the data from 15 different studies considered by Troeh et al. (1982), u ranged between 0 and 0.15, and v between 1.1 and 2.

CONCLUSIONS

The following conclusions can be drawn from the present study:

(i) Effective diffusion of reactive tracers like TCE and toluene can be determined from relatively limited experimental work; i.e., determination of D_P/D_0–ε relations for a nonreactive tracer and measurement of K_D, K_D', and K_H values for the reactive tracers.

(ii) This approach has better accuracy at higher water contents, where the relatively slower diffusion allows adsorption sites to be filled, and where vapor/solid partitioning is small. At very low water contents the approach highly under-predicts the diffusion coefficients. This might be explained by faster diffusion, lack of equilibrium and uncertainties in the K_D' values.

(iii) For the investigated Yolo silt loam, Henry's Law is applicable for water contents higher than four molecular layers of water. Thus, for water contents greater than four molecular layers of water, retardation factors can be determined from knowledge of only K_D and K_H. For less than four layers, however, the approach is inaccurate, and K_D' should be measured.

(iv) The measured data for Yolo silt loam were fitted very well with the model that was introduced by Troeh et al. (1982), $D_P/D_0 = ((\varepsilon - u)/(1 - u))^v$. Values of u and v were determined to be 0.12 and 1.23 respectively.

ACKNOWLEDGMENTS

This research was supported by the NIEHS Superfund Basic Research Program (P42ESO4699), the Ecotoxicology Program of the University of California Toxic Substances Research and Teaching Program, the Center for Ecological Health Research (EPA-CR819659010), and the Danish Research Academy. Although the information in this document has been funded in part by the United States Environmental Protection Agency, it may not necessarily reflect the views of the Agency and no official endorsement should be inferred. A travel grant from the Japanese Ministry of Education (Monbusho International Scientific Research Program: Joint Research, no. 04044127) is gratefully acknowledged by the authors.

REFERENCES

Amali, S., L.W. Petersen, D.E. Rolston, and P. Moldrup. 1994. Modeling multicomponent volatile organic and water vapor adsorption on soils. Hazard. Mater. 36:89–108.

Armstrong, A.Q., R.E. Hodson, H.-M. Hwang, and D.L. Lewis. 1991. Environmental factors affecting toluene degradation in ground water at a hazardous waste site. Environ. Toxicol. Chem. 10:147–158.

Carter, D.L., M.M. Mortland, and W.D. Kemper. 1986. Specific surface. p. 413–423. *In* A. Klute, (ed.) Methods of soil analysis. Part 1. 2nd ed. Agron. Monogr. 9. ASA and SSSA, Madison, WI.

Chiou, C.T., and T.D. Shoup. 1985. Soil sorption of organic vapors and effects of humidity on sorptive mechanism and capacity. Environ. Sci. Technol. 19:1196–1200.

Cihacek, L.J., and J.M. Bremner. 1979. A simplified ethylene glycol monoethyl ether procedure for assessment of soil surface area. Soil Sci. Soc. Am. J. 43:821–822.

Claus, D., and N. Walker. 1964. The decomposition of toluene by soil bacteria. J. Gen. Microbiol. 36:107–122.

Currie, J.A. 1984. Gas diffusion through soil crumbs: The effects of compaction and wetting. J. Soil Sci. 35:1–10.

Eno, C.F., and H. Popenoe. 1964. Gamma radiation compared with steam and methyl bromide as a soil sterilizing agent. Soil Sci. Soc. Am. Proc. 28:533–535.

Ensley, B.D. 1991. Biochemical diversity of trichloroethylene metabolism. Annu. Rev. Microbiol. 45:283–299.

Fuller, E.N., P.D. Schettler, and J.C. Giddings. 1966. A new method for prediction of binary gas-phase diffusion coefficients. Ind. Eng. Chem. 58:19–27.

Garbarini, D.R., and L.W. Lion. 1985. Evaluation of sorptive partitioning of nonionic pollutants in closed systems by headspace analysis. Environ. Sci. Technol. 19:1122–1128.

Gee, G.W., and J.W. Bauder. 1986. Particle-size analysis. p. 383–411. *In* A. Klute (ed.) Methods of soil analysis. Part 1. 2nd ed. Agron. Monogr. 9. ASA and SSSA, Madison, WI.

Glauz, R.D., and D.E. Rolston. 1989. Optimal design of two-chamber, gas diffusion cells. Soil Sci. Soc. Am. J. 53:1619–1624.

Heilman, M.D., D.L. Carter, and C.L. Gonzalez. 1965. The ethylene glycol monoethyl ether (EGME) technique for determining soil-surface area. Soil Sci. 100:409–413.

Howard, P.H. (ed.). 1989. Handbook of environmental fate and exposure data for organic chemicals. 3rd ed. Lewis Publ., Chelsea, MI.

Jury, W.A., D. Russo, G. Streile, and H.E. Abd. 1990. Evaluation of volatilization by organic chemicals residing below the soil surface. Water Resour. Res. 26:13–20.

Livingston, H.F. 1949. The cross-sectional areas of molecules adsorbed on solid surfaces. J. Colloid Sci. 4:447–458.

McLaren, A.D., R.A. Luse, and J.J. Skujins. 1962. Sterilization of soil by irradiation and some further observations on soil enzyme activity. Soil Sci. Soc. Am. Proc. 26:371-377.

Millington, R.J., and J.M. Quirk. 1961. Permeability of porous solids. Trans. Faraday Soc. 57:1200-1207.

Nelson, D.W., and L.E. Sommers. 1982. Total carbon, organic carbon, and organic matter. *In* A.L. Page et al. (ed.) Methods of Soil Analysis. Part 2. 2nd ed. Agron. Monogr. 9. ASA and SSSA, Madison, WI.

Nelson, M.J.K., S.O. Montgomery, W.R. Mahaffey, and P.H. Pritchard. 1987. Biodegradation of trichloroethylene and involvement of an aromatic biodegradative pathway. Appl. Environ. Microbiol. 53:949-954.

Ong, S.K., and L.W. Lion. 1991a. Mechanisms for trichloroethylene vapor sorption onto soils minerals. J. Environ. Qual. 20:180-188.

Ong, S.K., and L.W. Lion. 1991b. Effects of soil properties and moisture on the sorption of trichloroethylene vapor. Water Res. 25:29-36.

Penman, H.L. 1940a. Gas and vapour movements in the soil: I. The diffusion of vapours through porous solids. J. Agric. Sci. 30:437-462.

Penman, H.L. 1940b. Gas and vapour movements in the soil: II. The diffusion of carbon dioxide through porous solids. J. Agric. Sci. 30:570-581.

Peterson, M.S., L.W. Lion, and C.A. Shoemaker. 1988. Influence of vapor-phase sorption and diffusion on the fate of trichloroethylene in an unsaturated aquifer system. Environ. Sci. Technol. 22:571-578.

Rao, P.S.C., R.A. Ogwanda, and R.D. Rhue. 1989. Adsorption of volatile organic compounds on anhydrous and hydrated sorbents: Equilibrium adsorption and energetics. Chemosphere 18:2177-2191.

Rhue, R.D., K.D. Pennell, P.S.C. Rao, and W.H. Reve. 1989. Competitive adsorption of alkylbenzene and water vapors on predominantly mineral surfaces. Chemosphere 18:1971-1986.

Sallam, A., W.A. Jury, and J. Letey. 1984. Measurement of gas diffusion coefficient under relatively low air-filled porosity. Soil Sci. Soc. Am. J. 48:3-6.

Schwarzenbach, R.P., and J. Westall. 1981. Transport of nonpolar organic compounds from surface water to groundwater: Laboratory Sorption Studies. Environ. Sci. Technol. 15:1360-1367.

Shimamura, K. 1992. Gas diffusion through compacted sands. Soil Sci. 153:274-279.

Thibodeaux, L.J., K.C. Nadler, K.T. Valsaraj, and D.D. Reible. 1991. The effect of moisture on volatile organic chemical gas-to-particle partitioning with atmospheric aerosols – competitive adsorption theory predictions. Atmos. Environ. 25A:1649-1656.

Troeh, F.R., J.D. Jabro, and D. Kirkham. 1982. Gaseous diffusion equations for porous materials. Geoderma 27:239-253.

Valsaraj, K.T., and L.J. Thibodeaux. 1988. Equilibrium adsorption of chemical vapors on surface soils, landfills and landfarms – A Review. J. Hazard. Mater. 19:79-99.

van Bavel, C.H.M. 1952. Gaseous diffusion and porosity in porous media. Soil Sci. 73:91-104.

Wesseling, J., and W.R. Van Wijk. 1957. Land drainage in relation to soil and crops. 1. Soil physical conditions in relation to drain depth. p. 461-504. *In* J.D. Luthin (ed.) Drainage of Agricultural Land. Agron. Monogr. 7. ASA, CSSA, and SSSA, Madison, WI.

Article II.

Reprinted from the *Journal of Environmental Quality*
Volume 24, no. 4, July–August 1995. Copyright © 1995, ASA, CSSA, SSSA
677 South Segoe Rd., Madison, WI 53711 USA

The Effect of Moisture and Soil Texture on the Adsorption of Organic Vapors

L. W. Petersen,* P. Moldrup, Y. H. El-Farhan, O. H. Jacobsen, T. Yamaguchi, and D. E. Rolston

ABSTRACT

The fate of volatile organic compounds (VOCs) moving as vapors in the subsurface is dependent on their interaction with the soil. Adsorption of VOC vapors is greatly influenced by soil texture and soil-water content. The effects of differences in texture and soil-water content on vapor partition coefficients for trichloroethylene (TCE) were examined. Batch experiments were conducted for a variety of soils and at different soil-water contents, w, to determine the relationship between the vapor/solid partition coefficient, K_D', and w. In dry soils, K_D' was nonlinearly related to soil-water content because, in that range, water molecules compete with VOC molecules for adsorption sites on the soil surface. Under wet conditions, K_D' became linearly related to water content according to Henry's law, indicating that adsorbed water molecules were acting as a solvent for VOC molecules. In general, K_D' under oven-dry conditions did not relate well to total specific surface area of soils, most likely because VOC molecules adsorb only on the outside surfaces of soil particles (due to their nonpolarity), rather than the total surface area present. In the dry range, adsorption was dominated by soils with high specific areas (i.e., high clay content), while soils with higher organic carbon content manifested higher adsorption amounts in the wet moisture range. A one-parameter, exponential model well described the log K_D'-w curve in the nonlinear region. The model parameter, α, was found to be highly dependent on the specific surface area of the soil. The proposed $K_D'(w)$ model incorporated in conventional VOC transport models seems promising for analyzing the effects of VOC vapor adsorption on VOC subsurface transport.

THE EXTENT of pollutant sorption on soils is greatly influenced by the physical and chemical composition of soils. Properties like soil organic matter and clay content can be directly linked to magnitudes of chemical adsorption. In addition, when VOC vapors are involved, soil water content, w, (g water/g soil) becomes another factor greatly affecting sorption. Numerical analysis by Culver et al. (1991) and Ong et al. (1992) suggested that vapor sorption onto soil minerals significantly retards the transport of VOCs under dry conditions. Thus, in modeling the transport and fate of VOC vapors, the relationship between the vapor partition coefficient and the soil water content must be fully determined to obtain correct estimates of chemical amounts adsorbed onto the soil.

In general, soil-water content defines whether clay content or organic carbon content dominate adsorption. In dry soils, surface reactivity is dominated by the clay fraction of the soil. Under oven-dry conditions, solid/vapor partition coefficients have been correlated to the specific surface area of soils and, thus, their clay content (e.g., Jurinak, 1957; Rhue et al., 1988; Ong and Lion, 1991a,b). On the other hand, under wet conditions the aqueous/solid partition coefficient has been highly correlated to the organic carbon content of a soil (e.g., Chiou et al., 1979; Ong and Lion, 1991b). Methods for predicting vapor sorption coefficients across water contents and various soil types do not exist.

The relationship between the vapor partition coefficient and water content consists of two regions: linear and

---

L.W. Petersen and O.H. Jacobsen, Danish Ministry of Ariculture, Institute of Plant and Soil Science, Research Centre Foulum, P.O. Box 23, DK-8830 Tjele, Denmark; P. Moldrup, Environmental Engineering Lab., Dep. of Civil Engineering, Aalborg Univ., Sohngaardsholmsvej 57, DK-9000 Aalborg, Denmark; Y.H. El-Farhan and D.E. Rolston, Soils and Biogeochemistry, Dep. of Land, Air, and Water Resources, Univ. of California, Davis, CA 95616, USA; and T. Yamaguchi, Dep. of Civil and Environmental Engineering, Faculty of Engineering, Hiroshima Univ., 1-4-1 Kagamiyama, Higashi-Hiroshima, 724, Japan. Received 6 June 1994. *Corresponding author (lwp@dina.foulum.min.dk).

Published in J. Environ. Qual. 24:752–759 (1995).

Abbreviations: VOC, volatile organic compound; BET, Brunauer-Emmett-Teller; EGME; Ethylene Glycol Monoethyl Ether; EPICS : Equilibrium Partitioning In Closed Systems; GC, gas chromatograph; TCE, trichloroethylene; RMSE, root mean square error.

nonlinear. The linear region occurs in the wet soil range in which dissolution of VOCs can be described by Henry's law. The nonlinear region occurs in soils at the very dry water content range. Ong and Lion (1991a, b) and Petersen et al. (1994) presented data sets for very different textured soils, illustrating this highly nonlinear behavior. It is important to note, however, that the concept of partition coefficients only applies at the low range of VOC relative vapor pressures, at which adsorption is linearly related to the vapor pressure. At high vapor pressures, the Brunauer-Emmett-Teller (BET) theory (Jurinak and Volman, 1957; Chiou and Shoup, 1985; Poe et al., 1988; Amali et al., 1994) can be used to describe the whole adsorption isotherm over the full range of relative vapor pressures.

The main objective of this work is to determine the shape of the curve relating vapor partition coefficients to soil-water content over the full range of water contents at low VOC relative vapor pressures, and to present a realistic VOC vapor adsorption model for water contents from oven-dry to saturation. The VOC used was TCE (toluene data from Petersen et al. [1994] were included in the model analysis). This work also attempts to describe how different soil fractions dominate adsorption as water contents vary.

THEORY

The aqueous/solid partition coefficient, K_D (cm^3/g), can be determined as the slope obtained from plotting the left-hand side of Eq. [1] against $M/(V_{LS} + \lambda K_H V_{GS})$ (Peterson et al., 1988). Equation [1] arises from combining mass-balance equations for bottles containing sorbent, a gas phase, and a liquid phase with bottles containing only a gas phase and a liquid phase to give

$$\frac{C_{GB}(\lambda K_H V_{GB} + V_{LB})}{C_{GS}(\lambda K_H V_{GS} + V_{LS})} = K_D \frac{M}{V_{LS} + \lambda K_H V_{GS}} + 1 \quad [1]$$

where V_{LB} and V_{GB} are liquid and gas volumes in a bottle without sorbent (cm^3), V_{LS} and V_{GS} are liquid and gas volumes in bottles with sorbent, C_{GB} and C_{GS} are headspace concentration in bottles without and with sorbent (g/cm^3), M is mass of sorbent (g), K_H is the dimensionless Henry's constant, and λ is the activity coefficient for VOC in 0.1M NaCl. NaCl is used because it adequately swamps out any ionic influences attributed to the sorbent (Gabarini and Lion, 1985). Values of λ and K_H must be determined separately. Petersen et al. (1994) determined these to be $K_H = 0.397$ cm^3 air/cm^3 H_2O and $\lambda = 1.06$ which are in agreement with the values measured by Garbarini and Lion (1985).

For linear isotherms, the solid/vapor partition coefficient, K_D'(cm^3/g), can be determined as the slope obtained from plotting the left hand side of Eq. [2] against M/V_s (Ong and Lion, 1991a, b). Equation [2] arises from equating mass balance equations for bottles with sorbent to bottles without sorbent:

$$\frac{V_B C_B}{V_S C_S} - 1 = K_D' \frac{M}{V_S} \quad [2]$$

where V_B and C_B are the gas volume and concentration in bottles without sorbent and V_S and C_S are the gas volume and concentration in bottles with sorbent. For nonlinear isotherms, the Langmuir equation is used to determine K_D' as follows (Ong and Lion, 1991a,b):

$$W = \frac{C_B V_B - C_S V_S}{M} = \frac{W^m k C_S}{1 + kC_s} \quad [3]$$

where W is amount adsorbed per mass of soil (g VOC/g soil), W^m is the monolayer capacity (g VOC/g soil), k is a constant related to the binding energy, and K_D' is given by $W^m k$ and is applicable to the linear region of the isotherm (i.e., low C_S).

MATERIALS AND METHODS

Adsorption experiments were conducted on four different soils: a coarse aquifer sand, a Yolo silt loam (fine-silty, mixed, nonacid, thermic Typic Xerorthent), a sandy loam (Ødum, Denmark) (fine-sandy, mixed, mesic, calcareous, Typic Agrudalf), and a sand (Lundgaard, Denmark) (coarse sand, mixed, mesic, Orthic Haplohumod). The soils were initially air-dried, passed through a 2.0-mm sieve (no. 10), and mixed thoroughly to obtain a homogeneous mixture. Some characteristics of the soils are given in Table 1.

Total surface area was determined by the Ethylene Glycol Monoethyl Ether (EGME) method (Heilman et al., 1965; Carter et al., 1986). Pretreatments to remove organic matter and saturation with Ca^{2+} were omitted (Cihacek and Bremner, 1979). The organic carbon content of the soils was analyzed by a modified Walkley and Black method (Nelson and Sommers, 1982). The pH was measured on saturated paste by a pH meter while electrical conductivity (EC) was measured on saturation extracts using a conductivity meter. Cation exchange capacity (CEC) was determined by saturation with barium acetate. Particle-size analysis to determine sand, silt, and clay size fractions was performed by hydrometer (Gee and Bauder, 1986) and sieve. The soil-water content corresponding to a specific amount of molecular layers of water was calculated using the total surface area determined by the EGME method, assuming that a water molecule occupies an area of 10.8×10^{-20} m^2 (Livingston, 1949).

In addition, different soils from the Danish Soil Library (#54-70) were used in this study. Characteristics for these soils are given in Hansen (1976). Specific surface areas were determined for all these soils using the EGME method, and adsorption isotherms at oven-dried conditions were determined for selected soils.

The headspace technique, Equilibrium Partitioning In Closed Systems (EPICS) (e.g., Peterson et al., 1988; Ong and Lion, 1991 a, b; Petersen et al., 1994; Amali et al., 1994) was used for determining partition coefficients. The method can briefly be described as a mass-balance technique that involves measurements by gas chromatography of the headspace vapor concentration in sealed glass bottles. A system with known gas volume and mass of sorbent is compared to a control that contains no sorbent. The sorbent masses ranged from 0.2 to 60 g. The amount of sorbent was increased for increasing water content. For each adsorption isotherm, six different

Table 1. Characteristics of the soils used in the experiments.

	Aquifer	Yolo	Ødum	Lundgaard
Surface area, m^2/g	18.7	80.6	40.1	10.84
Organic carbon, %	<0.1	1.05	1.41	1.12
pH	8.2	7.9	7.1	6.1
EC, milli-mhos/cm	0.36	0.77	0.47	0.21
CEC, meq/100g	2.3	21.1	13.97	8.78
Sand, %	94	33	57.5	80.2
Silt, %	4	49	26.4	13.2
Clay, %	2	18	13.7	4.8
Water content at four molecular layers of H_2O coverage, g H_2O/g soil	0.021	0.089	0.044	0.012

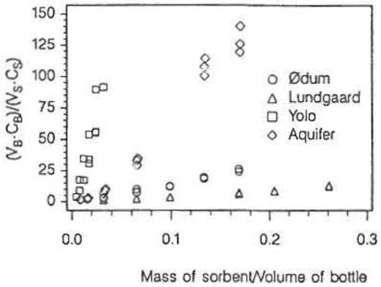

Fig. 1. Adsorption isotherms for oven-dried soils. K_D'-values were determined by fitting the measured data using Eq. [3]. V_B and C_B are the gas volume and concentration in bottles without sorbent and V_S and C_S are the gas volume and concentration in bottles with sorbent.

sorbent masses were used, with three replicates for each mass. The sorbent was introduced into amber glass bottles with a volume of 63 or 248 mL, which were then sealed with teflon Mininert valves (Dynatech, Baton Rouge, LA). A volume of 2.5 mL of air in each bottle was replaced by an equivalent volume of saturated VOC vapor. All bottles were rotated for 24 to 36 h at 25°C to reach equilibrium; earlier work showed that equilibrium was reached after this period of time (Petersen et al., 1994). One milliliter of headspace was removed from each bottle with a gas-tight syringe (Hamilton 1001, Hamilton Co., Reno, NV) and analyzed on a Hewlett-Packard 5890 gas chromatograph (GC, Hewlett Packard, Avondale, PA), equipped with a flame-ionization detector. The packed GC column was a 10 ft 20% SP-2100, 0.1% Carbovax 1500, on 100/120 mesh Supelcoport (Supelco, Inc., Bellefonte, PA), operated isothermally at 140°C.

For each of the four soils, adsorption isotherms were determined for up to 10 different water contents ranging from 0 to 21 g H_2O/g soil. Water contents less than air-dry were obtained by mixing specific amounts of oven-dry and air-dry soils. After mixing the soils were left to equilibrate. Water contents higher than air dry were obtained by spraying air-dry soil with a predetermined mass of water. After the experiments the soil-water contents were measured by weighing samples dried in an oven for 24 h at 105°C on a five digit scale.

RESULTS AND DISCUSSION

Figure 1 shows adsorption isotherms for the four different sorbents under oven-dry conditions. The shapes of the isotherms are all nonlinear, which is in agreement with what other researchers have found for oven-dry soils (e.g., Amali et al., 1994; Ong and Lion, 1991a, b). The K_D' values therefore are determined by fitting Eq. [3] to the data. Table 2 gives K_D' values for the four soils under oven-dry conditions along with K_D'-values for six different soils from the Danish Soil Library. As can be seen, there is a tremendous difference between the adsorption capacities of the 10 different soils. This might be explained by differences in texture and, hence, in specific surface area. Soil specific surface area is highly correlated to clay content, as can be seen from Fig. 2, in which surface areas, determined by the EGME method for the four soils and several soils from the Danish Soil Library, are plotted against clay size fraction. The data correlate very well ($R^2 = 0.91$) and the scatter can mainly be explained by differences in surface areas for different clay minerals. In this case it may be more correct to use a nonlinear expression since, as seen from Fig. 2, with a clay-content of 0 there is some surface area present corresponding to the silt and sand fractions.

Table 2. Vapor/solid partition coefficients K_D', under oven-dry conditions and aqueous/solid partition coefficients, K_D.

	K_D' (oven-dry)	K_D	Clay size fraction
	cm³/g	cm³/g	%
Aquifer	1464	0.52	2
Yolo	3401	0.58	18
Ødum	174.3	1.21	13.7
Lundgaard	60.8	0.69	4.8
Rønhave (58A)	2174		16.3
Askov (54C)	7246		23.2
Jyndevad (56A)	24.3		3.9
Roskilde (57D)	6579		27.6
Årslev (60A)	110.4		10.9
Silstrup (64B)	6060.6		23.5

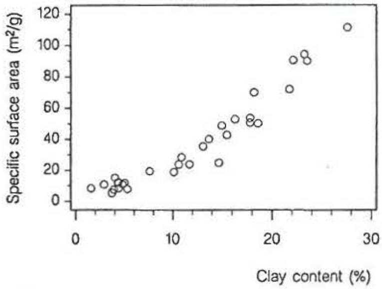

Fig. 2. Relationship between total specific surface area and clay content. The surface areas were determined by using the ethylene glycol monoethyl ether (EGME) technique.

In Fig. 3, K_D'-values for oven-dry soils are plotted against EGME surface areas. Included in the plot are K_D'-values reported by Ong and Lion (1991b). K_D'-values do not correlate well with specific surface area ($R^2 = 0.61$). Although surface area and clay size fraction is well correlated independent of the mineralogical components, the VOC sorptive affinity for different minerals may be independent of bulk surface area and dependent more on the mineralogical composition. The low correlation may also partly be explained by the fact that mainly the

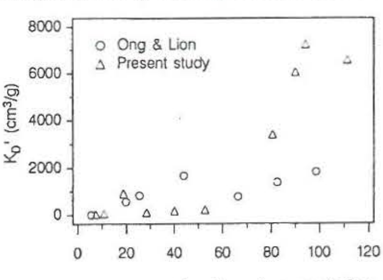

Fig. 3. Relationship between K_D'-values for oven-dry soil and total specific surface area. K_D'-values reported by Ong and Lion (1991b) and Petersen et al. (1994) are included.

external surface area of soil particles contribute to the adsorption capacity of VOC gases (Amali et al., 1994), whereas the surface areas determined in this study are total surface areas. The EGME method to determine surface area was used in the present study because of its simplicity and to be able to compare results with the measurements performed by Ong and Lion (1991a,b) since this is the only study, to our knowledge, which presents data for K_D' at oven-dry conditions and specific surface area. In conclusion we recommend that K_D'-values for oven-dried conditions be determined experimentally and not by using empirical equations relating surface area and K_D'.

In general, as water content increases, adsorption isotherms tend to take on a linear form and the adsorption capacity decreases. This is due to water molecules outcompeting VOC molecules for adsorption sites, since the former is highly polar. Figure 4 shows adsorption isotherms for Ødum sandy clay at five different water contents. The slope of the isotherms, and hence the K_D'-values, decreases with increasing water content and then stabilize at an almost constant value. This phenomenon is illustrated in Fig. 5 for all four soils. K_D' values are plotted against the numbers of molecular layers of H_2O equivalent to the different water contents used in the experiments. The solid and dashed lines are produced from Eq. [4] (Ong and Lion, 1991b; Petersen et al., 1994):

$$K_D' = \frac{K_D}{K_H} + \frac{w}{K_H \varphi \rho} \qquad [4]$$

where w is the water content by weight (g H_2O/g soil), φ is the aqueous activity coefficient (≈ 1), and ρ is the density of water ($= 1 g/cm^3$). The points at which measured K_D'-values fall on the lines indicate the applicability of Henry's law; this point seems to be located at approximately four molecular layers of water for all soils except the aquifer material. We believe that the problem with the placement of the line for the aquifer material, lies in the determination of K_D. The regression of Eq. [1] to the data only had an R^2 of 0.71 (several repetitions of the experiment did not increase the accuracy) whereas for the other soils it was close to 1. Using the EPICS method and Eq. [1] can give problems on soils with very low adsorption capacity, since experimental errors overwhelm measurable differences due to different treatments. Ong and Lion (1991a) found the applicability of Henry's law to be above approximately five molecular layers of water for TCE adsorption on a variety of minerals, and thus in agreement with our findings. K_D'-values increase slightly for water contents higher than four molecular layers. This is due to dissolution of VOC molecules in the surface-bound water, that is, the adsorbed water molecules start to act as real water when sufficient amount of layers are present. Aqueous/solid partition coefficients, K_D, used in Eq. [4], were determined at saturated moisture conditions by the EPICS method and Eq. [1]. K_D-values for the four soils are given in Table 2. K_D-values are highest for the two Danish soils, which was expected because of their higher organic carbon contents. Figure 6 shows the relation between K_D and percentage organic carbon; using results from this study together with values from Ong and Lion (1991b). The correlation is very good ($R^2 = 0.97$). The adsorptive effect of the amount of organic carbon can also be seen in Fig. 5. At very low water contents the mineral surfaces are the main contributor to the sorption capacity. The two American soils adsorb the highest

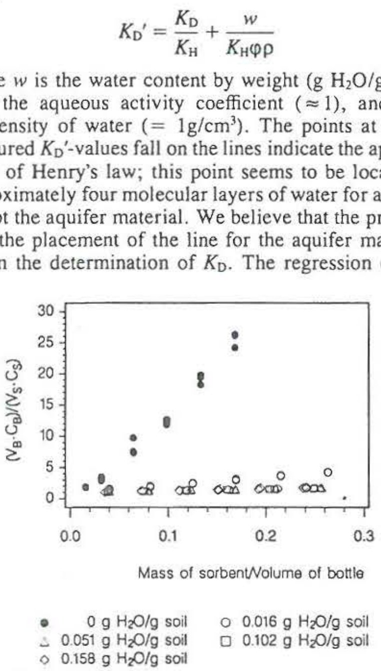

Fig. 4. Adsorption isotherms for Ødum sandy loam at five different water contents. K_D' were determined by fitting the measured data using Eq. [3].

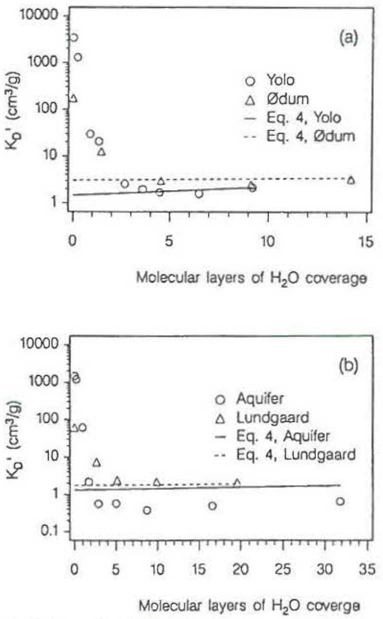

Fig. 5a-b. Relationship between K_D'-values and soil-water content expressed as number of molecular layers of water molecules adsorbed on the total specific soil surface. Values of K_D' falling on the solid and dashed lines indicates the applicability of Henry's law.

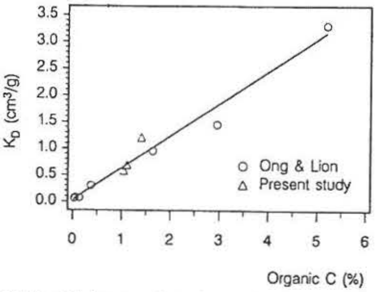

Fig. 6. Relationship between K_D and percentage organic carbon. K_D-values reported by Ong and Lion (1991b) are included. The K_D value for the aquifer material was omitted.

amounts which for the aquifer material cannot be explained by the total surface area and clay content. After only a few layers of water molecules have been adsorbed the two Danish soils with the higher amount of organic carbon adsorb the highest amount of VOC.

Petersen et al. (1994) concluded that accurate determination of K_D should be done experimentally and not from the widely used empirical equations. We suggest that a whole curve (like the one in Fig. 5) describing the K_D'-values dependency on water content can be determined by only a few experiments: First determination of total surface area to determine the water content equivalent to four molecular layers of water, and determination of K_D (aqueous/solid partition coefficient) to be used along with Eq. [4] to describe the curve for water contents higher than four molecular layers of water molecules. To describe the shape of the curve from oven-dry conditions to four molecular layers of water molecules (non-Henry-range) we have used a one-parameter, exponential model for log K_D' as a function of w, Eq. [5],

$$A = (A_0 - \beta)e^{-\alpha w} + \beta \qquad 0 \leq w \leq w_{4m} \qquad [5]$$

where $A = \log K_D'(w)$, $A_0 = \log K_D'(w = 0)$, w is water content by weight, w_{4m} is the water content at four molecular layers of water, β is a fitting parameter which also is introduced to handle possible negative log K_D' values and α is a function of β. To observe the criteria $A = A_0$ for $w = 0$ and $A = \log K_D'$ $(w = w_{4m}) = A_4$ for $w = w_{4m}$, α as a function of β is given by Eq. [6],

$$\alpha = -\frac{\ln\left[\dfrac{A_4 - \beta}{A_0 - \beta}\right]}{w_4} \qquad [6]$$

yielding

$$A = (A_0 - \beta)e^{\left(\ln\left[\frac{A_4 - \beta}{A_0 - \beta}\right]\right)\frac{w}{w_4}} \qquad [7]$$

Equation [7] can be curve-fitted to the measured $\log K_D'$-w data by finding the β-value that minimizes the root mean square error (RMSE),

$$\text{RMSE} = \sqrt{\left(\frac{1}{n}\sum_{i=1}^{n}(A_{\text{measured}} - A_{\text{estimated}})^2\right)} \qquad [8]$$

where n is number of data points.

Table 3. Result of curve-fitting Eq. [7] to the measured VOC adsorption data (K_D'-w) within the non-Henry range (water content less than four molecular layers) for the different soil types. The table shows the measured $A = \log K_D'$ values at the start ($A = A_0$) and the end ($A = A_4$) of the non-Henry range, the number of data points (n), the fitted β values, the corresponding root mean square error (RMSE) and the α values calculated from Eq. [6].

	A_0	w_{4m}†	A_4‡	n	β	RMSE	α
Yolo (TCE)	3.532	0.088	0.294	6	0.17	0.105	37.5
Yolo (toluene)§	4.336	0.092	0.549	6	0.38	0.078	34.3
Aquifer (TCE)	3.166	0.015	−0.252	5	−1.9	0.215	74.9
Ødum (TCE)	2.241	0.050	0.483	3	0.39	0	58.9
Lundgaard (TCE)	1.784	0.015	0.389	3	−0.22	0	77.3

† Chosen as the actual w value (g H_2O/g soil) closest to the estimated soil water content at four molecular layers.

‡ The log K_D' value measured at the specific water content w_{4m}.

§ Adsorption data from Petersen et al. (1994) used.

Values of β, determined by using the least square fit of Eq. [7] to the measured data, and α calculated from Eq. [6] are given in Table 3 along with the RMSE of the fit. Equation [7] gives a very close fit to the measured data. Note that α increases with decreasing surface area of the soils as expected. For Yolo loam we have included adsorption data for toluene. Data for Yolo loam were measured by Petersen et al. (1994). It is interesting to note that α-values for TCE and toluene are almost identical. Thus α seems to be independent of the nature of the VOC, which is only bound by weak van der Waals forces, and indeed dependent on the surface area of the soil. Comparisons between the α-values (Table 3) and the measured total surface areas (Table 1) show that α is related to the specific surface area of a soil in a highly linear fashion. This is illustrated in Fig. 7. With an R^2 of 0.994, α relate linearly to the specific surface area, SA, as given in Eq. [9],

$$\alpha = 84.1 - 0.585 \times SA \qquad [9]$$

Figure 8a–d show the curve-fits to measurements for TCE or toluene on three soils using Eq. [7] and [8]. As seen, the extreme increase in K_D' with decreasing soil-water content, w, is accurately represented by an exponential relationship between log K_D' and w. The suggested model (Eq. [7]) therefore seems appropriate to include in VOC transport models to analyze the effects of VOC vapor sorption onto soil minerals. We note that a simple, exponential relationship between K_D' and water

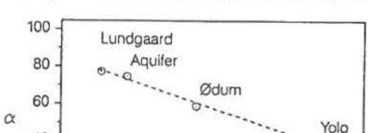

Fig. 7. Relationship between α (Eq. [5] and [6]) and specific surface area for the four soils.

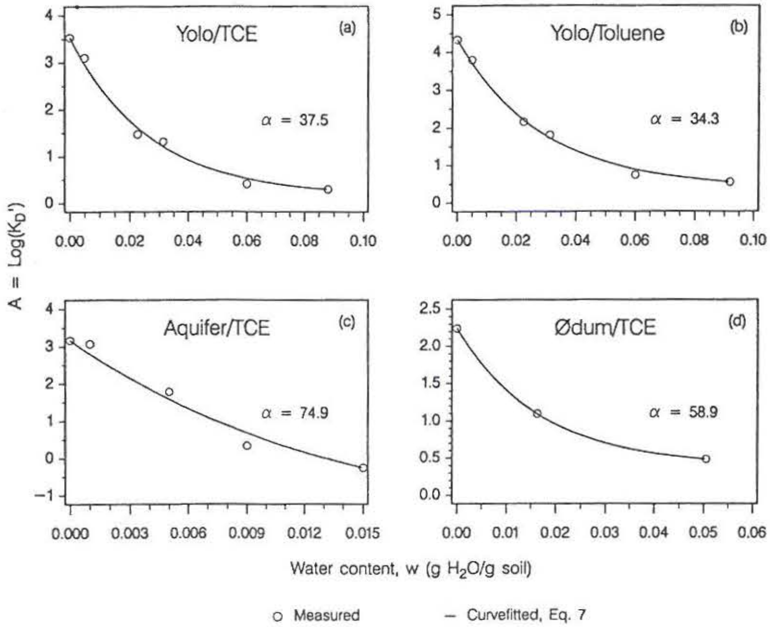

Fig. 8a–d. Examples of curve-fitting Eq. [7] to measurements of K_D'-values at different water contents. Toluene data from Petersen et al. (1994).

content within the non-Henry range as assumed in the numerical analysis of Culver et al. (1991) did not fit our data well. This relationship would indicate that the log K_D'-w curves shown in Fig. 8a–d should be straight lines which is obviously not the case. Hence, Culver et al. (1991) may have underestimated the nonlinearity of the K_D'-w relation in their calculations.

To reduce the numbers of experiments necessary to establish the K_D'-w curve in the non-Henry range we have investigated whether the K_D'-w curve could be estimated correctly from only three data sets [w; A]. The data points at $w = 0$ ($A = A_0$) and $w = w_{4m}$ ($A = A_4$) must be used (cf. Eq. [7]) along with a point at $w = w_x$ ($A = A_x$) placed somewhere in between these two target points. We have concluded that w_x should be chosen well within the non-Henry range in such a way that A_x be placed approximately between A_0 and A_4 that is, $A_x \approx 0.5\ A_0$. Since typical values of A_4 and β are negligible compared to A_0 (cf. Table 3), A_x can be expressed as $A_x \approx A_0e^{-\alpha w}$ (cf. Eq. [7]). The corresponding optimal water content at which to conduct the adsorption experiment can therefore be determined from Eq. [10],

$$w_x = \frac{\ln[0.5]}{-\alpha} \qquad [10]$$

where an estimate for α may be obtained from Eq. [9]. Applying this procedure on the Yolo silt loam data using $w_x = 0.02$ g H$_2$O/g soil (corresponding to the w value calculated from Eq. [10] and [9]) yielded nearly the same α-values (α = 43.1 for TCE and α = 35.6 for toluene) compared to fitting Eq. [7] to all six measured data points within the non-Henry range (α = 37.3 for TCE and α = 34.3 for toluene cf. Table 3).

In the above model (Eq. [5]–[7]) the point of four molecular layers coverage of water has been chosen as the matching point in agreement with the findings of Ong and Lion (1991a, b). In some applications it could be an advantage to apply a continuous function covering the whole range of soil-water contents from oven-dry conditions to saturation, instead of a two-part model.

For this purpose we suggest the model given in Eq. [11] and [12], which results in a smoother transition between the nonlinear and linear regions

$$A = (A_0 - \beta(w))e^{-\alpha w} + \beta(w) \qquad [11]$$

where

$$\beta(w) = \log\left(\frac{K_D}{K_H} + \frac{w}{K_H\varphi\rho}\right) \qquad [12]$$

For this suggested approach (Eq. [11] and [12]), physical significance is attached to the variable β(w) because it represents the aqueous/solid and vapor/aqueous components of the overall partitioning. The parameter α is still a function of the minimum $A(w)$ and the degree of curvature of the nonlinear part of the curve. The results of a sensitivity analysis using Eq. [1]) and [12] with different choices of α is given in Fig. 9a.

The model given by Eq. [11] and [12] has an disadvantage in a fitting process since many measurement points are needed to establish a good fit. For our data it was

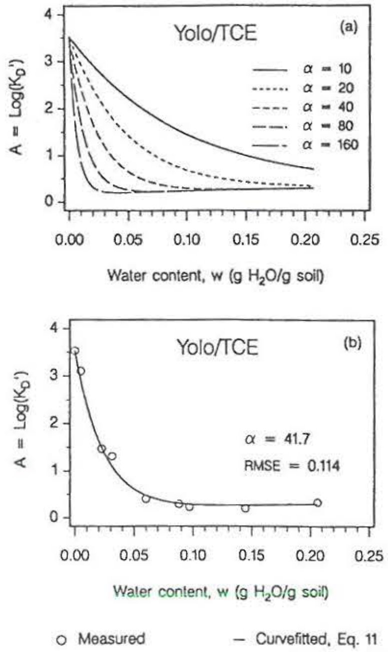

Fig. 9a-b. Alternative, continuous model for VOC vapor adsorption as function of soil-water content (Eq. [11] and [12]). (*a*) Used for sensitivity analysis to illustrate the effects of changing α values and (*b*) fitted to TCE data for Yolo silt loam. α is defined by Eq. [11], $A_0 = \log K_D'(w = 0)$, and β(*w*) is given by Eq. [12].

only possible for the TCE data on Yolo silt loam. This is illustrated in Fig. 9b. On the contrary it obviously has an advantage (no discontinuities) when used for sensitivity analysis in, for example, existing chemical transport models. Here it could be used as an easy approach to evaluate the effects of vapor/solid adsorption on chemical fate and transport.

The EPICS method used to determine the above adsorption isotherms is only valid for the relatively low vapor pressure range (Peterson et al., 1988; Ong and Lion, 1991b; Amali et al., 1994), since the K_D'-values are determined for the linear part of the adsorption isotherms. For high concentrations and hence high relative vapor pressures of VOCs, adsorption isotherms can be described by the BET-theory (e.g., Jurinak and Volman, 1957; Chiou and Shoup, 1985; Poe et al., 1988; Amali et al., 1994).

CONCLUSIONS

1. For VOC adsorption, at oven-dry conditions, K_D' does not correlate well to the total specific surface area of soils. Thus, K_D' at these conditions should be determined experimentally and not from empirical equations relating total specific surface area to K_D'.

2. Water molecules apparently start acting as a solvent to VOC molecules at water contents equal to or greater than four molecular layers, for all soils examined in this paper. Consequently, that is also the point where Henry's law becomes applicable.

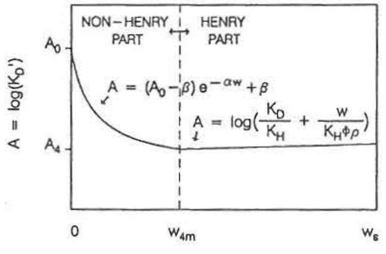

Fig. 10. Suggested two-part model concept for VOC vapor adsorption as function of soil-water content. $A_0 = \log K_D'(w = 0)$, β is a fitting parameter, α is given by Eq. [6], and w_s is the saturated soil-water content (g H_2O/g soil).

3. For the lower VOC concentration range where the partition coefficient concept is applicable, we have suggested a two-part model for $A = \log K_D'$ as function of the soil-water content (w). Part 1: An exponential, closed-form model (Eq. [7]) within the non-Henry part (water contents less than four molecular layers) where the model parameter α is shown to be highly dependent on the specific surface area of the soils. Part 2: A linear model within the Henry part according to Henry's law [yielding $A = \log [K_D / K_H + w/(K_H\ \varphi\ \rho)]$]. The two-part model concept for VOC-vapor adsorption ($\log K_D'$-w) is illustrated in Fig. 10. Inclusion of this two-part model concept and especially Eq. [7] in simulation models for VOC transport is suggested for analyzing the effects of VOC vapor sorption onto soil minerals.

4. The K_D'-w curve should be determined experimentally. This, though, can be done by relatively few experiments: 1. Determination of total specific surface area to determine the water content equivalent to four molecular layers of water. 2. Determination of K_D which along with Eq. [4] describe the curve for w higher than or equal to four molecular layers of water. 3. Determination of K_D' at oven-dry conditions, and finally 4. Determination of K_D' at one or more water contents between oven dry and four molecular layers of water. For choosing at which intermediate water content K_D' should be determined we suggest using Eq. [10].

ACKNOWLEDGMENTS

This research was supported by the Danish Ministry of Agriculture, the Danish Environmental Protection Agency, the Danish Research Academy, the NIEHS Superfund Basic Research Program (P42ESO4699), the Ecotoxicology Program of the University of California Toxic Substances Research and Teaching Program, and the USEPA (R819658) Center for Ecological Health research at Univ. of California-Davis. Although the information in this document has been funded in part by the U. S. Environmental Protection Agency, it may not necessarily reflect the views of the Agency and no official endorsement should be inferred. A travel grant from the Japanese Ministry of Education (Monbusho International Scientific

Research Program: Joint Research, no. 06044158) is gratefully acknowledged by the authors.

REFERENCES

Amali, S., L.W. Petersen, D.E. Rolston, and P. Moldrup. 1994. Modeling multicomponent volatile organic and water vapor adsorption on soils. J. Hazard. Mater. 36:89-108.

Carter, D.L., M.M. Mortland, and W.D. Kemper. 1986. Specific surface. p. 413-423. *In* A. Klute (ed.) Methods of soil analysis. Part 1. 2nd ed. Agron. Monogr. 9. ASA and SSSA, Madison, WI.

Chiou, C.T., L.J. Peters, and V.H. Freed. 1979. A physical concept of soil water equilibria for nonionic organic compounds. Science (Washington, DC) 206:831-832.

Chiou, C.T., and T.D. Shoup. 1985. Soil sorption of organic vapors and effects of humidity on sorptive mechanism and capacity. Environ. Sci. Technol. 19:1196-1200.

Cihacek, L.J., and J.M. Bremner. 1979. A simplified ethylene glycol monoethyl ether procedure for assessment of soil surface area. Soil Sci. Soc. Am. J. 43:821-822.

Culver, T.B., C.A. Shoemaker, and L.W. Lion. 1991. Impact of vapor sorption on the subsurface transport of volatile organic compounds: A numerical model and analysis. Water Resour. Res. 27:2259-2270.

Garbarini, D.R., and L.W. Lion. 1985. Evaluation of sorptive partitioning of nonionic pollutants in closed systems by headspace analysis. Environ. Sci. Technol. 19:1122-1128.

Gee, G.W., and J.W. Bauder. 1986. Particle-size analysis. p. 383-411. *In* A. Klute (ed.) Methods of soil analysis. Part 1. 2nd ed. Agron. Monogr. 9. ASA and SSSA, Madison, WI.

Hansen, L. 1976. Soil types at the Danish state experimental stations. Tidsskr. Planteavl. 80:742-758.

Heilman, M.D., D.L. Carter, and C.L. Gonzalez. 1965. The ethylene glycol monoethyl ether (EGME) technique for determining soil-surface area. Soil Sci. 100:409-413.

Jurinak, J.J. 1957. Adsorption of 1,2-dibromo-3-chloropane vapor by soils. J. Agric. Food Chem. 5:598-601.

Jurinak, J.J., and D.H. Volman. 1957. Application of the Brunauer, Emmett, and Teller equation to ethylene dibromide adsorption by soils. Soil Sci. 83:487-496.

Livingston, H.F. 1949. The cross-sectional areas of molecules adsorbed on solid surfaces. J. Colloid Sci. 4:447-458.

Nelson, D.W., and L.E. Sommers. 1982. Total carbon, organic carbon, and organic matter. p. 539-579. *In* A.L. Page (ed.) Methods of soil analysis. Part 2. 2nd ed. Agron. Monogr. 9. ASA and SSSA, Madison, WI.

Ong, S.K., and L.W. Lion. 1991a. Mechanisms for trichloroethylene vapor sorption onto soil minerals. J. Environ. Qual. 20:180-188.

Ong, S.K., and L.W. Lion. 1991b. Effects of soil properties and moisture on the sorption of trichloroethylene vapor. Water Res. 25:29-36.

Ong, S.K., T.B. Culver, L.W. Lion, and C.A. Shoemaker. 1992. Effects of soil moisture and physical-chemical properties of organic pollutants on vapor-phase transport in the vadose zone. J. Contam. Hydrol. 11:273-290.

Petersen, L.W., D.E. Rolston, P. Moldrup, and T. Yamaguchi. 1994. Volatile organic vapor diffusion and adsorption in soils. J. Environ. Qual. 23:799-805.

Peterson, M.S., L.W. Lion, and C.A. Shoemaker. 1988. Influence of vapor-phase sorption and diffusion on the fate of trichloroethylene in an unsaturated aquifer system. Environ. Sci. Technol. 22:571-578.

Poe, S.H., K.T. Valsaraj, L.J. Thibodeaux, and C. Springer. 1988. Equilibrium vapor phase adsorption of volatile organic chemicals on dry soils. J. Hazard. Mater. 19:17-32.

Rhue, R.D., P.S.C. Rao, and R.E. Smith. 1988. Vapor phase adsorption of alkylbenzenes and water on soils and clays. Chemosphere 17:727-741.

Article III.

Reprinted from the *Journal of Environmental Quality*
Volume 25, no. 5, September–October 1996, Copyright © 1996, ASA, CSSA, SSSA
677 South Segoe Rd., Madison, WI 53711 USA

Transient Diffusion, Adsorption, and Emission of Volatile Organic Vapors in Soils with Fluctuating Low Water Contents

L. W. Petersen,* Y. H. El-Farhan, P. Moldrup, D. E. Rolston, and T. Yamaguchi

ABSTRACT

Laboratory experiments were conducted on large packed soil columns (15 cm diam., 40 cm length) under unsaturated conditions. Trichloroethene (TCE) was introduced at the bottom of the columns. The emissions of TCE from the soil surface were monitored. The soil-water content at the soil surface was changed by alternating dry and water-saturated air sweeping over the column surface, thus changing the vapor sorption capacity of the soil. The retardation of VOC gas transport, due to the change in adsorption capacity with change in soil-water content, was determined by sampling the soil-air and the sweep air flushing the column headspace. Soil-water content was monitored by the time-domain reflectometry (TDR) technique. The transport of VOC gases from experiment initiation until steady-state was simulated using a numerical simulation model, in which diffusion and equilibrium partition theory were incorporated. Measured and simulated concentration profiles as well as volatilization fluxes agreed very well. The decrease in soil-water content, caused by sweeping dry air over the column surface, resulted in an increase in the soil adsorption capacity up to several orders of magnitude (mainly in the top few centimeters of soil). Both increase and decrease in soil-water content affected the volatilization flux manifested in large rapid peaks of TCE volatilizing from the surface. This behavior was likewise simulated using a numerical model with changing diffusion coefficients and retardation factors as function of soil-air content, and good agreement was obtained between model simulations and measured data.

THE PRESENCE AND PERSISTENCE of volatile organic compounds (VOCs) in soil and groundwater systems are of serious concern, due to their potential hazardous effect on human health. Accurate prediction of the movement and fate of these compounds is very complex, since many of the processes occur simultaneously, interact among themselves and have high dependency on changes in soil physical properties. Because of their volatile character, VOCs readily partition to the gas-phase and thereby increase the overall spreading of the contamination in soil. This contamination front will eventually reach the soil surface and cause emissions into the atmosphere, creating potential for human exposure. Emissions take place from industrial sites, hazardous waste treatment and disposal facilities, above shallow groundwater plumes, and anywhere the contamination might have spread due to transport in soil or migration in groundwater. Emissions of VOCs are highly dependent on their transport (especially gaseous diffusion) in the vadose zone. Emissions of chemicals have been studied for pesticides (e.g., Spencer and Cliath, 1973), and recently research has been conducted on the emissions to the atmosphere of VOCs (e.g., Drivas, 1982; Stiver and Mackay, 1984; Jury et al., 1990; Shonnard and Bell, 1993; Nye et al., 1994).

Both experimental work (e.g., Chiou et al., 1985; Chiou and Shoup, 1985; Peterson et al., 1988; Rhue et al., 1988; Ong and Lion, 1991a,b; Petersen et al., 1994, 1995a) and computer models (e.g., Culver et al., 1991; Ong et al., 1992) have shown that vapor-phase sorption in dry soils is substantially higher (several orders of magnitude) than in wet soils. This is due to the extremely high sorptive capacity of dry soil particles. This behavior will also have an impact on the emissions of VOCs to the atmosphere, since the top soil layer can become very dry, and therefore have the potential of *putting a cap* on the emission of VOCs from the soil.

The objectives of the present work are (i) to examine the effects of alternating soil-water contents on the diffusion, adsorption, and emissions of TCE in and from unsaturated soil above a liquid contamination source; (ii) to examine whether simple equilibrium partition theory, incorporated into a numerical diffusion model, can be used to describe experiments on transient transport and emission of TCE at constant and fluctuating low soil-water content; and (iii) to examine whether a layer of dry soil at the soil surface potentially can put a cap on the emissions of VOCs.

MATERIALS AND METHODS

Transient diffusion, adsorption, and emission experiments were conducted on Yolo silt loam (fine-silty, mixed, non-acid, thermic Typic Xerorthent) and a sandy loam from Ødum, Denmark (fine-sandy, mixed, mesic, calcareous, Typic Agrudalf). Some relevant characteristics of the two soils are given in Table 1. Analysis methods are described by Petersen et al. (1994, 1995a).

The experiments were conducted in a diffusion apparatus consisting of only stainless steel and polytetrafluoroethene (PTFE) to prevent the VOC from adsorbing on or diffusing through the walls. The apparatus consisted of a bottom reservoir containing pure liquid TCE and TCE vapor in air, a middle column (15 cm in diam. and 40 cm high) packed with prewetted soil, and a top chamber through which sweep-air could be flushed over the surface of the soil column (Fig. 1). Initial soil-water contents and bulk-density for the different experiments are given in Table 2. Additional columns were attached to each end of the soil column before packing. The middle part, which was expected to have the most homogeneous packing, was used in the experiments. Immediately after pack-

---

L.W. Petersen, Danish Inst. of Plant and Soil Science, Res. Center Foulum, P.O. Box 23, DK-8830 Tjele, Denmark; Y.H. El-Farhan and D.E. Rolston, Soils and Biogeochemistry, Dep. of Land, Air, and Water Resources, Univ. of California, Davis, CA 95616; P. Moldrup, Environ. Eng. Lab., Dep. of Civil Eng., Aalborg Univ., Sohngaardsholmsvej 57, DK-9000 Aalborg, Denmark; and T. Yamaguchi, Dep. of Civil and Environ. Eng., Faculty of Engineering, Hiroshima Univ., 1-4-1 Kagamiyama, Higashi-Hiroshima, 739, Japan. Received 26 June 1995. *Corresponding author (lwp@dina.foulum.min.dk).

Published in J. Environ. Qual. 25:1054–1063 (1996).

Abbreviations: VOC, volatile organic chemical; TCE, trichloroethene; TDR, time-domain reflectometry; GC, gas chromatograph.

ing, two stainless steel screens were placed at the bottom of the soil column. One was a fine-mesh screen to prevent grains from falling through (but not affecting diffusion) and the other a strong coarse-mesh screen to carry the weight of the soil. Finally, the bottom and the top chambers were attached to the column.

Thirteen mini TDR-probes were installed horizontally into the soil column at the following depths from the soil surface: 1, 2, 4, 6, 8, 10, 12, 14, 16, 20, 25, 30, and 35 cm. The probes were constructed as described in Petersen et al. (1995b), with a rod diameter, rod spacing, and rod length of 2 mm, 2 cm, and 12 cm, respectively. The only exception was the probe placed closest to the soil surface. This probe had a rod spacing of 1 cm to achieve a smaller sample volume around the probe (Petersen et al., 1995b) and thus provided the ability to measure close to the soil-surface without any influence on the measurement from the higher impedance of the air above the soil. The TDR rods were fitted with small PTFE plugs to prevent any contact between the rods and the stainless steel wall. Miniature o-rings were placed on the outside of the PTFE plugs, making a compression fit against the steel wall and thus preventing any VOC leaks around the TDR rods (Fig. 1). The TDR probes were pressed against the column wall by a plastic bar screwed into the column as indicated in Fig. 1.

Each TDR probe was calibrated individually to obtain the correct relationship between the volumetric soil-water content and the soil dielectric constant. Calibration curves were obtained by fitting measured values of the dielectric constant and the volumetric soil-water content to a third-order polynomial. These calibration curves were used along with probe-specific values of trace offset and probe length (Petersen et al., 1995b) to determine the volumetric soil-water content at each depth as a function of time.

The TDR measurements were done automatically using a Tektronix 1502B cable tester (Tektronix Inc., Beaverton, OR) equipped with an RS 232 computer interface (Tektronix model SP232 option port module) and connected to a Tektronix TSS 45, 13 port relay scanner, a control box, and a personal computer (Fig. 1). Software for controlling the total TDR system and collecting and analyzing TDR traces is described by Thomsen and Thomsen (1994), Thomsen (1994), and Petersen et al. (1995b). The TDR measurements were taken once every hour.

Gas samples could be obtained at the outlet of the top sweep-air chamber and at 13 locations in the soil column. In the top chamber, a Mininert (Dynatech, Baton Rouge, LA) PTFE sampling valve was screwed directly into a specially made, stainless-steel fitting, thus allowing for gas sampling. In the soil column, the same principle was used along with 3 cm long needles that were introduced into the column after packing (Fig. 1). Before installment, a metal wire was placed inside the needle to prevent clogging during the installment. The Mininert provided a compression fit onto the needle and thus prevented any leakage. The needles were placed in the soil column at the same depths as, but in a 90 degree angle from, the TDR probes. During gas sampling, 25 μL of gas was removed from each sampling valve. Since gas samples were only 25 μL out of a total vapor phase in the column of approximately 3 L, convective flow of gas due to sampling was not likely to be induced. Gas samples were analyzed on a Varian 3000 Series gas chromatograph equipped with a flame ionization detector (FID). The packed GC column was a 3 m (10 ft) 20% SP-2100, 0.1% Carbowax 1500, on 100/120 mesh Supelcoport (Supelco Inc.), operated isothermally at 140°C with N_2 as the carrier gas.

The experiments were initiated by separating the bottom chamber from the apparatus by a stainless steel/PTFE piston (Fig. 1). The liquid TCE was introduced into the bottom reservoir and left to equilibrate for approximately 20 min. At time zero, the piston was pulled back and diffusion through the soil column initiated. Simultaneously, a constant flow of air was swept over the soil surface through the top flow chamber. The flow was controlled by an ADC air supply unit with mass flowmeter (Analytical Development Co. Ltd., Herts, UK) that adequately swept away TCE emissions from the soil surface. The flow rate was kept constant at 400 mL $\min^{-1}$ and 350 mL $\min^{-1}$ for experiments on Yolo silt loam and Ødum sandy loam, respectively, replacing the air of the flow chamber every few minutes. The relative humidity of the sweep air was alternated between 100 and 0% (measured with a Testo 610 Hygrometer, Buhl & Bønsøe A/S, Denmark) by either bubbling it through four bottles of distilled water or passing the sweep air through bottles containing silica gel.

Table 1. Characteristics of the soils used in the experiments. Analysis methods are described by Petersen et al. (1994, 1995a).

Characteristic	Yolo	Ødum
Surface area, $m^2\ g^{-1}$	80.6	40.1
Organic carbon, %	1.05	1.41
pH	7.9	7.1
EC, milli-mhos cm^{-1}	0.77	0.47
CEC, meq 100 g^{-1}	21.1	13.97
Sand, %	33	57.5
Silt, %	49	26.4
Clay, %	18	13.7
Four molecular layers of H_2O, g H_2O g^{-1} soil	0.089	0.044

The course of the experiments was divided into three periods: *Period I*, which covers from the start of the experiment until the concentration profile was at steady-state – during this period the relative humidity of the sweep air was kept constant at 100%; *Period II* (drying), in which the relative humidity of the sweep air was changed to 0% and kept constant; and *Period III* (wetting), in which the relative humidity of the sweep air was changed to 100% and kept constant.

Adsorption isotherms, and partition coefficients at different soil-water contents for the two soils are presented in Petersen et al. (1994, 1995a) and will not be discussed here.

THEORY

Under conditions where the VOC is only a small fraction in the VOC-air mixture, Ficks 2nd law can be used to describe diffusion (Amali and Rolston, 1993). Very high relative vapor pressure of TCE was only present in the vicinity of the bottom chamber containing liquid TCE. Baehr and Bruell (1990) did not observe any significant deviation from Ficks law when ternary systems containing one VOC diffused in a stagnant mixture of O_2 and N_2. Therefore, in this study, Ficks law was thought to be applicable to describe diffusion in favor of the Stefan-Maxwell equations. Also the soil-gas diffusivity, D_P (cm^3 soil air cm^{-1} soil $\min^{-1}$), can be assumed to be independent of the gas concentration, C (g VOC cm^{-3} air). Hence, the unsteady gaseous diffusion with dissolution and sorption in soils, under steady state water regime corresponding to Period I of the experiments, is given by

$$\varepsilon \frac{\partial C}{\partial t} = D_P \frac{\partial^2 C}{\partial x^2} - \frac{\partial S_W}{\partial t} - \frac{\partial S_S}{\partial t} \qquad [1]$$

where ε is the volumetric soil-air content (cm^3 air cm^{-3} soil), x is distance (cm), t is time (min), S_W is amount of VOC-vapor dissolved in water (g VOC cm^{-3} soil), and S_S is amount of

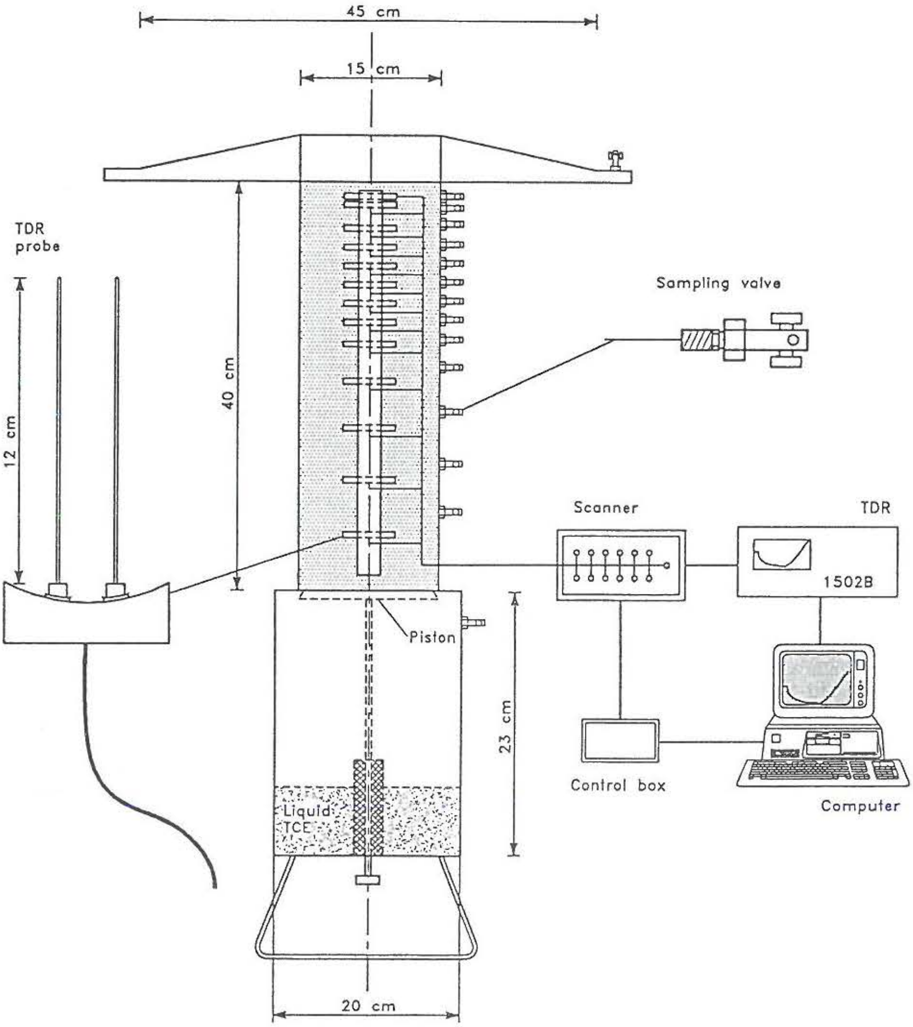

Fig. 1. Experimental apparatus. The middle compartment was packed with soil. TDR probes and PTFE Mininerts were installed for measurement of volumetric soil-water content and gas sampling, respectively. The bottom compartment was filled with liquid TCE maintaining a constant concentration boundary. Through the top-compartment air swept through maintaining a zero concentration boundary. TDR measurements were done automatically with a computer-controlled multiplexing system.

VOC-vapor adsorbed to soil solids (g VOC cm^{-3} soil). For high soil-water contents, w (higher than four molecular layers) (Petersen et al., 1994, 1995a), dissolution of VOCs can be described by Henry's Law (Eq. [2]), which governs the equilibrium distribution of the VOC between aqueous and vapor phase

$$C = K_H C_{AQ} \qquad [2]$$

where C_{AQ} is the VOC concentration in the aqueous phase, and K_H is the dimensionless Henry's constant (0.397 for TCE; Petersen et al., 1994), yielding

$$S_W = \frac{C\theta}{K_H} \qquad [3]$$

where θ is the volumetric soil-water content (cm^3 H_2O cm^{-3} soil).

Under the same assumptions, and neglecting adsorption kinetics, the sorption of dissolved VOCs onto soil particles can be described by the aqueous/solid partition coefficient, K_D (cm^3 g^{-1}), yielding

$$S_S = K_D \frac{C}{K_H} \rho_b \qquad [4]$$

where ρ_b is the soil bulk density (g soil cm^{-3} soil). Taking the derivatives of S_W and S_S with respect to time and substituting into Eq. [1] gives

Table 2. Initial soil-water and soil-air contents and dry bulk density in packed columns. Calculated number of molecular layers of water correspond to the initial soil-water content.

Soil type	Yolo	Ødum
Soil-water content, g H_2O g^{-1} soil	0.074	0.1187
Dry bulk density, g soil cm^{-3} soil	1.3	1.4
Soil-air content, cm^3 air cm^{-3} soil	0.4132	0.3027
Initial number of molecular layers of H_2O	3.3	10.7

$$R\,\varepsilon \frac{\partial C}{\partial t} = D_P \frac{\partial^2 C}{\partial x^2} \qquad [5]$$

where R is the retardation factor and is given by

$$R = 1 + \frac{\theta}{\varepsilon K_H} + \frac{\rho_b K_D}{\varepsilon K_H} \qquad [6]$$

For low soil-water contents (<4 molecular layers of H_2O) the adsorption capacity of soils increases drastically (Ong and Lion, 1991a,b; Petersen et al., 1994, 1995a), and Henry's Law is no longer valid. Thus, the adsorption/dissolution should instead be described by applying the solid/vapor partition coefficient K'_D (cm^3 g^{-1}), yielding

$$S_S + S_W = K'_D\, C\, \rho_b \qquad [7]$$

Using the same procedure as above, the retardation factor for this case can be described as

$$R = 1 + \frac{K'_D\, \rho_b}{\varepsilon} \qquad [8]$$

It is assumed that sorption will be linear. This assumption is correct for low relative vapor pressures. Also, above relative humidities (RH) of 0.5, sorption isotherms for VOCs are linear when their relative vapor pressures are less than 0.5 (Chiou and Shoup, 1985). Since relative vapor pressures were very high only at the bottom of the soil column where also RH was constantly high the assumption of linear isotherms will only introduce minor errors.

For the conditions of the experimental apparatus given schematically by Fig. 2, the following transport equations apply

$$R\,\varepsilon \frac{\partial C}{\partial t} = D_P \frac{\partial^2 C}{\partial x^2} \qquad x_1 \le x \le x_2 \qquad [9a]$$

$$\frac{\partial C}{\partial t} = D_0 \frac{\partial^2 C}{\partial x^2} \qquad 0 \le x \le x_1, x_2 \le x \le x_3 \qquad [9b]$$

where D_0 is the gaseous diffusion coefficient in free air (cm^2 min^{-1}) and with the initial and boundary conditions as follows.

Initial Conditions

Liquid TCE was introduced to the inlet chamber with the surface of the liquid TCE being at $x = x_3$ and $t = -t_1$ with the soil column isolated from the bottom TCE reservoir using a piston mechanism (see the Materials and Methods section). After a period of time ($t = t_1$) passed, the piston was slowly pulled back from the soil surface ($t = 0$) and the experiment initiated. Some mixing of the VOC vapor might have occured during movement of the piston. This will influence the concentration profile only at very early times. The vapor concentration as a function of distance within the bottom chamber was calculated according to Eq. [9b] for the period $t_1 < t < 0$ as well as for the period $t > 0$. The initial conditions can be represented mathematically by

$$C(x,-t_1) = 0 \qquad \text{for all } x \qquad [10a]$$

$$C(x,0) = 0 \qquad 0 \le x < x_2 \qquad [10b]$$

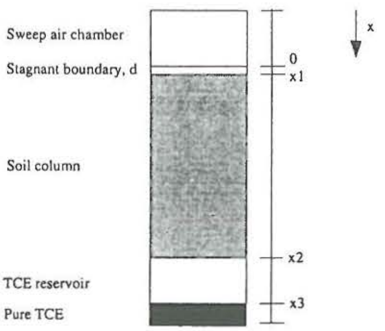

Fig. 2. Schematic of initial and boundary conditions for the diffusion apparatus.

$$C(x,0) = f(x) \qquad x_2 \le x < x_3 \qquad [10c]$$

where Eq. [10c] represents the vapor concentration profile within the TCE reservoir at $t = 0$.

Boundary Conditions

$$C(0,t) = 0 \qquad [11a]$$

$$C(x_3,t) = C_0 \qquad [11b]$$

$$-D_0 \frac{\partial C}{\partial x} = -D_p \frac{\partial C}{\partial x} \qquad x = x_1 \text{ and } x = x_2 \qquad [11c]$$

where C_0 is the vapor concentration of TCE at the surface of the liquid TCE.

VOC Diffusion and Adsorption during Unsteady Water Regime

During unsteady water regime, corresponding to Period II and III, the retardation factor and the volumetric soil-air content are changing with time. Likewise, the soil-gas diffusivity is varying in space. Therefore, the following transport equation applies instead of Eq. [9a] during Period II and III:

$$\frac{\partial}{\partial t}(\varepsilon R C) = \frac{\partial}{\partial x}\left(D_p \frac{\partial C}{\partial x}\right) \qquad [12]$$

For Yolo loam, the soil-gas diffusivity function, $D_P(\varepsilon)$, could be determined from the relationship given in Eq. [13] (Troeh et al., 1982; Petersen et al., 1994), which was established specifically for this soil.

$$D_P = D_0 \left(\frac{\varepsilon - 0.12}{1 - 0.12}\right)^{1.23} \qquad [13]$$

The value of the diffusion coefficient in free air, D_0, was calculated using the Fuller correlation (Fuller et al., 1966) to

Table 3. Parameter values used in Eq. [14] and [15]. Values are from Petersen et al. (1995a); details on the determination of the parameters can be found herein.

Parameter	Yolo silt loam	Ødum sandy loam
A_0	3.532	2.241
A_4	0.294	0.483
α	37.5	58.9
β	0.17	0.39
w_4†	0.088	0.050

† Chosen as the actual w value (g H_2O g^{-1} soil) closest to the estimated soil-water content at four molecular layers (Petersen et al., 1995a).

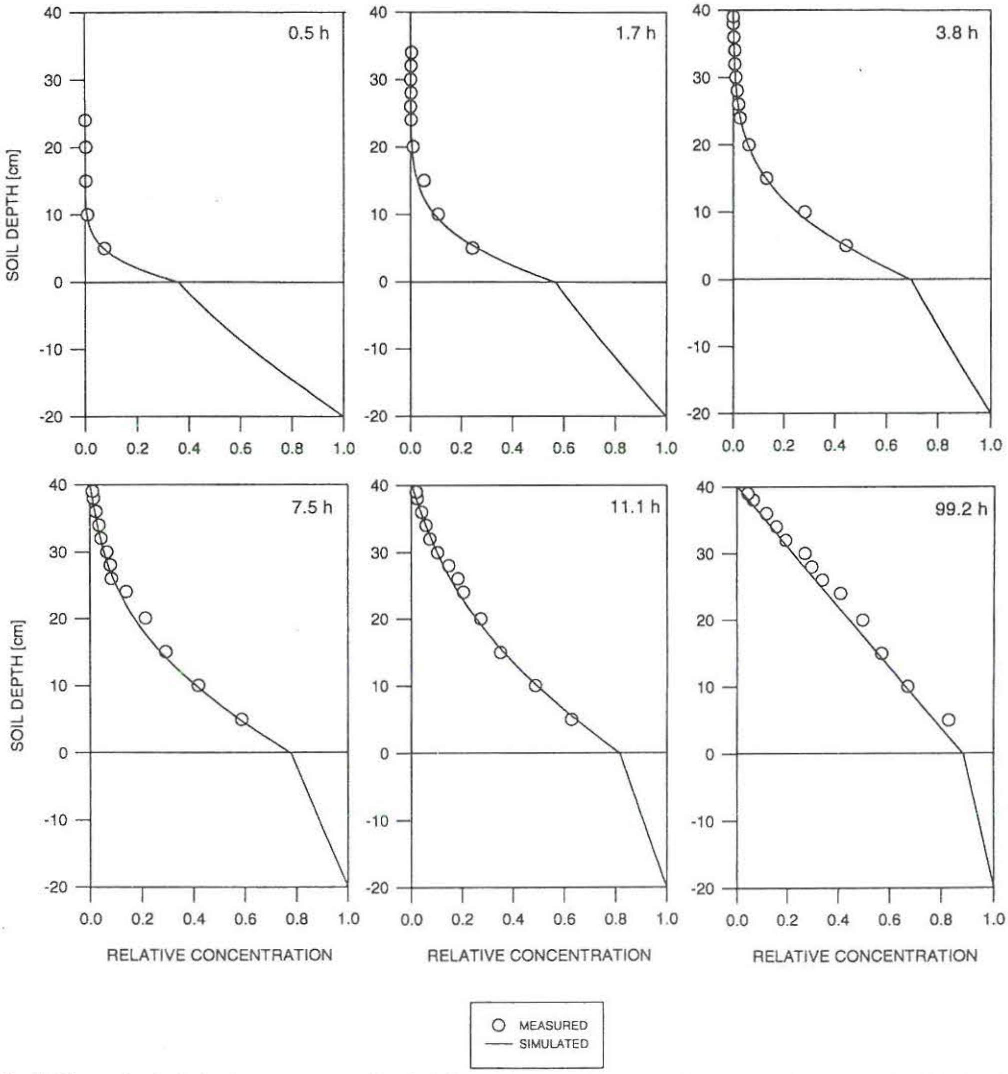

Fig. 3. Measured and simulated concentration profiles for TCE transport, in Yolo silt loam, from start of the experiment until steady-state (Period I). The sweep-gas was kept with a constant relative humidity of 100% to prevent evaporation and thus drying of the soil surface. The depths −20 to 0 cm (below the solid horizontal line) represent the bottom VOC chamber. Depths 0 to 40 cm is the soil column.

give 0.0835 $cm^2\ s^{-1}$ for TCE (at 25°C). For the Ødum sandy loam, a D_P value was determined from the transient flux data (Fig. 5b). This value agreed well with the D_P value predicted from Eq. [13]; thus, Eq. [13] was also used for calculating D_P for this soil.

The change in TCE retardation and thus in K'_D with changing soil-water content is predicted by applying Eq. [14] and [15] (Petersen et al., 1995a) for soil-water contents less than the equivalent of four molecular layers of water as follows

$$A = (A_0 - \beta)\, e^{-\alpha w} + \beta \quad (0 \le w \le w_4) \qquad [14]$$

where $A = \log K'_D(w)$, $A_0 = \log K'_D(w = 0)$, w is water content by weight, w_4 is the water content at four molecular layers of water, β is a fitting parameter, and α as a function of β is given by

$$\alpha = \frac{\ln\left(\dfrac{A_4 - \beta}{A_0 - \beta}\right)}{w_4} \qquad [15]$$

where α is a constant related to the specific surface area of

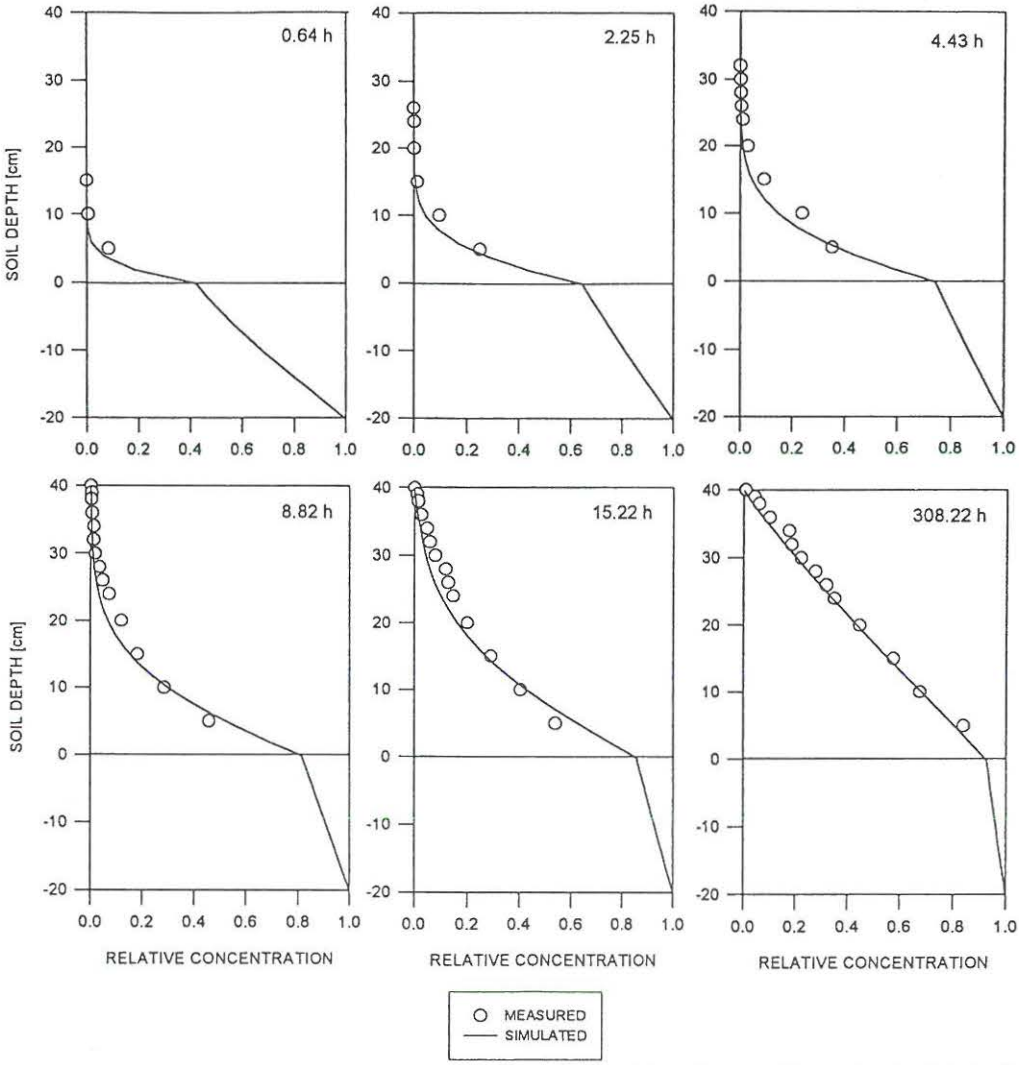

Fig. 4. Measured and simulated concentration profiles for TCE transport, in Ødum sandy loam, from start of the experiment until steady-state (Period I). The sweep-gas was kept with a constant relative humidity of 100% to prevent evaporation and thus drying of the soil surface. The depths −20 to 0 cm (below the solid horizontal line) represent the bottom VOC chamber. Depths 0 to 40 cm is the soil column.

the soil, and $A_4 = \log K'_D(w_4)$. Values of A_0, A_4, α, β, and w_4 for TCE adsorption onto Yolo silt loam and Ødum sandy loam were determined by Petersen et al. (1995a) and are given in Table 3. For soil-water contents higher than four molecular layers, Eq. [16] is used instead to determine K'_D as a function of w

$$K'_D = \frac{K_D}{K_H} + \frac{w}{K_H \varphi \rho} \qquad [16]$$

where φ is the aqueous activity coefficient (= 1), and ρ is the density of water (= 1 g cm^{-3}).

RESULTS AND DISCUSSION

Period I: From Start until Steady-State

The concentration profiles along the soil column at different times after the start of the experiment and until steady-state are given in Fig. 3 and 4 for Yolo silt loam and Ødum sandy loam, respectively. The profile reached steady state relatively fast where the concentrations increased linearly toward the TCE reservoir. During this period the soil-water content was constant with depth.

The transport and retardation of TCE can be simulated numerically by discretizing Eq. [9a,b]. The Crank-Nicholson Finite Difference method was used to solve the equations for the three regions – (i) TCE vapor reservoir; (ii) soil; (iii) the stagnant air boundary layer – with the continuity of flux condition enforced at each interface between the different regions. Depth increments used were 0.1 cm and time increments were adjusted to maintain mass balance (typically 0.001-5 min). No model parameters were fitted; instead, all were taken from related studies (Petersen et al., 1994, 1995a).

Results of the numerical simulations are shown by the solid lines in Fig. 3 and 4. For Yolo silt loam, the soil was initially dryer than what is equivalent to four molecular layers; hence, the retardation factor (R) was determined by Eq. [8] using a K_b' value of 2.147 cm^3 g^{-1} (from Eq. [14]). The air-filled porosity for Yolo silt loam was fairly high (see Table 2). Thus, the diffusion was fast compared with Ødum sandy loam, and equilibrium was therefore reached sooner. In general, measured and simulated values agree extremely well with slightly more noise in the data for the Ødum sandy loam. This may be attributed to the smaller air-filled porosity in this soil due to its high water content causing the accuracy of soil-air sampling to decrease.

The amount of VOC lost by emission from the soil compartment can be simulated by assuming that the gas escapes by molecular diffusion in the gaseous phase through a stagnant air layer, d, at the soil surface. Assuming that the concentration above the stagnant layer is zero, the volatilization flux, q (g VOC cm^{-2} soil min^{-1}), can be calculated using Eq. [17]

$$q = D_0 \frac{C_{x=dx}}{dx} \qquad [17]$$

where $C_{x=dx}$ is the concentration of VOC at a distance dx from the top of the stagnant air layer. The distance dx is smaller than d, where d is the thickness of the stagnant boundary layer. A value of 0.1 cm (equivalent to the general depth increment used in the simulations) was used for dx for the determination of the flux in Eq. [17]. A value of $d = 0.475$ cm was used in the simulations (Jury et al., 1990). Sensitivity analysis showed that the simulated emission was virtually unaffected by changing d between 0.2 and 1.0 cm.

The measured flux of TCE from the soil surface was determined using Eq. [18]

$$q = \frac{CQ}{A_s} \qquad [18]$$

where C is the TCE concentration in the outlet sweep air (g VOC cm^{-3} air), Q is the sweep-air flow rate (cm^3 air s^{-1}), and A_s is the cross sectional area of the soil-column surface (cm^2). Measured and simulated volatilization fluxes from the start of the experiments until steady state was reached are shown in Fig. 5a and 5b for both soils. Measured and simulated fluxes agreed very well, indicating that simple partition theory can be applied to describe gaseous diffusion and emission of VOC in these experiments.

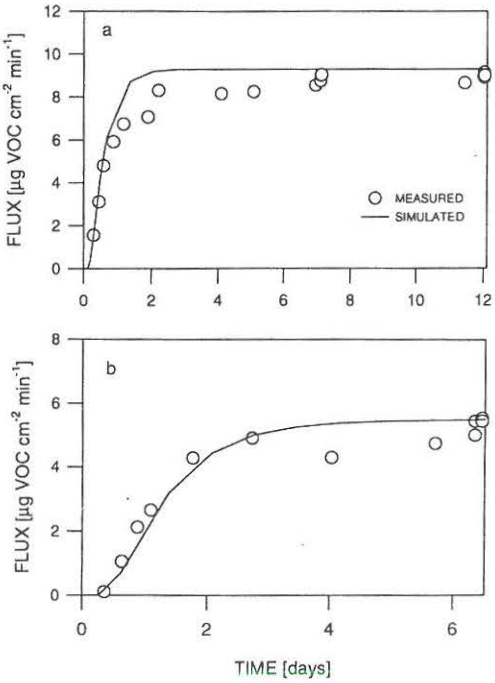

Fig. 5. Measured and simulated volatilization fluxes for (*a*) Yolo silt loam, and (*b*) Ødum sandy loam. From start of the experiment until steady state (Period I).

Periods II and III: Drying and Wetting

After steady-state was reached, the relative humidity of the sweep air was changed to 0% RH (Period II). The change in soil-water content with time at selected depths (measured with TDR) is shown in Fig. 6 and 7. The predicted increase in adsorption capacity (K_b') due to the decrease in soil-water content (molecular layers of water) is shown in the same figures.

The increase in adsorption capacity was very pronounced in the top 1 cm of the soil columns, especially for Yolo silt loam. The lowest soil-water contents obtained for Yolo silt loam and Ødum sandy loam was equivalent to 0.22 and 0.88 molecular layers of water, respectively. If the soils simultaneously had been influenced by increased temperature and all water molecules removed (even chemically bonded water), K_b' would increase to 3401 and 174 cm^3 g^{-1} for Yolo silt loam and Ødum sandy loam, respectively (Petersen et al., 1995a). One would expect this phenomenon to greatly restrict the volatilization from the soil compartment and into the atmosphere. Hence, even a few millimeters of soil could store large amounts of adsorbed VOC gases, which would be released as soon as water molecules were reintroduced to the soil surface (represented here in Period III by sweeping air with RH 100% over the soil surface after the drying period). Figure 8 shows the

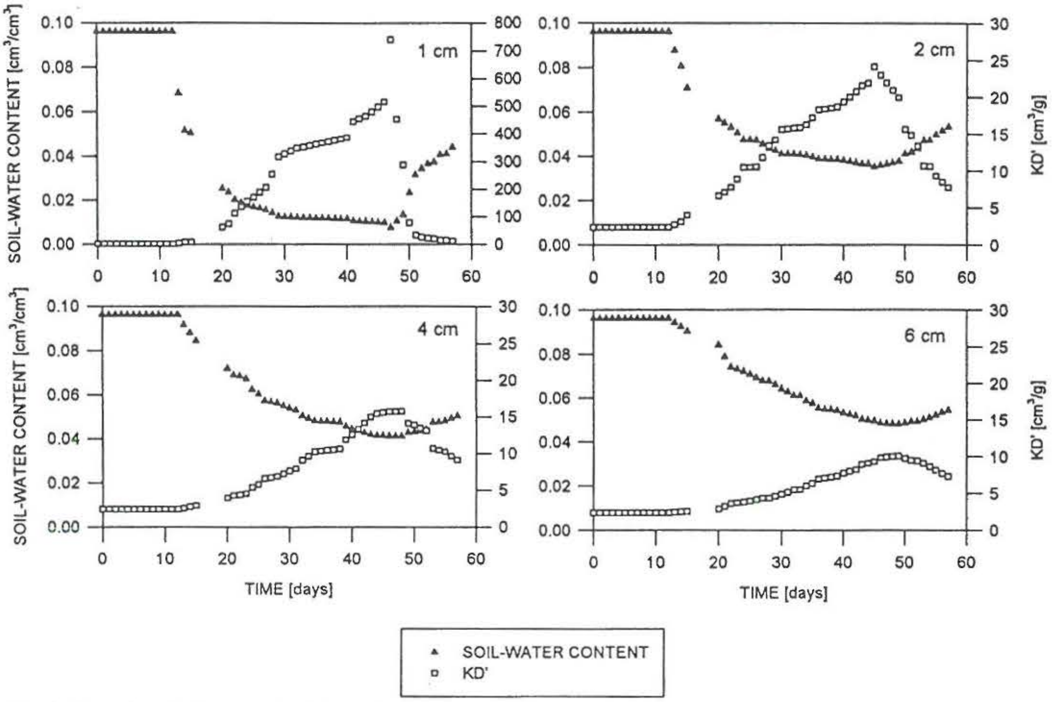

Fig. 6. Change in soil-water content and K_D' for Yolo silt loam in four depths as a function of time after start of the experiment. Note the different *y*-axis for the 1-cm depth.

response in volatilization fluxes for the two different soils due to the decrease in soil-water content (Fig. 6 and 7), obtained by sweeping dry air over the soil surface, and hence an increase in adsorption capacity. Also, the figures show the response to the later increase in soil-water content. The decreased soil-water content did not seem to have the expected effect of decreasing the volatilization fluxes. Immediately after drying was initiated, the volatilization flux increased in a rapid peak. This phenomenon may be explained by the fact that the water that immediately started to evaporate contained dissolved VOC. This led to a sudden increase in VOC concentration in the liquid phase which, by Henry's partitioning, would have resulted in a corresponding increase in VOC concen-

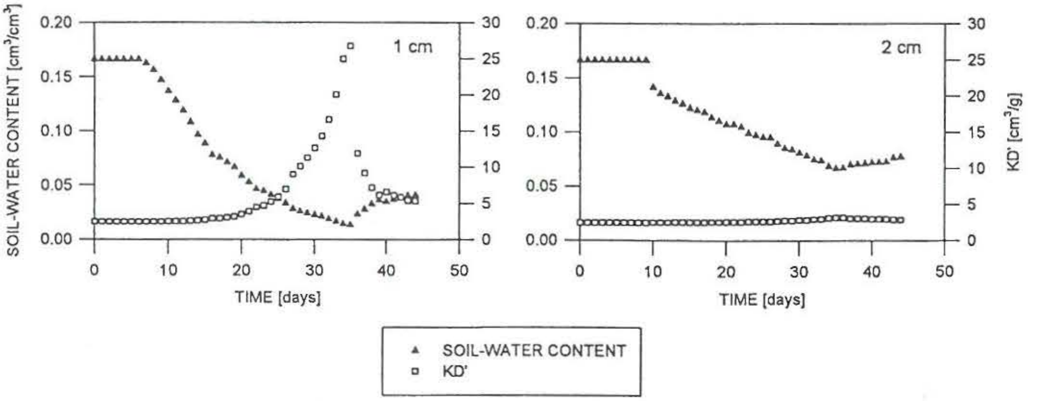

Fig. 7. Change in soil-water content and K_D' for Ødum sandy loam in two depths as a function of time after start of the experiment.

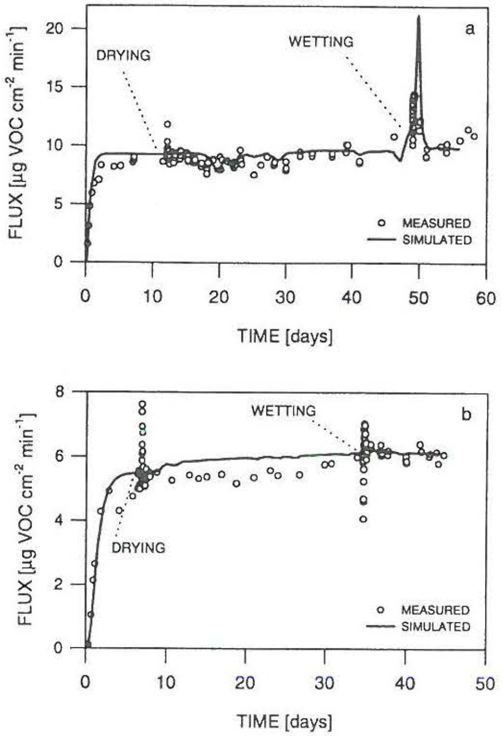

Fig. 8. Response in volatilization flux due to drying (Period II) and wetting (Period III) as a function of time for (*a*) Yolo silt loam and (*b*) Ødum sandy loam. The lines show the simulated volatilization fluxes.

tration in the gas phase. This effect was especially pronounced in the Ødum sandy loam, which had the higher water content, and hence more VOC mass in the liquid before the initiation of drying.

Despite the large decrease in soil-water content and consequently the increase in adsorption capacity during the drying period, the soil mineral adsorption did not seem to restrict the volatilization flux. This could be explained by the fact that the constant, very high flux of gaseous VOCs from the bottom of the soil column constantly maintained all adsorption sites occupied. Evidently, the increase in the adsorption capacity was gradual enough that it did not decrease the volatilization flux significantly. Even though K'_D was increasing, so was the flux, q (since the air-filled porosity and therefore D_P was increasing). It seems that the relative increase in q was more than enough to overwhelm the gradual increase in the adsorption capacity. Overall, the flux kept gradually increasing. The situation is analogous for example to a leaky container of VOC, buried relatively close to the soil surface. This is, however, in contrast to situations where the source of contamination is deep under the soil surface and concentrations at the surface are quite low. For these conditions, we suggest that the top few millimeters of soil, in periods when the soil-water content is low and adsorption capacity is high, may still temporarily restrict the volatilization flux of VOCs to the atmosphere.

When rewetting was initiated (Period III), the volatilization flux again increased drastically for both soils and especially for Yolo silt loam (Fig. 8a,b), which was expected since the adsorption capacity had increased greatly during the drying cycle (Fig. 6 and 7). This behavior is a reflection of water molecules out competing the VOC molecules sorbed on soil particle surfaces. We cannot explain the sudden decrease in the volatilization flux that occur for the experiment on Ødum loam. After the initial peak resulting from wetting, the fluxes remained at a higher level than during Period II. This might be due to the water molecules slowly penetrating the dry soil and desorbing VOC molecules from adsorption sites. The rapid peak observed during this stage emphasizes the importance of knowing changes in soil-water contents when studying emissions. To quantify the maximum VOC emissions from a soil surface, two- or threefold error in the prediction may occur if measurements were made with disregard to sudden changes in soil-water contents (for example such changes may occur in the morning where the soil surface dries out or evenings when water vapor condenses on the soil surface).

Figure 8 also shows simulations of the emissions of TCE during period II and III. In these simulations, it is taken into account that D_P becomes a variable since ε is changing with time and D_P is a function of ε. For this purpose soil-water contents measured with the TDR were read into the numerical model, and, using linear interpolation, soil-water contents were determined for each time step, which consequently allowed for the explicit determination of D_P, R, and ε throughout the simulation. For both soils, the second peak resulting from wetting is predicted by the model whereas the first peak is not predicted for any of the soils. For the Ødum soil the simulated second peak is smaller than the measured. As discussed, the first peak must be caused by other physical phenomena than those incorporated into the numerical model. In general, measured and simulated volatilization fluxes agree well for the whole duration of the experiment.

CONCLUSIONS

The transient diffusive transport and volatilization fluxes of gaseous VOCs could be described well by applying simple partitioning theory. Simulations of gaseous emissions were not highly dependent on the size of the stagnant boundary layer.

Theoretically, a decrease in soil-water content should greatly increase the adsorption capacity of the soil. When decreasing the soil-water content in the experiments, the increased adsorption capacity had some effect on the volatilization flux, but not as much as expected. This may partly be explained by the fact that a constant high flux of VOC vapor from the source of contamination was maintaining all adsorption sites occupied.

Measurements of VOC emissions are extremely dependent on soil-water contents. Full knowledge of fluctuations in soil-water content can be critical for measuring emissions correctly. A sudden increase in soil-water content can cause a sharp increase in VOC emissions that may be overlooked if the measurements were not concurrent to the soil-water changes.

ACKNOWLEDGMENTS

This research was supported by the Danish Ministry of Agriculture and Fisheries, the Danish Environmental Protection Agency, the Danish Research Academy, the NIEHS Superfund Basic Research Program (P42ES04699), the Ecotoxicology Program of the University of California Toxic Substances Research and Teaching Program, and the USEPA (R819658) Center for Ecological Health research at U.C. Davis. Although the information in this document has been funded in part by the USEPA, it may not necessarily reflect the views of the Agency and no official endorsement should be inferred. A travel grant from the Japanese Ministry of Education (Monbusho International Scientific Research Program: Joint research, no. 06044158) is gratefully acknowledged by the authors.

REFERENCES

Amali, S., and D.E. Rolston. 1993. Theoretical investigation of multicomponent volatile organic vapor diffsuion, steady-state fluxes. J. Environ. Qual. 22:825-831.

Baehr, A.L., and C.L. Bruell. 1990. Application of the Stefan-Maxwell equations to determine limitations of Fick's Law when modeling organic vapor transport in sand columns.

Chiou, C.T., and T.D. Shoup. 1985. Soil sorption of organic vapors and effects of humidity on sorptive mechanism and capacity. Environ. Sci. Technol. 19:1196-1200.

Chiou, C.T., T.D. Shoup, and P.E. Porter. 1985. Mechanistic roles of soil humus and minerals in the sorption of nonionic organic compounds from aqueous and organic solutions. Org. Geochem. 8:9-14.

Culver, T.B., C.A. Shoemaker, and L.W. Lion. 1991. Impact of vapor sorption on the subsurface transport of volatile organic compounds: A numerical model and analysis. Water Resour. Res. 27:2259-2270.

Drivas, P.J. 1982. Calculation of evaporative emissions from multicomponent liquid spills. Environ. Sci. Technol. 16:726-728.

Fuller, E.N., P.D. Schettler, and J.C. Giddings. 1966. A new method for prediction of binary gas-phase diffusion coefficients. Ind. Eng. Chem. 58:19-27.

Jury, W.A., D. Russo, G. Streile, and H.E. Abd. 1990. Evaluation of volatilization by organic chemicals residing below the soil surface. Water Resour. Res. 26:13-20.

Jury, W.A., W.F. Spencer, and W.J. Farmer. 1983. Behavior assessment model for trace organics in soil: I. Model description. J. Environ. Qual. 12:558-564.

Nye, P.H., B. Yaron, Ts. Galin, and Z. Gerstl. 1994. Volatilization of a multicomponent liquid through dry soils: Testing a model. Soil Sci. Soc. Am. J. 58:269-277.

Ong, S.K., and L.W. Lion. 1991a. Mechanisms for trichloroethylene vapor sorption onto soil minerals. J. Environ. Qual. 20:180-188.

Ong, S.K., and L.W. Lion. 1991b. Effects of soil properties and moisture on the sorption of trichloroethylene vapor. Water Res. 25:29-36.

Ong, S.K., T.B. Culver, L.W. Lion, and C.A. Shoemaker. 1992. Effects of soil moisture and physical-chemical properties of organic pollutants on vapor-phase transport in the vadose zone. J. Contam. Hydrol. 11:273-290.

Petersen, L.W., P. Moldrup, Y.H. El-Farhan, O.H. Jacobsen, T. Yamaguchi, and D.E. Rolston. 1995a. The effect of moisture and soil texture on the adsorption of organic vapors. J. Environ. Qual. 24:752-759.

Petersen, L.W., D.E. Rolston, P. Moldrup, and T. Yamaguchi. 1994. Volatile organic vapor diffusion and adsorption in soils. J. Environ. Qual.23:799-805.

Petersen, L.W., A. Thomsen, P. Moldrup, O.H. Jacobsen, and D.E. Rolston. 1995b. High-resolution time domain reflectometry: Sensitivity dependency on probe-design. Soil Sci. 159:149-154.

Peterson, M.S., L.W. Lion, and C.A. Shoemaker. 1988. Influence of vapor-phase sorption and diffusion on the fate of trichloroethylene in an unsaturated aquifer system. Environ. Sci. Technol. 22:571-578.

Rhue, R.D., P.S.C. Rao, and R.E. Smith. 1988. Vapor phase adsorption of alkylbenzenes and water on soils and clays. Chemosphere 17:727-741.

Shonnard, D.R., and R.L. Bell. 1993. Benzene emissions from a contaminated air-dry soil with fluctuations of soil temperature or relative humidity. Environ. Sci. Technol. 27:2909-2913.

Spencer, W.F., and M.M. Cliath. 1973. Pesticide volatilization as related to water loss from soil. J. Environ. Qual. 2:284-289.

Stiver, W., and D. Mackay. 1984. Evaporative rate of spills of hydrocarbons and petroleum mixtures. Environ. Sci. Technol. 18: 834-840.

Thomsen, A. 1994. Program AUTOTDR for making automated TDR measurements of soil water content. User's guide, vers. 01, January 1994. Danish Inst. of Plant and Soil Science Internal SP Rep. 38. Danish Inst. of Plant and Soil Science, Lyngby, Denmark.

Thomsen, A., and H. Thomsen. 1994. Automated TDR measurements: Control box for Tektronix TSS 45 Relay Scanners. Danish Inst. of Plant and Soil Science Internal SP Rep. 10. Danish Inst. of Plant and Soil Science, Lyngby, Denmark.

Troeh, F.R., J.D. Jabro, and D. Kirkham. 1982. Gaseous diffusion equations for porous materials. Geoderma 27:239-253.

Article IV.

Journal of Hazardous Materials, 36 (1994) 89–108
Elsevier Science Publishers B.V., Amsterdam

Modeling multicomponent volatile organic and water vapor adsorption on soils

S. Amali[a,*], L.W. Petersen[b] and D.E. Rolston[a]

[a] *Land, Air, and Water Resources Department, University of California, Davis, CA 95616 (USA)*
[b] *Environmental Engineering Laboratory, Department of Civil Engineering, Aalborg University, Sohngaardsholmsvej 57, DK-9000 Aalborg (Denmark)*

Received March 16, 1993, revised manuscript received July 21, 1993

Abstract

Volatile organic chemical (VOC) and water vapors are present simultaneously in the soil gas phase. Any modeling of VOC vapor flow must account for the strong competition they experience from water and any competition between themselves. To account for these competitions, the multicomponent form of the Brunauer–Emmett–Teller equation with finite number of adsorption layers was tested. Of the three input constants required in the multicomponent model, two can be obtained from single species adsorption experiments. The third constant was found to be bounded within a fairly narrow range; although its physical meaning is debatable, its value can be approximated fairly accurately. The data used to check the applicability of this model were for the adsorption of trichloroethylene and toluene on a sand and Yolo silt loam (fine-silty, mixed, nonacid, thermic Typic Xerorthent). For relative humidities (RHs) corresponding to less than one molecular layer of water coverage and at low to very low toluene and trichloro ethylene (TCE) vapor pressures, it underpredicted the adsorbed amounts of both species from their binary mixtures with water on both soils. At RHs corresponding to between one and two molecular layers of water coverage, predictions compared well with data. At RHs corresponding to about two layers of water, the model overpredicted the adsorbed amounts. At toluene relative vapor pressures above 0.1 the model reasonably described the adsorbed amount on sand at two RHs corresponding to one to two water layers. This model was further tested on published adsorption data of *para*-xylene and water on soil. It was reasonably successful in describing adsorption of *para*-xylene from its binary mixture with water above *para*-xylene relative vapor pressure of 0.069 and water relative humidity of 0.084. No competition between TCE and toluene was observed at the low vapor pressures in our experiments. Simulations of adsorption in the ternary systems of TCE, toluene, and water followed the same pattern as for the binary simulations.

1. Introduction

Realistic modeling of vapor flow for volatile organic chemicals (VOCs), especially in fairly dry soils, requires models of adsorption of these vapors to

---

[*] Corresponding author.

0304-3894/94/$07.00 © 1994 Elsevier Science B.V. All rights reserved.
SSDI 0304-3894(93)E0082-D

soil particles. The strong competition of polar water with nonpolar VOC molecules for adsorption sites has been recognized by many researchers [1–5]. Under dry conditions, adsorption on the external surfaces of minerals is the primary VOC vapor sorption mechanism [4, 6–9]. The vapor adsorption isotherms on dry soils follow the Brunauer–Emmett–Teller (BET) isotherms [3, 6, 8]. The most observed of the BET isotherms is the Type II which is characteristic of vapor condensation forming multilayer adsorbates on nonporous or macro-porous adsorbents [10]. As the relative humidity (RH) in the soil increases from zero, strong polar interactions between water molecules and soil minerals predominate over the relatively weak Van der Waals forces between the VOC vapor molecules and mineral surfaces [7, 8]. Chiou and Shoup [3] showed that BET adsorption isotherms of a few chlorobenzenes became linear as RH increased to 0.50. Above a RH of 0.50, isotherms became linear for VOC relative vapor pressures (actual vapor pressure/saturated vapor pressure) of less than 0.50. Rhue et al. [9] found that at RH values close to a monolayer of water coverage on a kaolinitic soil and on a silica gel, the adsorption of *para*-xylene decreased much more noticeably than at lower or higher RH values. At higher RH values, Henry's partitioning into water and partitioning into soil organic matter become the dominant uptake mechanisms for VOC vapors over adsorption on external mineral surfaces [5]. Jurinak and Volman [6] obtained data on adsorption of ethylene dibromide on soils up to a relative vapor pressure of 0.9. They obtained a good fit of the BET equation to the data up to relative vapor pressures of 0.6–0.7. Poe et al. [8] used the BET equation to fit adsorption data of a few widely different chemicals on four types of soils. Their correlation coefficients indicate good fits over the range of data used. The success of the BET equation to fit single vapor adsorption data, particularly in the 0.05–0.3 relative vapor pressure range, has prompted its widespread use in calculations of monolayer coverage and soil surface area from nonpolar compounds (Sing et al. [10]).

Models of multicomponent adsorption must account for the competition of water vapor with the VOC vapors and any competition between the individual VOC vapors. Even though competition between nonpolar VOC species for adsorption sites is expected to be much less intense than competition with water, the strength of competition is expected to increase with the polarity of the species [3, 8]. The extension of the single component multilayer BET isotherm to a multicomponent form presented by Hill [11, 12] may offer some possibilities in this regard. Valsaraj and Thibodeaux [4] used a binary form of Hill's general equation to get simplified isotherms to estimate partial pressures of VOCs above soils. They point out that this equation applies best to results at low VOC relative vapor pressures. Their equation allows an infinite number of adsorption layers thereby assuming that a free liquid surface can be formed on the surface of soil minerals. Thibodeaux et al. [13] used a similar equation to theoretically investigate the adsorption of slightly volatile organic chemical (SVOC) vapors and water on atmospheric aerosols. Their equation indicated the correct behavior of the SVOC isotherm at various RHs. However, the applicability of their equation to soils is not clear. Rhue et al. [9] proposed a formula for the mass fraction of an adsorbed species in the total mass adsorbed from a binary vapor system. An equation derived based on their equation greatly overpredicts the total mass adsorbed at low water contents but its predictions are reasonably close to measured values at higher RHs. Pennel et al. [14] compared the results of the Valsaraj and Thibodeaux [4] equation and Rhue et al. [9] equation. They collected single and binary adsorption data of *para*-xylene on a kaolinitic soil at low to medium *para*-xylene relative vapor pressure ranges and at RHs corresponding to less than one molecular water layer. The models used in their paper also assume that an infinite number of adsorption layers could form on the surface. They concluded that at low RHs, the binary BET equation underestimated the adsorption of both water and *para*-xylene due to noncomplete monolayer coverage by water. However, it is not known how the BET equation performs at higher RHs and VOC relative vapor pressures.

In this paper we will investigate the applicability of the multicomponent BET model to adsorption of VOC vapors in the presence of water on soils. We will set the maximum number of adsorbed layers (n) to be finite and investigate the implications of this choice for multicomponent adsorption modeling. The predictions of the multicomponent BET equation can be compared theoretically against the forms used by Valsaraj and Thibodeaux [4] and Thibodeaux et al. [13], to investigate the possible strengths and limitations of choosing a finite n value. Moreover, we will compare the predictions of the multicomponent BET model with measured trichloro ethylene (TCE) and toluene vapor adsorption data from binary and ternary mixtures with water on a sand and a Yolo silt loam. Finally, we will compare the multicomponent BET model predictions with the results obtained using the equation of Rhue et al. [9] and with their measured data on adsorption of *para*-xylene on Na-saturated kaolin at various water contents.

2. Theory

The single species multilayer BET model [15, 16] is based on the following assumptions: (1) energetically and geometrically homogeneous adsorbent surface, (2) no lateral interaction among the adsorbed molecules, (3) adsorption of the molecules of the second and higher adsorbed layers follows the condensation–evaporation properties of the liquid state. Hill [11] assumes the last postulate to be equally applicable to adsorption from a mixed vapor system. Assuming that the adsorbed solution obeys Raoult's law, namely that the mixture of sorbed species behaves as an ideal solution at all compositions, eq. (14) in Hill [11] takes the following form for adsorption of species i from a vapor mixture containing s species,

$$w_i = \frac{w_i^{\mathrm{m}} E_0 x_i}{(1-E)+E_0(1-E^n)}\left[\frac{B_i(1-E^n)}{E_0} + \sum_{k=2}^{n} E^{k-2}(1-E^{n-k+1})\right] \qquad (1)$$

where $E_0=\sum_{i=1}^{s}x_iB_i$, $E=\sum_{i=1}^{s}x_i$, w_i is sorbed mass of species i per soil mass, $w_i^{\rm m}$ is mass of species i required to form a monolayer coverage on adsorbent surface per soil mass, x_i is relative vapor pressure (vapor pressure/saturated vapor pressure), and B_i is related to the molar heat of adsorption of the adsorbate on bare mineral surface [3]. Finally, in eq. (1), n is an integer signifying the maximum possible number of layers of i on the adsorbent surface for single-species systems. In eq. (1) the summation is only taken when $n \geq 2$.

In eq. (1), the assumption of ideality leads to the simplified form of the parameter E. However, one would expect eq. (1) to be less applicable to sparingly soluble compounds than to more soluble ones. Furthermore, the applicability range would be expected to be restricted to lower VOC relative vapor pressures.

All the various forms of the BET equation presented in the literature are simplifications of the general multicomponent BET (MBET) form. When considering adsorption of a single species and $n=\infty$, eq. (1) reduces in a linear form to

$$\frac{x_i}{w_i(1-x_i)}=\frac{1}{w_i^{\rm m}B_i}+\frac{(B_i-1)x_i}{w_i^{\rm m}B_i} \tag{2}$$

This form is applied to $0.05 \leq x_i \leq 0.3$ to obtain $w_i^{\rm m}$, B_i, and adsorbent surface area [10]. For single species adsorption and finite n, eq. (1) gives the form used by Jurinak and Volman (1957) and Poe et al. (1988) to fit adsorption data of single species of VOC vapors on dry soils. When applied to a binary vapor system and $n=\infty$, it furnishes the form used by Valsaraj and Thibodeaux [4], Thibodeaux et al. [13], and Pennell et al. [14]. When $n=1$ (i.e., adsorption is restricted to a monolayer), the single species form of eq. (1) reduces correctly to a Langmuir type equation.

The effect of the parameters B and n on the shape of eq. (1) for adsorption of a hypothetical VOC species on dry soils is plotted in Fig. 1. As B increases, a 'knee' is formed at the lower x_i values and $w/w_i^{\rm m}$ increases to give a sharp drop to zero. The point where the knee occurs is often taken to indicate the stage at which monolayer coverage is complete and multilayer adsorption is about to begin [10, 17]. As n increases, higher adsorption is predicted at higher x_i values until for $n=\infty$, $w_i \rightarrow 1$ as $x_i \rightarrow 1$. As x_i decreases, the difference in adsorption between isotherms for various values of n also decreases. This shows that the choice of $n=\infty$ in the MBET equation may be appropriate in modeling multicomponent adsorption at low VOC relative vapor pressures but leads to gross overestimation of adsorption capacity at high relative vapor pressures. Even though the BET theory does not provide a physical basis for why the number of layers should be restricted to a finite value, the presence of capillaries in soils is possibly one cause of this [17]. Fig. 1 indicates that proper choice of n and B may allow various isotherms to be fitted if the monolayer capacity $w_i^{\rm m}$ is known. In binary form, eq. (1) can be used to look at the effect of increasing RH on the shape of the isotherm and strength of adsorption for a given VOC on

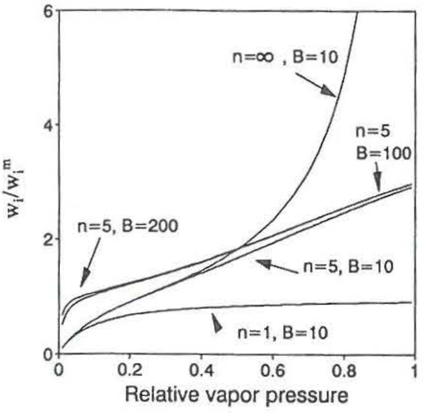

Fig. 1. The effect of *B* and *n* on the shape of eq. (1) applied to a single vapor system.

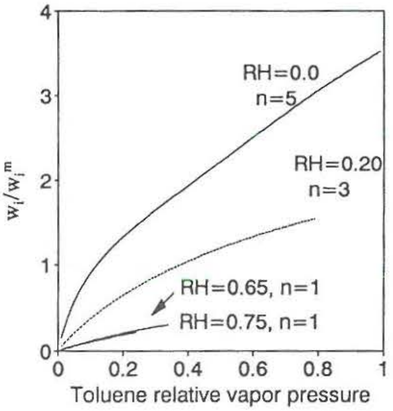

Fig. 2. Effect of water relative vapor pressure (RH) on MBET isotherms of toluene adsorption on Yolo silt loam at 25 °C.

soil. Fig. 2 illustrates theoretical isotherms for toluene on Yolo silt loam at various RH values. The major effects are a linearization of the isotherm with an accompanying reduction in adsorption amounts as RH increases. These effects have been experimentally documented by Chiou and Shoup [3], Rao et al. [18], and Rhue et al. [9], among others.

Rhue et al. [9] presented equations similar to BET which could be used to quantify competitive adsorption in a binary system. Their derivation assumes that the two adsorbates form immiscible films on the adsorbent surface. This assumption is opposite to what is used in deriving eq. (1) which requires the adsorbates to form an ideal solution on the adsorbent surface. When S_0 (bare mineral surface) in their equations is substituted by the external surface area for their soil (given in their paper), their equations lead to an expression giving the mass of a given compound in the total mass adsorbed from a binary vapor system. The final equation obtained is

$$w_i = \alpha_i B_i S_{\mathrm{ext}} \frac{x_i}{(1-x_i)^2} \tag{3}$$

where α_i is the mass of adsorbate i occupying unit area of surface and is given by Rhue et al. [9] to be 0.50 mg/m^2 for *para*-xylene, S_{ext} is the soil specific external surface area (m^2/g), and additional parameters have previously been defined.

The parameter n in eq. (1), when applied to single species adsorption, signifies the maximum number of adsorption layers. However, in a multicomponent situation, the physical meaning of n requires further investigation. A first hypothesis is that as in a single species system, n in a multispecies system refers to the maximum number of layers of the multispecies adsorbate. A second hypothesis is that n refers to an 'equivalent' maximum number of layers of species i on the surface of a soil–water adsorbent complex. We will look at which of these hypothesis may better explain the data.

3. Materials and methods

Adsorption was measured on a coarse riverbed sand and Yolo silt loam (fine-silty, mixed, non-acid, thermic Typic Xerorthent). Some relevant characteristics of the two soils are given in Table 1. Total surface areas were determined by the ethylene glycol monoethyl ether (EGME) method [19, 20]. Pretreatment to remove organic matter and saturation with Ca^{2+} were omitted [21]. The organic carbon content of the soils was analyzed by a modified Walkley and Black method [22]. The pH was measured in a saturated paste by pH electrode, while electrical

TABLE 1

Characteristics of the soils used in adsorption experiments

Characteristic	Riverbed sand	Yolo silt loam
EGME surface area (m^2/g)	18.7	80.6
Organic carbon (%)	<0.1	1.05
pH	8.2	7.9
EC (milli mho/cm)	0.36	0.77
CEC (meq/100 g)	2.3	21.1
Sand (%)	94	33
Silt (%)	4	49
Clay (%)	2	18

conductivity (EC) of saturation extracts was measured using a platinized platinum–iridium conductivity electrode and a conductance–resistance meter. Cation exchange capacities (CECs) were determined by saturation with barium acetate [23]. Particle size analysis to determine sand, silt, and clay fractions was performed by hydrometer [24]. Initially the soils were air dried, passed through a 2.0-mm sieve (No. 10), and mixed thoroughly to obtain a homogeneous mixture.

To obtain adsorption data in the very low relative vapor pressure range, the equilibrium partitioning in closed systems (EPICS) method [5, 25] was used. The method can briefly be described as a mass balance technique that involves measurement of the headspace vapor concentration in sealed glass bottles by gas chromatography. A system with known gas volume and mass of adsorbent is compared to a control which contains no adsorbent. The adsorbent masses ranged from 0.2 to 60 g. Amount of adsorbent was increased for increasing water content. For each adsorption isotherm, six different adsorbent masses were used with three replicates for each mass. The adsorbent was introduced into glass bottles with a volume of 63 or 248 ml. The bottles were wrapped in paper to prevent photo-decomposition of the VOCs and sealed with teflon Mininert valves (Dynatech, Baton Rouge, LA). A volume of 2.5 ml of air in each bottle was replaced by an equivalent volume of saturated VOC vapor. All bottles were rotated for 24–36 h at 25 °C to reach equilibrium. Preliminary work showed that equilibrium was reached after this period of time. One ml of headspace was removed from each bottle with a gas-tight syringe (Hamilton 1001) and analyzed on a Hewlett-Packard 5890 gas chromatograph equipped with a flame ionization detector. The relative humidity at each water content was determined by measuring it in similarly prepared bottles. Relative humidity of the samples was measured with a certified NIST traceable digital hygrometer (Fisherbrand) with an error of ±1.5% in the 10 to 90% range. Water contents were measured by weighing samples dried in an oven for 24 h at 105 °C. The water contents and the corresponding relative humidities used in the EPICS experiments are summarized in Table 2.

A high vacuum (HV) technique [26] was used to obtain data at the higher relative vapor pressure range than was obtained with the EPICS method up to near saturation. In this technique, an electrobalance located inside a glass vacuum chamber measured the weight change of about 0.5 g of a soil sample upon adsorption. The chamber is evacuated with a mechanical pump and a turbomolecular pump to vacuums as low as 10^{-3} Pa. Care was taken so as not to have any static charge interference with the weight measurements. The temperature measured at the vicinity of the soil sample was monitored continuously and was within ±0.5 °C of the experimental temperature of 25 °C. Liquid sources of water, TCE, and toluene connected to the chamber via Kontes high vacuum glass valves were opened to allow evaporation into the chamber. The vapor pressures were determined by a capacitance manometer. The relative vapor pressures were then determined by dividing the measured vapor pressures by the published values of the saturated vapor pressure at 25 °C. For binary experiments of water and toluene, water was first allowed to evaporate

TABLE 2

Water content (W) (mg/g, dry weight basis) and corresponding relative humidities (RH) in the soils used in the adsorption experiments

EPICS[a]	Toluene on sand		TCE on sand		Toluene on loam[b]		TCE on loam		Toluene and TCE on			
									sand		loam	
	W	RH	W	RH	W	RH	W	RH	W	RH	W	RH
	1	0.12	<1	0.07	8	0.16	8	0.16	2	0.13	32	0.65
	5	0.32	5	0.25	24	0.38	23	0.38				
	7	0.65	7	0.65	31	0.65	31	0.65				
HV[c]	Toluene on sand											
	W	RH										
	1	0.10										
	7	0.656										

[a] EPICS = equilibrium partitioning in closed system technique.

[b] Yolo silt loam.

[c] HV = high vacuum technique.

from the liquid reservoir into the chamber. Once equilibrium at the desired relative humidity was reached, toluene was allowed to evaporate in increments until equilibrium was attained. One set of measurements of toluene adsorption at each relative humidity was obtained. The water content and relative humidity data are given in Table 2.

4. Results and discussion

4.1. Single species systems

Figs. 3 and 4 contain isotherms of TCE and toluene adsorption on the oven-dried Yolo silt loam and sand at 25 °C, respectively. They indicate that the EPICS data connect reasonably well with the HV data for TCE and less so for toluene. The EPICS data are used to investigate the applicability of MBET at low x_i values. The value of B_i and w_i^{m} for our VOCs and soils were obtained by fitting eq. (2) to the x_i range between 0.05 and 0.3. These values were then used to fit the linearized form of eq. (1) for single species adsorption [27] to the full range of the adsorption data to find the best value of n. These data and the R^2 values for the fit of eq. (2) are summarized in Table 3. Figs. 3a and 4a show that the MBET equation generally underpredicts adsorption capacity at low x_i values. Even though there was some difficulty in obtaining a good match between the EPICS and the HV data for toluene, the underprediction is most likely the result of the presence of adsorption sites of a higher heat of adsorption than those which are occupied at monomolecular surface coverage [28]. After the most active sites have been covered, the properties of the rest of the

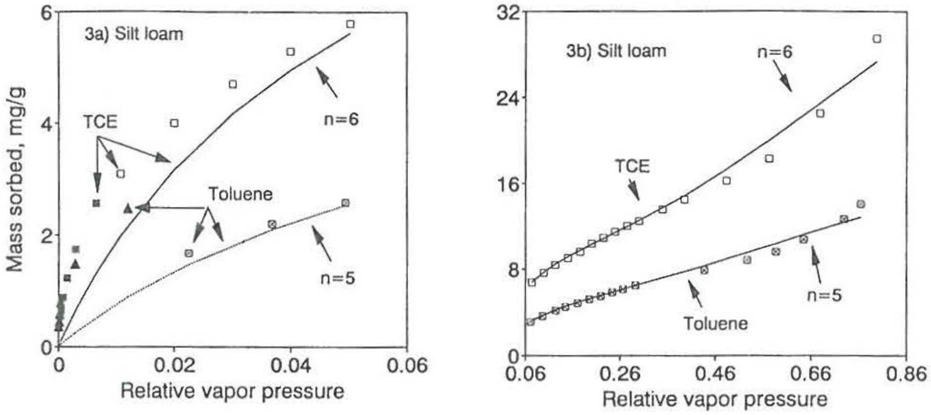

Fig. 3. Adsorption isotherms of TCE and toluene on Yolo silt loam at 25 °C. The values of n given on the figures are the best fit values and the solid lines are the resulting curves. Fig. 3a shows the EPICS method as well as the first few of the HV method data. Fig. 3b includes only the HV data at higher x range.

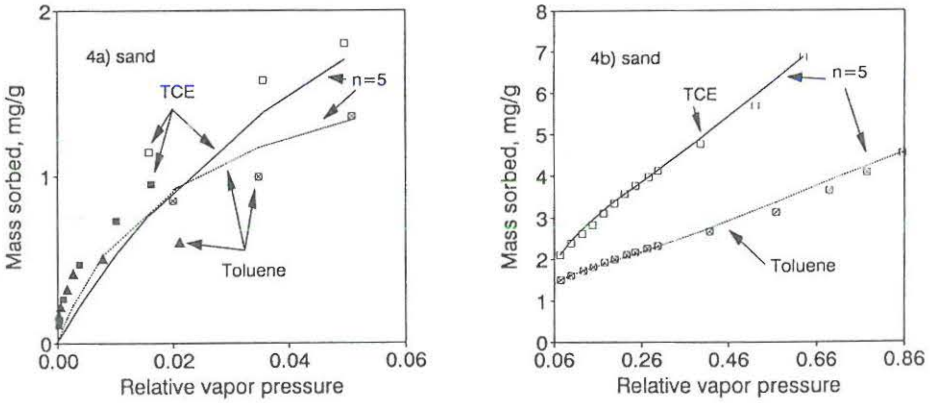

Fig. 4. Adsorption isotherms of TCE and toluene on sand at 25 °C. The values of n given on the figures are the best fit values and the solid lines are the resulting curves. Fig. 4a shows the EPICS method as well as the first few of the HV method data. Fig. 4b includes only the HV data at higher x range.

surface are similar to those of a homogeneous surface for which the MBET is much more suited. We subsequently used the method of Joyner et al. [27] in which the full range of adsorption data (EPICS + HV) is used to fit B_i, w_i^m, and n. However, the resulting values did not model the low x_i range any better (data not shown).

Table 3 indicates that the monolayer capacities, w_i^m, are higher on Yolo silt loam than on sand in accordance with the silt loam's higher external surface

TABLE 3

Values of B_i, w_i^m, and the goodness-of-fit R^2 values for the fit of eq. (2) to the appropriate range (relative vapor pressure from 0.05 to 0.3) of the adsorption data for TCE, toluene, and water on dry sand and Yolo silt loam. The value of n was then obtained by fitting the single species form of eq. (1) to the full range of adsorption data with the calculated values of B_i and w_i^m

Compound	Quantitiy	Adsorbent	
		Sand	Yolo silt loam
TCE	B	18.4	23.1
	w^m (mg/g)	3.3	9.7
	R^2	0.998	0.999
	n	5	6
Toluene	B	55.3	16.1
	w^m (mg/g)	1.7	5.3
	R^2	1.000	1.000
	n	5	5
Water	B	25.7	17.6
	w^m (mg/g)	2.3	8.5
	R^2	0.999	0.999
	n	5	7

area. The monolayer capacity for water should probably be accepted only as a fitting parameter since water does not coat the surface uniformly [29]. The B values for Yolo silt loam and sand do not correlate well with the trend in polarity. The B values for water are expected to be higher than the VOC species considering energy of adsorption alone. The B values reported by Chiou and Shoup [3] increase as polarity of adsorbates increases. The data of Poe et al. [8] indicate similar behavior for adsorption of nonpolar to more polar compounds on a sandy loam and a silty loam soil. However, the correlation between B and polarity breaks down in their silty clay loam soil. On this soil, the least and the most polar compounds have similar B values which are smaller than the values for compounds of intermediate polarity. The parameter B directly reflects the relative strength of adsorption arising from the different heats of adsorption. Higher strengths of adsorption are signified by higher negative values of ΔH_s. Therefore, the actual value of B is indicative of the degree to which a compound might compete for adsorption sites with other compounds and would be expected to increase with the polarity of adsorbate species. However, the exact relationship between B and ΔH_s is at best only qualitative [10]. This is since, firstly, the actual amount adsorbed depends on the site distribution of energies for adsorption. The uniform distribution of site energies, as assumed by the BET theory, cannot be assumed for soils due to differences in the chemical nature of the surfaces [30] and the nature of the cations present on different exchange sites [14]. Secondly, porous adsorbents like soils are characterized by a range of pore sizes arising from particle size distribution, structure, and packing [31]. The actual surface area available for

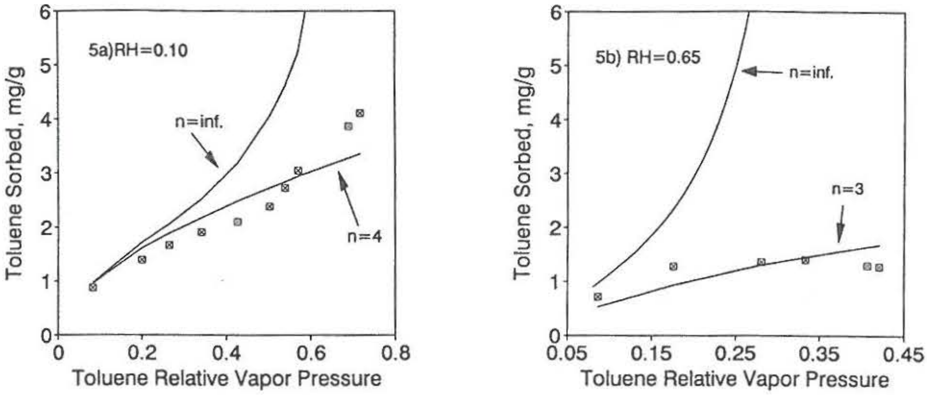

Fig. 5. Toluene vapor adsorption isotherms on sand at two relative humidities. Squares are data measured using the HV apparatus and the lines are from the MBET model with the given best-fit n.

adsorption of any given compound depends on whether the adsorbate molecule can reach the adsorbing sites. The larger the adsorbate molecule relative to the pore size, the less adsorption is expected to occur at any given relative vapor pressure.

4.2. Binary systems

Fig. 5 contains the fit of the MBET model to toluene adsorption data on sand at two relative humidities. At $\mathrm{RH}=0.10$ the mass of toluene adsorbed is only slightly less than for adsorption on dry sand (Fig. 4b). At this RH, the amount of water is less than half a monolayer of water coverage on sand (Table 1). According to Quirk [29], water adsorbed at this RH is not thought to cover the soil surfaces uniformly but to congregate around high adsorption sites. Even though the adsorption of toluene on mineral matter is expected to be mostly curtailed by the presence of water molecules [3], higher energy (possibly still bare) sites are apparently still available for toluene adsorption. A similar conclusion was reached by Pennell et al. [14] when looking at *para*-xylene adsorption on Na-saturated kaolin at RHs lower than required to form a monolayer of water coverage. The value of $n=4$ fitted to the data is one less than $n=5$ fitted to the dry adsorption data on the same soil. At $\mathrm{RH}=0.65$ (Fig. 5b), sorbed amount levels out with increasing toluene relative vapor pressure. The last two measurement values are actually slightly less than the previous two possibly from electrical drift of the microbalance [26]. The value of n used to fit the data is reduced to three in accordance with lower adsorption amounts at the higher water contents.

Figs. 6a–d contain the fit of the MBET model to adsorption data of toluene and TCE at low x_i range on sand and Yolo silt loam at several RH values. The lowest RH values in each graph correspond to less than one molecular layer of

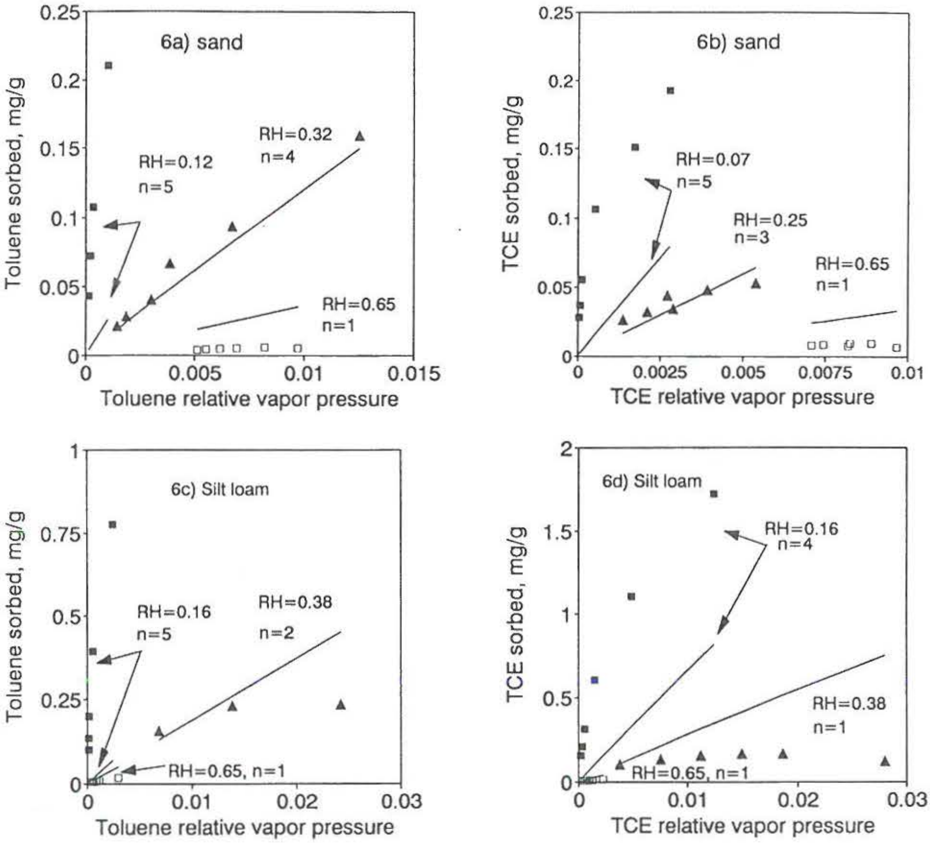

Fig. 6. Binary vapor adsorption of TCE or toluene at several RHs on sand and Yolo silt loam. The solid lines are the MBET predictions with the corresponding RH and the best-fit value of n. (a) Toluene on sand, (b) TCE on sand, (c) toluene on silt loam, and (d) TCE on silt loam.

water coverage on the adsorbent surface. At the lowest RHs, the MBET underpredicts the sorbed mass for values of n ranging from 2 to the value fitted to dry adsorption data. This behavior is similar to the underprediction of adsorption on dry adsorbents in the low vapor pressure range. The explanation of this behavior is similar to the one given for the single-species cases and indicates that water does not coat the soil surfaces uniformly as Quirk [29] has discussed. No such behavior was seen at the higher toluene vapor pressures (Fig. 5a) most likely because a monolayer of water and toluene was already formed on the sand surface. Further adsorption, therefore, took place on a more energetically uniform surface.

The intermediate RH values correspond to water contents between one and two molecular layers of coverage. The fit of the MBET model is much better than for the low RH cases. Most, if not all, of the energetic heterogeneity on sand surfaces has been eliminated by water coverage [28], resulting in a more homogeneous surface for further adsorption. The MBET fit is less satisfactory on the more heterogeneous silt loam than the sand. Notice that the fitted values of n are becoming smaller as RH increases and are associated with lower adsorption amounts of TCE and toluene.

At RH = 0.65, or about two molecular layers of water coverage, the measured isotherms show reduced adsorption capacity. The MBET overpredicts adsorption for both VOCs on both soils even at the lowest possible n value. The MBET assumes ideal mixed liquid adsorbate corresponding to complete miscibility of adsorbed species. As the number of water layers on the adsorption surface increases, the dissolution in water is thought to dominate the uptake process of VOCs on saturated soils [5]. The adsorption process of water and VOCs on mineral matter changes to a dissolution process of VOCs in water. It is, however, doubtful that the MBET equation leads to an adequate vapor–liquid solution theory at this and higher RH values [13].

The final binary system studied is that of *para*-xylene and water adsorption on Na-saturated kaolin performed by Rhue et al. [9]. Their measured adsorption values, the MBET model predictions, and the predictions using eq. (3) which was derived from the basic equations given in the Rhue et al. (1989) paper are included in Table 4. The B and w_i^{m} values used in the MBET model were obtained by fitting eq. (2) to appropriate range (x from 0.05 to 0.3) of the single-species data given in their paper. The lowest and the highest *para*-xylene relative vapor pressures are within the range of HV data used in our experiments with TCE and toluene. At low to intermediate RH values, the fit of the MBET equation to the *para*-xylene adsorption data is much better than the fit of eq. (3). The predictions of eq. (3) become comparable to MBET only at high RH values when both predict the sorbed mass of *para*-xylene well. At lower RHs, the MBET slightly underpredicts the measured sorbed amount. However, at RHs close to 0.65, the measured sorptions are predicted well. The *para*-xylene solubility in water is 198 mg/l (25 °C) compared with 1100 mg/l for TCE (25 °C) and 515 mg/l for toluene (20 °C) [32]. Even though solubility values alone cannot be used to partition adsorption between water and mineral phases at these water contents [5], we would still expect the ideal solution assumption in MBET to be more restrictive for less soluble *para*-xylene than the more soluble toluene and TCE. The relatively good prediction of *para*-xylene adsorption at these higher water contents is perhaps indicative of the fact that the ideality of the adsorbed mixture is not a very restrictive assumption in developing the MBET model at these water contents. The MBET model shows much improvement over eq. (3) in predicting adsorbed amounts of *para*-xylene over a relatively wide range of water and *para*-xylene vapor pressures.

4.3. Ternary systems

Data were obtained on adsorption of TCE and toluene from mixtures with water on our adsorbents using the EPICS method. The comparisons between

TABLE 4

Comparison of MBET model predictions with predictions from eq. (3) and with the measured values of adsorption of *para*-xylene and water vapors on Na-saturated kaolin reported in Rhue et al. [9]

Water relative vapor pressure	*para*-Xylene relative vapor pressure	*para*-Xylene mass sorbed (mg/g)	Simulated sorbed mass (mg/g)		Best fit *n*
			Eq. (3)	MBET	
0.084	0.390	7.11	31.15	5.90	6
0.095	0.379	6.56	29.55	5.54	5
0.100	0.132	3.96	10.18	2.45	5
0.190	0.086	2.61	5.37	1.40	4
0.22	0.18	3.87	10.43	2.63	5
0.228	0.424	7.04	24.06	5.70	5
0.239	0.281	5.23	15.49	3.89	5
0.262	0.171	3.5	8.87	2.43	5
0.39	0.156	2.34	5.53	2.08	5
0.517	0.187	1.85	4.15	1.75	3
0.658	0.069	0.45	0.77	0.34	2
0.67	0.286	2.77	2.97	2.87	4
0.676	0.164	1.41	1.64	1.38	3

TABLE 5

Comparison of measured and calculated adsorption of TCE and toluene from their ternary mixture with water on the adsorbents. The *n* values given are the best fit values. Measured RHs are 0.10 for sand and 0.65 for loam

TCE relative vapor pressure	Toluene relative vapor pressure	Mass TCE sorbed (mg/g)	Mass toluene sorbed (mg/g)	Simulated sorbed mass (mg/g)	
				TCE	Toluene
Sand				$n=4$	$n=4$
0.034	0.036	0.543	0.530	0.428	0.571
0.014	0.004	0.516	0.244	0.231	0.084
0.012	0.003	0.419	0.184	0.198	0.066
0.008	0.002	0.386	0.152	0.142	0.041
Silt loam				$n=1$	$n=1$
0.0021	0.0016	0.0126	0.0080	0.0379	0.0109
0.0012	0.0007	0.0084	0.0038	0.0218	0.0048
0.0010	0.0006	0.0071	0.0030	0.0176	0.0038
0.0008	0.0005	0.0061	0.0024	0.0147	0.0031
0.0005	0.0003	0.0049	0.0018	0.0096	0.0022
0.0005	0.0003	0.0044	0.0016	0.0082	0.0019

measured values and values from the MBET model are summarized in Table 5 for sand at RH = 0.10 and Yolo silt loam at RH = 0.65, respectively. With two or more VOCs adsorbing, the adsorption sites not occupied by water molecules are divided between the VOC species based on their strength of adsorption. The higher value of parameter B for toluene compared with TCE on sand indicates higher preference of this soil for toluene than TCE. Not much difference was, however, observed between the adsorption strengths of either TCE or toluene compared with their binary adsorption experiments. At these low concentrations, the major competition for each VOC species seems to be with water and not with each other. At the low RH on sand, the MBET simulates lower adsorbed amounts than what is measured. This is similar to what occurred in the single and binary experiments. At the higher RH on Yolo silt loam, the MBET overpredicts the measured amounts for both VOCs at this RH as similarly occurred in the binary cases. At low VOC relative vapor pressures at these two RHs, their behavior is mainly determined by the presence of water and not the other species.

4.4. *Significance of n*

The fitting of n in addition to B and w^{m} enables the single-species isotherms to be well characterized over a good portion of their vapor pressure range. The physical meaning of this parameter in such systems is straightforward and is the maximum number of adsorbed layers which can be formed on the adsorbent surface [6]. By analogy, this parameter is the number of layers of mixed adsorbate layers in a multicomponent case [11]. In binary formulations used to date [4, 13], there was no need to define n, since $n = \infty$ was used. This is because the amount adsorbed is independent of n at low relative vapor pressures as shown in Fig. 1. The same behavior is observed in Fig. 5 for binary systems of toluene adsorption on wet sand. It is only at the relatively higher x_i range that the $n = \infty$ formulation diverges from a finite n formula. The extent of divergence increases as x_i increases and leads to serious overpredictions of adsorption amounts. Many contaminations of soil and groundwater involve low concentrations of the VOC species. Therefore, setting $n = \infty$ in eq. (1) is a good approximation at low x_i (Fig. 1). However, in cases where higher concentrations are involved, as with concentrations existing close to immobile residual liquid VOCs or around high liquid concentrations from accidental spills or deliberate dumpings, an $n = \infty$ would lead to overestimation of adsorption.

Two hypotheses were proposed earlier to elucidate the correct physical significance of the parameter n. The first one is that n is the maximum number of mixed adsorbate layers on the adsorbent surface as in Hill's original paper. In this case, when one species has a much higher relative vapor pressure compared with other species, the value of n in the isotherm for all species is expected to approach the n for the one species with high relative vapor pressure. However, in our simulations the value of n for all VOC adsorbents decrease as RH increases rather than approaching the n values fitted to water adsorption data. We therefore investigate our second hypothesis in which n is an 'equivalent' maximum number of layers. It applies to adsorption of VOCs onto a soil–water complex and is a function of RH (or water content). In this soil–water system, VOC molecules can penetrate the surface (e.g., dissolve in water) as well as adsorb onto mineral surfaces directly. The minimum value of n ($n_{\min}$) is equal to the total amount adsorbed w_i spread over the adsorbent external surface area S_{ext}. It is given by

$$n_{\min}=\frac{w_i A_i N}{M_i S_{\text{ext}}} \tag{4}$$

where w_i is a measured mass of adsorbate per mass of adsorbent (g/g), A_i is the projected area of one molecule (m^2/molecule), N is the Avogadro number ($=6.022\times10^{23}$ molecules/mol), and M_i is the molecular weight for species i (g/mol). The parameter $A_i=1.091(M_i/d_iN)^{2/3}$ [33], where d_i is the liquid density of the species. Eq. (4) indicates that $n_{\min}$ increases as w_i increases. Note that the value obtained from eq. (4) is not an integer. The value of n chosen for fit to eq. (1) must at least be the integer higher than $n_{\min}$ determined from an experiment which involves the highest VOC concentration deemed probable for the case being modeled. The value of n ranges from this minimum value to the maximum used to fit the dry adsorption isotherm. For example, for toluene adsorption data on sand (Fig. 5), the highest measured w_i at an RH of 0.18 and 0.65 give $n_{\min}=2.3$ and $n_{\min}=0.73$, respectively. The fitted values of n are 4 and 3, respectively. Both of the fitted n values are higher than $n_{\min}$ and lower than the n fitted to dry adsorption data ($n=5$, cf. Table 1). Similar results were observed for Rhue et al. [9] data. For ternary and larger multinary cases, the value of n for less highly adsorbed species would not only depend on RH but also on the vapor pressures of the other more highly adsorbed species. Based on these data alone, the second hypothesis cannot be exclusively accepted or rejected. However, the decrease of the value of n is over a relatively small range which would make its use as a fitting parameter relatively convenient in modeling multicomponent adsorption.

5. Conclusions

The extension of the general BET adsorption equation to multicomponent adsorption as proposed by Hill [11, 12] was tested on binary and ternary systems of TCE, toluene, and water vapors on a sand and Yolo silt loam soil. The model inputs are the monolayer adsorption capacity (w_i^{m}), a constant related to heats of adsorption (B_i), and a constant signifying the number of adsorbed layers on the adsorbent surface (n). The first two constants were obtained by application of the model to single-species adsorption isotherms. The last constant ranges from a minimum integer value larger than the total amount adsorbed spread over the soil external surface area to a maximum value obtained from the single species adsorption isotherm.

This model was reasonably successful in describing adsorption of toluene from its binary vapor mixture with water on the sand over toluene vapor pressures range above about 0.1 and at two relative humidities (RH) corresponding to less than one and about two molecular layers of water. At lower TCE and toluene relative vapor pressures, the model was applied to their adsorption on the sand and Yolo silt loam at three RH values. At RH values corresponding to less than a monolayer of water coverage, it underpredicted adsorbed amounts. At intermediate RH values corresponding to between approximately one and two molecular layers of water coverage, predictions were successful. At the highest RH value of 0.65, corresponding to about two molecular layers of water, the MBET equation overpredicted the adsorbed amounts. The MBET equation was more successful than a method based on the equations of Rhue et al. [9] in describing adsorption of *para*-xylene from its binary mixture with water over a wide range of *para*-xylene and water relative vapor pressures. Adsorption experiments in the ternary systems of TCE, toluene, and water did not indicate any major decrease in adsorption of any of the VOCs as a result of the presence of the other compounds at the RHs studied.

The maximum number of adsorption layers is an important parameter in correctly modeling multicomponent adsorption. Even though its physical significance is still somewhat ambiguous, its value was confined to a narrow range for the VOCs and soils tested in this study. For simulations at low VOC relative vapor pressures, the amount adsorbed is irrespective of the value of n and a simplified equation based on $n=\infty$ can be used. At higher relative vapor pressures, the choice of $n=\infty$ leads to overestimation of adsorption and a finite n should be used.

The MBET equation can successfully be used to model VOC adsorption on geological material and soil over the range of water content corresponding to between one and two molecular layers. It underpredicts the adsorption amount at lower water contents and low VOC relative vapor pressures. At higher water contents it lacks a suitable vapor solution theory so that the measured adsorption isotherms have to be employed. However, the amount of overprediction may be small enough to render its use for modeling purposes worthwhile.

Acknowledgements

This research was funded (in part) by the Kearney Foundation of Soil Science, the NIEHS Superfund Basic Research Program P42ES04699, the Ecotoxicology Program of the University of California Toxic Substances Research and Teaching Program, the Center for Ecological Health Research (EPA-CR819658-010), and the Danish Research Academy. Although the information in this document has been funded wholly or in part by the United States Environmental Protection Agency, it may not necessarily reflect the views of the Agency and no official endorsement should be inferred. We would also like to thank Professor A.P. Jackman and Yan Wang of the Chemical Engineering Department for the use of and help with the high vacuum adsorption apparatus.

References

1 W.F. Spencer, M.M. Cliath and W.J. Farmer, Vapor density of soil-applied dieldrin as related to soil-water content, temperature, and dieldrin concentration, Soil Sci. Soc. Am. Proc., 33 (1969) 509–511.

2 W.F. Spencer and M.M. Cliath, Desorption of lindane from soil as related to vapor density, Soil Sci. Soc. Am. Proc., 34 (1970) 574–578.

3 C.T. Chiou and T.D. Shoup, Soil sorption of organic vapors and effects of humidity on sorptive mechanism and capacity, Environ. Sci. Technol., 19 (1985) 1196–1200.

4 K.T. Valsaraj and L.J. Thibodeaux, Equilibrium adsorption of chemical vapors on surface soils, landfills and landfarms — a review, J. Hazardous Mater., 19 (1988) 79–99.

5 S.K. Ong and L.W. Lion, Effects of soil properties and moisture on the sorption of trichloroethylene vapor, Wat. Res., 25(1) (1991) 29–36.

6 J.J. Jurinak and D.H. Volman, Application of the Brunauer, Emmett, and Teller equation to ethylene dibromide adsorption by soils, Soil Sci., 83 (1957) 487–496.

7 B.K.G. Theng, The Chemistry of Clay–Organic Reactions, Wiley, New York, 1974, pp. 128–135.

8 S.H. Poe, K.T. Valsaraj, L.J. Thibodeaux and C. Springer, Equilibrium vapor phase adsorption of volatile organic chemicals on dry soils, J. Hazardous Mater., 19 (1988) 17–32.

9 R.D. Rhue, K.D. Pennell, P.S.C. Rao and W.H. Reve, Competitive adsorption of alkylbenzene and water vapors on predominantly mineral surfaces, Chemosphere, 18 (1989) 1971–1986.

10 K.S.W. Sing, D.H. Everett, R.A.W. Haul, L. Moscou, R.A. Pierotti, J. Rouquerol and T. Siemieniewska, Reporting physisorption data for gas/solid systems, Pure and Appl. Chem., 57(4) (1985) 603–619.

11 T.L. Hill, Theory of multimolecular adsorption from a mixture of gases, J. Chem. Phys., 14 (1946) 268–275.

12 T.L. Hill, Theory of multimolecular adsorption from a mixture of gases, J. Chem. Phys. (Notes), 14 (1946) 46–47.

13 L.J. Thibodeaux, K.C. Nadler, K.T. Valsaraj and D.D. Reible, The effect of moisture on volatile organic chemical gas-to-particle partitioning with atmospheric aerosols — competitive adsorption theory predictions, Atm. Environ., 25A (1991) 1649–1656.

14 K.D. Pennell, R.D. Rhue and A.G. Hornsby, Competitive adsorption of *para*-xylene and water vapors on calcium, sodium, and lithium-saturated kaolinite, J. Environ. Qual., 21 (1992) 419–426.

15 S. Brunauer, P.H. Emmett and E. Teller, Adsorption of gases in multimolecular layers, J. Am. Chem. Soc., 60 (1938) 309–319.

16 S. Brunauer, The Adsorption of Gases and Vapors, Vol. 1, Princeton University Press, Princeton, NJ, 1945, pp. 149–162.

17 A.W. Adamson, Physical Chemistry of Surfaces, Wiley, New York, 5th edn., 1990, pp. 609–614.

18 P.S.C. Rao, R.A. Ogwada and R.D. Rhue, Adsorption of volatile organic compounds on anhydrous and hydrated sorbents: equilibrium adsorption and energetics, Chemosphere, 18 (1989) 2177–2191.

19 M.D. Heilman, D.L. Carter and C.L. Gonzalez, The ethylene glycol monoethyl ether (EGME) technique for determining soil surface area, Soil Sci., 100 (1965) 409–413.

20 D.L. Carter, M.M. Mortland and W.D. Kemper, Specific surface, in A. Klute (Ed.), Methods of Soil Analysis. Part 1. Physics and Mineralogical Methods, Agronomy Monograph No. 9, ASA/SSSA, Madison, WI, 2nd edn., 1986, pp. 413–423.

21 L.J. Cihacek and J.M. Bremner, A simplified ethylene glycol monoethyl ether procedure for assessment of soil surface area, Soil Sci. Soc. Am. J., 43 (1979) 821–822.

22 D.W. Nelson and L.E. Sommers, Total carbon, organic carbon, and organic matter, in A.L. Page (Ed.), Methods of Soil Analysis. Part 2. Chemical and Microbiological Properties, Agronomy Monograph No. 9, ASA/SSSA, Madison, WI, 2nd edn., 1982, pp. 539–579.

23 P. Janitzky, Cation exchange capacity, in M.J. Singer and P. Janitzky (Eds.), Field and Laboratory Procedures Used in a Soil Chromosequence Study, U.S. Geological Survey Bulletin 1648, US Governmental Printing Office, Washington, DC, 1986.

24 G.W. Gee and J.W. Bauder, Particle-size analysis, in A. Klute (Ed.), Methods of Soil Analysis. Part 1. Physical and Mineralogical Methods, Agronomy Monograph No. 9, ASA/SSSA, Madison, WI, 2nd edn., 1986, pp. 383–411.

25 M.S. Peterson, L.W. Lion and C.A. Shoemaker, Influence of vapor-phase sorption and diffusion on the fate of trichloroethylene in an unsaturated aquifer system, Environ. Sci. Tech., 22 (1988) 571–578.

26 D.R. Shonnard, An experimental and theoretical study of the effects of environmental conditions and nonlinear adsorption on the emission rates of volatile organic compounds from contaminated soils, Ph.D. Dissertation, University of California, Davis, CA, 1991, pp. 135–141.

27 L.G. Joyner, E.B. Weinberger and C.W. Montgomery, Surface area measurements of activated carbons, silica gel, and other adsorbents, J. Am. Chem. Soc., 67 (1945) 2182–2188.

28 V. Ponec, Z. Knor and S. Cerny, in D. Smith and N.G. Adams (Eds.), Adsorption on Solids (English Trans. from Czech), Butterworths, London, 1974, chaps. 10 + 11, p. 436.

29 J.P. Quirk, Significance of surface areas calculated from water vapor sorption isotherms by use of the BET equation, Soil Sci., 80 (1955) 423–430.

30 S. Sircar, Role of adsorbent heterogeneity on mixed gas adsorption, Ind. Eng. Chem. Res., 30 (1991) 1032–1039.

31 A.T. Corey, Mechanics of Immiscible Fluids in Porous Media, Water Resources Publications, Littleton, CO, 1986, p. 55.

32 K. Verschueven, Handbook of Environmental Data on Organic Chemicals, Van Nostrand Reinhold, New York, 1977.

33 P.H. Emmett and S. Brunauer, The use of low temperature Van der Waal's adsorption isotherms in determining the surface area of iron synthetic ammonia catalysts, J. Am. Chem. Soc., 59 (1937) 1553–1564.

ELSEVIER Journal of Hazardous Materials 37 (1994) 395

JOURNAL OF HAZARDOUS MATERIALS

Erratum

Modeling multicomponent volatile organic and water vapor adsorption on soils (*Journal of Hazardous Materials*, 36 (1994) 89–108)

S. Amali, L.W. Petersen, D.E. Rolston and P. Moldrup

The name of the fourth author was mistakenly left out of the article. His name and address are:

Per Moldrup
Environmental Engineering Laboratory, Department of Civil Engineering, Aalborg University, Sohngaardsholmsvej 57, 9000 Aalborg, Denmark

Article V.

0038-075X/95/1593-0149$03.00/0
SOIL SCIENCE
Copyright © 1995 by Williams & Wilkins

March, 1995
Vol. 159, No. 3
Printed in U.S.A.

HIGH-RESOLUTION TIME DOMAIN REFLECTOMETRY: SENSITIVITY DEPENDENCY ON PROBE-DESIGN

L.W. PETERSEN,[1] A. THOMSEN,[1] P. MOLDRUP,[2] O.H. JACOBSEN,[1] AND D.E. ROLSTON[3]

When using the time domain reflectometry (TDR) technique in laboratory experiments, e.g., with packed soils columns, it is often of great importance to obtain high depth resolution with minimal disturbance of the soil and to be able to measure close to the soil surface. This requires the use of fairly small TDR probes that can be placed near each other. In laboratory experiments on packed soil, we have examined the importance of relations between the probe-rod diameter, probe-rod length, distance between probe rods, and distance from the probe to the soil surface for accurate determination of volumetric water content. The experiments were conducted on a coarse sand with three different rod diameters (1, 2, and 3 mm), three different rod spacings (10, 20, and 50 mm), two rod lengths (50 and 150 mm), and at distances to the soil surface varying from 5 to 50 mm. Theoretical work by Knight et al. (1994, Symposium and workshop on time domain reflectometry in environmental, infrastructure and mining applications, Northwestern Univ., Evanston, Illinois, Sept 7–9, 1994, pp. 93-104) has been used to evaluate the results. In general, theory and measurements agreed very well. Both measurements and theory showed that the volume of soil contributing to the measurement is highly dependent on the spacing of the rods and, to a lesser degree, on the rod diameter. For rod spacings of 10, 20, and 50 mm, measurements were accurately made as close to the soil surface as 10, 15, and 20 mm, respectively.

During the last decade, Time Domain Reflectometry (TDR) has become a widely used technique for determining the volumetric water content of soils. Initially, it was used mainly in field experiments, but now it is also a popular method in laboratory experiments (Heimovaara et al. 1993; Plagge et al. 1992; Wraith and Baker 1991), in which probe diameter and distance between probes become relevant issues.

An important question when using this technique is: What is the region of influence around TDR rods? Topp and Davis (1985) stated that parallel transmission lines having rods with a center-to-center spacing of about 50 mm are a practical compromise to obtain reasonable resolution. They suggested that the soil measured by TDR is a cylinder whose axis lies midway between the rods and whose diameter is 1.4 times the spacing between the rods. For a spacing of 50 mm, this gives a sphere of influence covering an area of 38 cm^2 in a plane perpendicular to the axis of the transmission line. Baker and Lascano (1989) presented a more detailed study of the spatial sensitivity of TDR using water-filled glass tubes placed at various distances from the TDR probe axis. For their probe design, in which TDR rods were placed 50 mm apart, they found that probes can be placed as close to the soil surface as 20 mm with little loss in accuracy. De Clerck (1985) stated that for a probe with a rod spacing of 25 mm, 94% of the energy was restricted to a cylinder with a diameter equal to 50 mm (twice the distance between the two rods). For the same rod spacing, 99% of the energy would be within a diameter of 120 mm. Knight (1992) presented a theoretical investigation of the size of the cylinder of influence. He recommended that probes be designed with a ratio of rod diameter divided by spacing of rods (B/D) to be higher than 0.1, so that too much energy will not be concentrated closely around the rods. Additionally, Knight et al. (1994) presented a design rule for using a probe near a surface. They concluded that for all values of B/D, at least 94% of the energy is below a surface of height $y = \frac{1}{2}(B + D)$ when the probe is installed with its two wires in a plane at $y = 0$ and parallel to the surface.

The objective of this work was to examine how the spatial sensitivity (volume of influence) of the TDR technique is dependent on the design of the TDR probes, i.e., length, spacing, and diame-

---

[1] Danish Ministry of Agriculture, Institute of Plant and Soil Science, Research Center Foulum, P.O. Box 23, DK-8830 Tjele, Denmark; Dr. Petersen is corresponding author.

[2] Environmental Engineering Laboratory, Dept. of Civil Engineering, Aalborg University, Sohngaardsholmsvej 57, DK-9000 Aalborg, Denmark.

[3] Soils and Biogeochemistry, Dept. of Land, Air, and Water Resources, University of California, Davis, CA 95616.

Received March 17, 1994; accepted Oct 24, 1994.

ter of probe rods. This was done in laboratory experiments on packed soil. Only relatively short, unbalanced, two-rod probes suited for laboratory experiments were investigated in this study.

THEORY

Principles of the TDR technique have been described elsewhere (e.g., Topp et al. 1980; Topp and Davis 1985; Heimovaara 1993). Figure 1 shows the TDR probe configuration for the two-rod TDR probes used in this study.

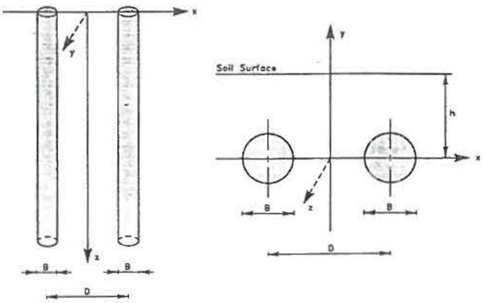

FIG. 1 TDR probe configuration. B is the diameter of the rods, and D is the center-to-center spacing between the rods.

Assuming that the soil-water content distribution differs only slightly from a uniform distribution, Knight et al. (1994) gave an approximation for the relative accumulated energy below a surface at height h above the probe axis ($h \geq \frac{1}{2} B$, $0 \leq P \leq 1$)

$$P(h,B,D) = 1 - \frac{\ln\left(1 + \frac{C_1}{h^2}\right)}{C_2}, 0 \leq P \leq 1 \quad (1)$$

where

$$C_1 = \frac{1}{4}(D^2 - B^2) \quad (2)$$

$$C_2 = 4 \ln\left(\frac{D}{B} + \sqrt{\left(\frac{D}{B}\right)^2 - 1}\right) \quad (3)$$

where B is the diameter of the rod, and D is the center-to-center distance between the rods (Fig. 1).

By inverting this equation, the critical height, h_c, below which a certain proportion, P_c, of the total energy is contained can be calculated as:

$$h_c = \sqrt{\frac{C_1}{(q - 1)}} \quad (4)$$

where

$$q = \left(\frac{D}{B} + \sqrt{\left(\frac{D}{B}\right)^2 - 1}\right)^{4(1 - P_c)} \quad (5)$$

Figure 2 illustrates the theoretical critical height $h = h_c$, below which a certain proportion, $P = P_c$, of total energy is contained. The h_c is especially dependent on rod spacing, e.g., for a 2-mm rod with $P_c = 0.95$, the critical height h_c will be 6.4, 11.0, and 22.9 mm for a spacing of 10, 20, and 50 mm, respectively. However, h_c is not as dependent on rod diameter. For a rod spacing of 1 cm, and with $P_c = 0.95$, h_c will be 5.5, 6.4, and 7.1 mm for a diameter of 1, 2, and 3 mm, respectively.

We note that by differentiating Eq. (1) with respect to h, applying the chain rule of differentiation, we determine what could be called the homogeneity or linearity of the energy distribution around the TDR probes as a function of h, B, and D:

$$\frac{dP(h,B,D)}{dh} = \frac{2}{C_2}\left(\frac{1}{h} - \frac{h}{h^2 + C_1}\right) \quad (6)$$

where C_1 and C_2 are given by Eqs. (2) and (3), respectively.

MATERIALS AND METHODS

The soil used in the experiments was a coarse sand (mixed, mesic, Orthic Haplohumod). It was collected from the top 20 cm of an agricultural field on the Danish Ministry of Agriculture's Experimental Field station in Lundgaard, Denmark. The soil was air dried, passed through a 2-mm sieve (No. 10), and mixed thoroughly to obtain a homogeneous mixture. Some characteristics of the soil are given in Table 1.

All measurements in this study were made with a Tektronix 1502B cable tester (Tektronix Inc., Beaverton, Oregon) equipped with an RS 232 computer interface (Tektronix model SP232 option port module). The transmission lines consisted of 2-m-long, 50-Ω coaxial cable leading from the cable tester directly to the two-rod probes, without impedance-matching balun between the rods and the coaxial cable (i.e., unbalanced probes). Eighteen different probes were fabricated. They differed regarding rod diameter (1, 2, and 3 mm), rod length (50 and 150 mm), and rod spacing (1, 2, and 5 cm). The probes were made of stainless-steel rods with the ends installed in a small Deldrin block. Holes were drilled in the Deldrin blocks, and the rods were

TABLE 1

Characteristics of the soil used in the experiments

Lundgaard Coarse Sand	
Sand/silt/clay (%)	80.2/13.2/4.8
Organic carbon (%)	1.12
Particle density (g/cm^3)	2.63
Surface area (m^2/g)	10.84
Bulk density (g/cm^3)	1.4
pH	6.1
CEC (meq/100g)	8.78
EC (milli-mhos/cm)	0.21

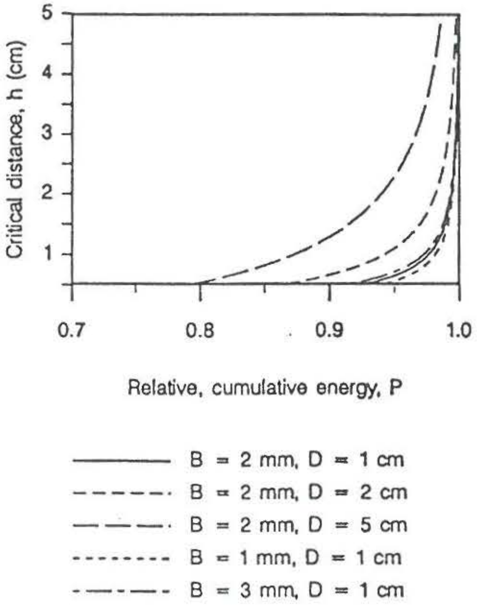

FIG. 2 Theoretical critical height below which a certain proportion of total energy is contained (calculated using Eqs. (4) and (5)).

inserted in the holes and soldered to the cable ends and then locked into place by filling the holes with a two-component adhesive, ensuring that the probes were waterproof. When cable and rods are soldered together inside the Deldrin block, the impedance of the transmission line increases sharply, resulting in a well defined trace segment. This reflection is used for locating the approximate beginning of the measuring probe. The true beginning, though, is offset by a small time difference proportional to the rod length embedded in the Deldrin block. This offset (Δt_0) [s] is a probe property (Heimovaara 1993). The electrical length of the probe embedded in soil (L) [m] is also a probe property. The shift and the electrical length of the probe were determined by measuring the travel time in air and in water at a known temperature as described by Heimovaara (1993). The travel time in the probe between the first reflection and the reflection from the open end (Δt_p(s)) is:

$$\Delta t_p=\Delta t_0+\Delta t_s=\Delta t_0+2L\sqrt{K_a}/c \qquad (7)$$

where K_a is the apparent dielectric constant, and c is the speed of light (m/s) in free space. The Δt_0 and L can be determined by substituting the correct values for K_a into Eq. (7). It is assumed that K_a for air is 1 (Weast 1980) and that K_a for water at a specific temperature can be determined from (Hasted 1973)

$$K_a=87.749-0.40008T+9.398\times10^{-4}T^2 -1.410\times10^{-6}T^3 \qquad (8)$$

where T is temperature (°C). For each probe, L and Δt_0 were used along with the empirical calibration function from Topp et al. (1980) when calculating the volumetric water content.

The soil was packed in a plastic box constructed such that the bottom could be moved upward with a small hydraulic jack with minimum disturbance of the soil. By raising the bottom and scraping off the excess soil extending above the top of the box, the installed probe was moved toward the soil surface. The bottom was raised in increments of 5 mm, and measurements were made at distances to the soil surface varying from 50 to 5 mm.

For every experiment, the box was packed with soil having a water content of W = 0.15 g H_2O/g soil, to a bulk density of 1.4. A probe was installed using specially fabricated guides to ensure the best installment possible. For every depth increment, five measurements of water content were performed. This was repeated for all 18 probes.

The TDR trace analysis was done automatically by a computer program (Thomsen 1994; available from the Danish Institute of Plant and Soil Science, Tjele, Denmark). The software, developed in Turbo Pascal and used for the analysis, is based on the work by Baker and Allmaras (1990), Heimovaara and Bouten (1990), and Thomsen and Schjønning (1994). The analysis included the following steps (see also Fig. 3, which shows an example of the TDR-trace output with indications of the following points 1–6):

1. The input trace is filtered using a moving average filter
2. The local slope (first derivative) of the smoothed trace is calculated

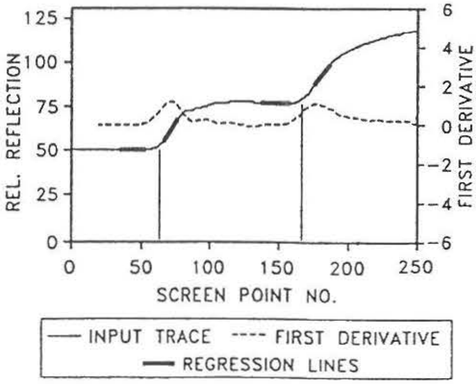

FIG. 3 Trace from cable tester. For explanation of TDR trace analysis, see points (1)–(6) in text.

3. x-values of the global minimum and maximum points on the first derivative curve are located
4. Regression lines are fitted to sections of the original trace, centered on the x-values of the first derivative curve maximum point
5. The initial reflection is located where the first regression line intersects a horizontal line through the minimum point of the initial reflection
6. The final reflection (end of transmission line) is located where the second regression line intersects a line following the trace segment before the final reflection.

RESULTS AND DISCUSSION

Figure 4 shows the measured dependency on rod diameter for 15-cm-long rods with a spacing of 1 cm. The critical height is not greatly affected by diameter, at least for the three fairly small diameters used in this work. This is also in agreement with Fig. 2. In a field situation, larger diameters might be desirable, and in that case the critical height might be affected. Scatter in the measurements increased slightly with increasing rod spacing and drastically with decreasing rod length (results not shown). This might be explained partly by the experience that probes with large rod spacings and small diameters are more difficult to accurately install. Also, Knight (1992) concluded that rod diameter should be as large as possible compared with the rod spacing to minimize the so called "skin-effect" with high energy density around the rods, resulting in local nonuniformities close to the rods having great effect on the determined water content. Measurement inaccuracy with short rods is attributable to much shorter pulse travel time. Therefore, errors with short probes will be larger than those with longer probes, and we suggest that probes be designed as long as practically possible.

Figure 5 shows the dependency on rod spacing for TDR-probes with 15-cm-long rods having diameters of 1, 2, and 3 mm. The relative soil-water content, S, is determined as the measured soil-water content at any specific depth divided by the soil water content measured at the 5-cm depth. Every plotted point is an average of five determinations of the volumetric soil-water content.

In general, the critical height decreases with decreasing spacing of rods (see Fig. 5). In situations where good depth resolution and measurements close to the soil surface are required, the smallest rod spacing possible should be used. It was possible, with minimal loss of accuracy, to place TDR probes as close to the surface as 1, 1.5, and 2 cm for probes with rod spacing of 1, 2, and 5 cm, respectively. The result for a rod spacing of 5 cm is in agreement with that found by Baker and Lascano (1989) for a probe with similar rod spacing. The solid lines in Fig. 5 (determined from Eqs. (1) through (5)) give the relative accumulated energy as a function of the critical height. It is evident that the theoretical critical height, h_c, agrees very well with the measured values. The reason the theory for balanced

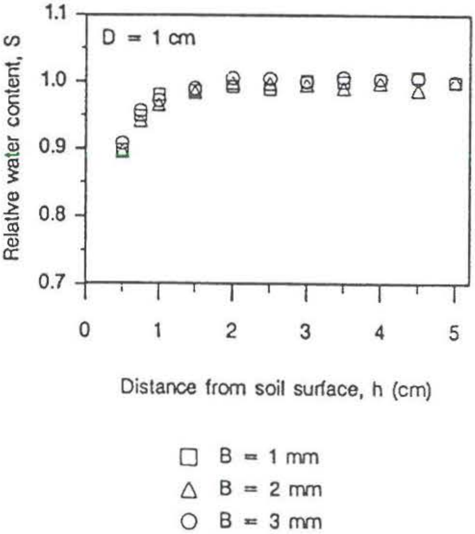

FIG. 4 Depth resolution dependency on TDR rod diameter.

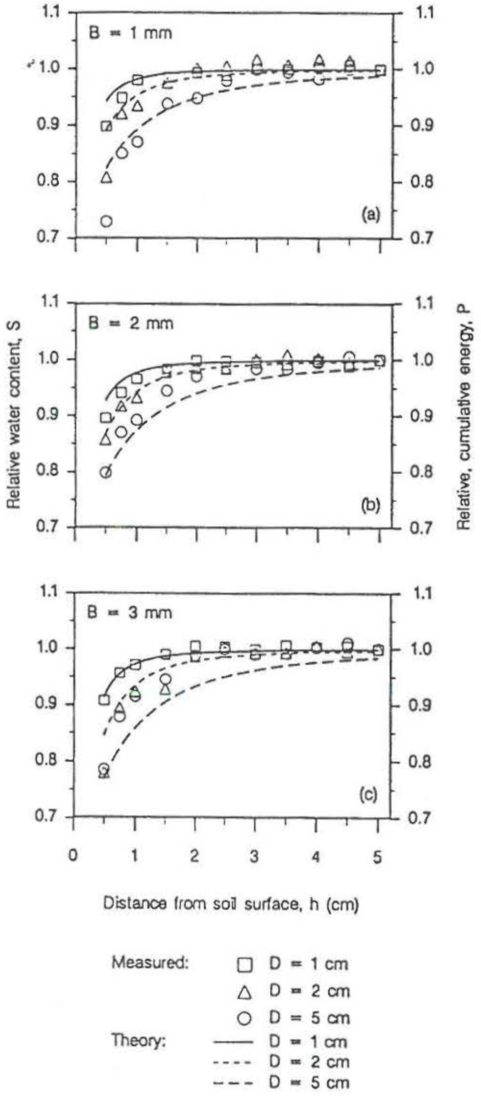

FIG. 5 Depth resolution dependency on TDR rod spacing. Theoretical curves are calculated using Eqs. (1)–(5).

probes agrees well with the measurements performed in the present study— with unbalanced probes—is because the unbalanced character probably does not have a major effect on the relative sensitivity in the vertical dimension for horizontally installed, unbalanced, two-rod probes. In the horizontal plane, though, most of the sensitivity resides in the vicinity of whichever waveguide is connected to the central conductor. This should be taken into account if probes are installed in small scale laboratory setups with short horizontal distances to, e.g., a column wall or if probes are installed with the rods placed on top of each other instead of next to each other, even though this would be rather unusual.

The volume of influence will be asymmetric in the vertical plane for both balanced and unbalanced probes for cases in which probes are placed close to a surface. This effect can be illustrated clearly by placing a TDR-probe at the soil surface, with half the diameter of the probe embedded in soil and the other half in free air; a determination of water content will not be 0.5 of a determination in which the probe is totally embedded in soil. The measured water content will instead be between 0.6 and 0.7 of an embedded probe because the probe "weighs" the contribution from the soil highest as a result of higher impedance in air than in soil.

Knight et al. (1994) states the probe-design rule that B/D should not be less than 0.1. We agree, as mentioned above, that one should attempt to have as large a rod diameter as possible compared with rod spacing. In the case of laboratory column experiments, one important option, though, is to minimize the disturbance of the soil. A small diameter (B) is thus desirable. We found good determination of water content with B/D = 0.02, but we agree that the smaller this ratio, the more caution should be taken during installation. When a small volume of influence is desired (i.e., good depth resolution), D should be as small as possible, which results in a higher B/D and subsequently less "skin-effect."

Figure 6 illustrates an example of what can be called the homogeneity of the energy distribution around the TDR-probes. The solid lines arise from Eqs. (6), (2), and (3) and the symbols from finding arithmetically the slope of the measured S values at two consecutive (neighboring) measurement points. This value is referred to an h value in between h values of the two measurement points. The shown data is for 15-cm rods with a diameter of 0.2 cm and three different spacings. Both data and theory show a fairly heterogeneous energy distribution, with a steep increase in energy close to the probes corresponding to the major part of the energy being located closely around the probes. Again, a good agreement between measured and calculated curves is seen.

CONCLUSIONS

By careful design, small TDR probes can be used in laboratory experiments where high reso-

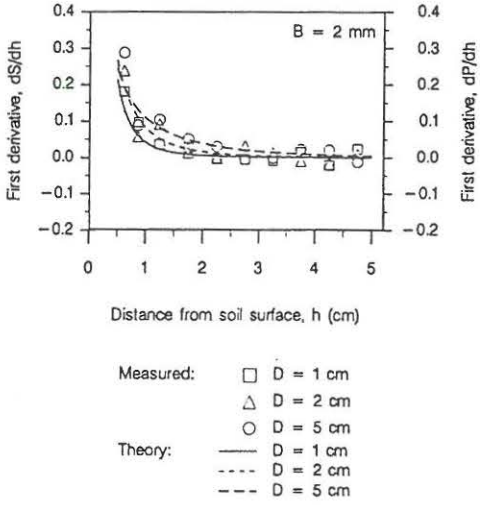

FIG. 6 Predicted and measured homogeneity of the energy distribution around TDR probes. Comparison of the theoretical dP/dh (Eqs. (6), (2), and (3)) and measured ds/dh first derivative.

lution is required, especially when computer software is used for analyzing TDR traces, making measurements fast and accurate.

The sphere of influence around the TDR rods is fairly independent of rod diameter (B) but highly dependent on rod spacing (D). The smaller the rod spacing, the higher the resolution and the closer measurements can be made to the soil surface. Good determination of water content was found with B/D as small as 0.02.

For rod spacings of 1, 2, and 5 cm, measurements were accurately made as close to the soil surface as 1, 1.5, and 2 cm, respectively, which is in excellent agreement with the theory presented by Knight et al. (1994).

ACKNOWLEDGMENTS

This research was supported by the Danish Environmental Protection Agency, the Danish Ministry of Agriculture, the Danish Research Academy, and the U.S. EPA (R819658) Center for Ecological Health Research at U.C. Davis. Although the information in this document has been funded in part by the United States Environmental Protection Agency, it may not necessarily reflect the views of the Agency and no official endorsement should be inferred. The authors want to sincerely thank Dr. J.H. Knight for providing us with a pre-print of the article "Sampling Volume of TDR probes used for Water Content Monitoring," which is published in the Proceedings of Symposium and Workshop on Time Domain Reflectometry, North Western University, Evaston, Illinois, Sept. 7–9, 1994.

REFERENCES

Baker, J. M., and R. R. Allmaras. 1990. System for automating and multiplexing soil moisture measurements by time-domain reflectometry. Soil Sci. Soc. Am. J. 54:1–6.

Baker, J. M., and R. J. Lascano. 1989. The spatial sensitivity of time-domain reflectometry. Soil Sci. 147:378–384.

De Clerck, P. 1985. Mesure de l'evolution de la teneur en eau des sols par voie electromagnetique. Tech. Routiere 3:6–15.

Hasted, J. B. 1973. Aqueous dielectrics. Chapman and Hall Ltd., London, p. 302.

Heimovaara, T. J., and W. Bouten. 1990. A computer-controlled 36-channel time domain reflectometry system for monitoring soil water contents. Water Resour. Res. 26:2311–2316.

Heimovaara, T. J. 1993. Time domain reflectometry in soil science: Theoretical backgrounds, measurements and models. Ph.D. Thesis, University of Amsterdam, Amsterdam, The Netherlands.

Heimovaara, T. J., J. I. Freijer and W. Bouten. 1993. The application of TDR in laboratory column experiments. Soil Technol. 6:261–272.

Knight, J. H. 1992. Sensitivity of time domain reflectometry measurements to lateral variations in soil water content. Water Resour. Res. 28:2345–2352.

Knight, J. H., I. White, and S. J. Zegelin. 1994. Sampling volume of TDR probes used for water content monitoring. Symposium and workshop on time domain reflectometry in environmental, infrastructure and mining applications, Northwestern University, Evanston, Illinois, Sept. 7–9, 1994.

Plagge, R., C. H. Roth, and M. Renger. 1992. A new laboratory method to rapidly determine the unsaturated soil hydraulic properties. *In*: M. Th. van Genuchten, F. J. Leij, and L. J. Lund (eds.). Proceedings of the international workshop on indirect methods for estimating the hydraulic properties of unsaturated soils. Riverside, California, October 11–13, 1989, pp. 653–663.

Thomsen, A. 1994. Program AUTOTDR for making automated TDR measurements of soil water content. User's guide. Internal document, Danish Institute of Plant and Soil Science. Dept. of Soil Physics, Tjele, Denmark.

Thomsen, A., and P. Schjønning (eds.). 1994. Time domain reflectometry (TDR): Aspects of its application to field measurements of soil water content. (In preparation).

Topp, G. C., J. L. Davis, and A. P. Annan. 1980. Electromagnetic determination of soil water content: Measurements in coaxial transmission lines. Water Resour. Res. 16:574–582.

Topp, G. C., and J. L. Davis. 1985. Time-domain reflectometry (TDR) and its application to irrigation scheduling. *In* Advances in irrigation 3:107–127. D. Hillel (ed.). Academic Press, New York.

Weast, R. C. 1980. Handbook of physics and chemistry, 60th Ed. CRC Press, Boca Raton, FL, pp. E58–61.

Wraith, J. M., and J. M. Baker. 1991. High resolution measurement of root water uptake using automated time-domain reflectometry. Soil Sci. Soc. Am. J. 55:928–932.

Article VI.

0038-075X/94/1581-0014$03.00/0
Soil Science
Copyright © 1994 by Williams & Wilkins

July 1994
Vol. 158, No. 1
Printed in U.S.A.

A SEMI-ANALYTICAL SOLUTION FOR ONE-DIMENSIONAL SOLUTE TRANSPORT IN SOILS[1]

T. YAMAGUCHI,[2] P. MOLDRUP,[3] D. E. ROLSTON,[4] AND L. W. PETERSEN[5]

Analytical solutions to the convection-dispersion model (CDM) of solute transport require linear reaction terms, strict initial and boundary concentration conditions, and are often complex to evaluate because of the inherent mathematical functions. We present a flexible and mathematically very simple solution to the CDM at steady water flow, labeled a semi-analytical (SA) solution. The SA solution allows for nonlinear reaction terms, variable initial and boundary conditions, and is based on the recently presented moving concentration slope (MCS) model for solute transport. To derive the SA solution, a solute flux approximation at the upper boundary and a small, constant depth increment of 0.5 cm are used, and two features of the MCS model are exploited, i.e., an explicit, depth-integrated flux equation is already inherent in the model and all numerical error and stability equations are unique functions of the solute unit mean travel distance (SUMTD). The SA solution contains seven constants; one is the solute dispersivity, and the remaining six are functions only of the SUMTD. Excellent agreement between the SA solution and ordinary analytical solutions to the CDM was obtained. For variable boundary conditions, the SA solution was also tested against data for chloride transport in sandy soil columns. Measured and calculated outlet concentrations compared well. The SA model allows for linear or nonlinear reaction terms without increasing the complexity of the solution. In the case of nonlinear reactions, the SA model offers a simple solution in situations where conventional analytical solutions are not available. This was illustrated by successfully comparing the SA solution, including a Michaelis-Menten reaction term, with measured data for simultaneous transport and reduction of nitrate in porous media columns.

Recently, we have presented a number of numerically simple but accurate models for transport processes in soil systems (Yamaguchi et al. 1992; Moldrup et al. 1989, 1992, 1993). Although easy to program and apply, these models still require the use of a traditional numerical calculation procedure, i.e., with special concern toward calculating the correct boundary fluxes and continuous control of numerical stability. In contrast, analytical solutions represent explicit functions to be solved directly but require strict boundary and initial conditions and evaluation of fairly complex mathematical functions (erfc, Bessel and others) that can represent problems at certain combinations of parameter values, time, and soil depth (van Genuchten 1985). Also, analytical solutions are not available in the case of nonlinear terms for adsorption, decay, and production.

The purpose of the present study was to derive a flexible, semi-analytical solution for solute transport, at steady water flow, that gives an accurate solution, avoids the use of complex mathematical functions, and allows for nonlinear reaction terms and variable initial and boundary solute concentrations. The derivation was based on the Moving Concentration Slope (MCS) solute transport model using the reasoning that i) all the numerical stability and error terms for the MCS model are unique functions of the pore-water velocity (u) times the time increment (Δt) "regardless of the individual values of u and Δt" (Moldrup et al. 1992); ii) numerical dispersion is efficiently removed in

---

[1] Contribution from Hiroshima University, Aalborg University, University of California, Davis, and Research Centre Foulum.

[2] Dept. of Civil and Environmental Engineering, Faculty of Engineering, Hiroshima University, 1-4-1 Kagamiyama, Higashi-Hiroshima, 724 Japan.

[3] Environmental Engineering Laboratory, Dept. of Civil Engineering, Aalborg University, Sohngaardsholmsvej 57, DK-9000 Aalborg, Denmark.

[4] Soils and Biogeochemistry, Dept. of Land, Air, and Water Resources, University of California, Davis, CA 95616, USA.

[5] Danish Ministry of Agriculture, Institute of Plant and Soil Science, Research Centre Foulum, P.O. Box 23, DK-8830 Tjele, Denmark.

Received Sept. 13, 1993; accepted Feb. 22, 1994.

the MCS model; and iii) an explicit, depth-integrated flux equation is already inherent in the MCS model.

DERIVATION OF A SEMI-ANALYTICAL (SA) SOLUTION

Solute transport and transformations are traditionally described by the convection-dispersion model (CDM), including a reaction term. The governing flux and continuity equations in case of steady water flow are, Eqs. (1) and (2),

$$J = -D\frac{\partial c}{\partial z} + uc \tag{1}$$

$$\frac{\partial c}{\partial t} = -\frac{\partial J}{\partial z} - S \tag{2}$$

where c is the solute concentration (mg L^{-1}), J is the solute flux (cm mg h^{-1} L^{-1}), u is the pore-water velocity (cm h^{-1}, assumed constant), D is the dispersion coefficient (cm^2 h^{-1}, assumed constant), t is time (h), z is soil depth (cm) and S is the solute removal rate (mg L^{-1} h^{-1}).

The MCS solution of Moldrup et al. (1992) to the CDM is shown in Eqs. (3)–(5),

$$J^t_{z+\frac{1}{2}\Delta z} = -\left(\frac{u}{e^{(u/D)\Delta z}-1} - \frac{D_{\text{num}}}{\Delta z}\right) \cdot (c^t_{z+\Delta z} - c^t_z) + uc_z{}^t \tag{3}$$

$$D_{\text{num}} = u\frac{\Delta z}{2} - u^2\frac{\Delta t}{2} + \frac{u\Delta z}{e^{(u/D)\Delta z}-1} - D \tag{4}$$

$$c_z{}^{t+\Delta t} = c_z{}^t + (J^t_{z-\frac{1}{2}\Delta z} - J^t_{z+\frac{1}{2}\Delta z})\frac{\Delta t}{\Delta z} - S_z{}^t\Delta t \tag{5}$$

where D_{num} is the numerical dispersion coefficient (cm^2 h^{-1}), which corrects the model for the artificial dispersion created by the calculation scheme itself; $\Delta t(h)$ is the time increment and Δz (cm) is the depth increment used in the calculations; the superscript t denotes time, the subscript z denotes depth (i.e., $J_{z+1/2\Delta z}$ is the solute flux on the grid boundary between the consecutive calculation depths z and $z + \Delta z$ in the soil profile); the power term $(u/D)\Delta z$ in Eq. (3) is equal to the Peclet number; and Eq. (3) represents the solute flux equation (Eq. (1)) integrated with respect to soil depth.

To enable the derivation of a simple, closed-form solution, the solute flux at the soil surface ($z = 0$) was approximated using Δz instead of 1/2 Δz in the first parenthesis of Eq. (3). Using 1/2 Δz was proposed by Moldrup et al. (1992) and corresponds to the distance between the soil surface and the first calculation point within the soil profile. However, both strategies are essentially non-accurate due to the ever-occurring upper boundary problem, i.e., the concentration and flux calculation points are both placed at the soil surface, which makes an approximation of the flux (Eq. (3)) and continuity (Eq. (5)) calculations necessary if a numerical solution is applied. Initial comparisons between the MCS model (using the two different flux approximations) and analytical solutions to the CDM showed that if $\Delta z \leq 0.5$ cm, the herein suggested flux approximation did not introduce significant errors compared with the flux approximation of Moldrup et al. (1992). Both MCS solutions yielded an accumulated error in concentration typically <1%, which was considered sufficiently accurate for most applications.

Using this suggested flux approximation at the soil surface, together with a small, constant $\Delta z = 0.5$ cm, and introducing the solute dispersivity (β) and the solute unit mean travel distance (Φ),

$$\beta = \frac{D}{u}\ (\text{cm}), \qquad \Phi = u\Delta t\ (\text{cm}) \tag{6}$$

the combined Eqs. (3)–(6) simply reduce to

$$\begin{aligned} c_z{}^{t+\Delta t} = {} & c_z{}^t - 2\,\Phi c_z{}^t + 4\Phi(0.5 - \Phi - 2\beta)c_z{}^t \\ & + 2\Phi c^t_{z-0.5} - 2\Phi(0.5 - \Phi - 2\beta)c^t_{z-0.5} \\ & - 2\Phi(0.5 - \Phi - 2\beta)c^t_{z+0.5} - S_z{}^t\Delta t \end{aligned}$$

i.e.,

$$\begin{aligned} c_z^{t+\Delta t} = {} & (\Phi + 2\Phi^2 + 4\Phi\beta)c^t_{z-0.5} \\ & + (1 - 4\Phi^2 - 8\Phi\beta)c_z{}^t \\ & + (-\Phi + 2\Phi^2 + 4\Phi\beta)c^t_{z+0.5} - S_z{}^t\Delta t \end{aligned} \tag{7}$$

where the time increment Δt must be chosen as (cf. Eq. (6))

$$\Delta t = \frac{\Phi}{u}\ (h) \tag{8}$$

Writing Eq. (7) in closed form gives the following expression for the solute concentration profile after $N_{\max}$ time steps, i.e., after $t = N_{\max}\ \Delta$t

$= N_{\max} \Phi/u,$

$$\begin{aligned} c_z^{N_{\max}\Delta t} = \sum_{N=1}^{N_{\max}} \sum_{z=0.5}^{z_{\max}} [(K_1 + K_2\beta) c_{z-0.5}^{(N-1)\Delta t} \\ + (K_3 + K_4\beta) c_z^{(N-1)\Delta t} \\ + (K_5 + K_6\beta) c_{z+0.5}^{(N-1)\Delta t} \\ - S_z^{(N-1)\Delta t} \cdot \Delta t] \end{aligned} \tag{9}$$

$K_1 = \Phi + 2\Phi^2$

$K_2 = 4\Phi$

$K_3 = 1 - 4\Phi^2$

$K_4 = -8\Phi$

$K_5 = -\Phi + 2\Phi^2$

$K_6 = 4\Phi$

where $N[1,2,3, \ldots, N_{\max}]$ is an integer representing the time step number, each time step is equal to Φ/u (h), and z $[0.5,1.0,1.5,..z_{\max}]$ are the soil distances (cm) under consideration. It is noticed that Eq. (9) also provides the temporal variation in solute concentration at any soil distance under consideration. We label the new solution semi-analytical (SA) because of the summation terms in Eq. (9) that makes an evaluation from time $t = 0$ necessary and, also, the inherent integrated flux equation (Eq. (3)). The latter is a parallel to the classical semi-analytical (or quasi-analytical) solutions for water infiltration problems (e.g., Philip and Knight 1974; Philip 1987).

Analytical solutions for simultaneous transport and nonlinear transformations are not available. Because of the separate reaction term in Eq. (9), the SA solution can easily incorporate any linear or nonlinear expressions for solute transformations without making the solution more complex. For example, in the case of a solute undergoing first-order adsorption, decay following Michaelis-Menten kinetics, and zero-order production, the reaction term of Eq. (9) simply becomes

$$S_z^{(N-1)\Delta t} \cdot \Delta t = \left(k_1 c_z^{(N-1)\Delta t} + \mu_{\max} \frac{c_z^{(N-1)\Delta t}}{K_m + c_z^{(N-1)\Delta t}} - k_0 \right) \frac{\Phi}{u} \tag{10}$$

where, for the processes under consideration, k_1 is the first order reaction rate coefficient (h^{-1}), $\mu_{\max}$ is the maximum reaction rate (h^{-1}), K_m is the Michaelis-Menten coefficient (mg L^{-1}), and k_0 is the zero order reaction rate coefficient (mg L^{-1} h^{-1}). Thus, any combination of linear and nonlinear processes can be accommodated.

The lower soil depth ($z_{\max}$) to be used in Eq. (9) should be chosen so the lower boundary is placed sufficiently deep to avoid any effects on the calculations. Based on our experiences, we recommend choosing

$$\begin{aligned} z_{\max} > \left(2 + \frac{D}{u}\right) N_{\max} u \Delta t \\ = (2 + \beta)\Phi N_{\max} \quad \text{(cm)} \end{aligned} \tag{11}$$

where $N_{\max}$ u Δt represents the mean travel distance of the solute front, the factor $(2 + D/u)$ represents a maximum additional travel distance for some of the solute due to hydrodynamic dispersion, and where u and D are in units of cm h^{-1} and cm^2 h^{-1}, respectively. In cases of long-term or rapid flow simulations where the $z_{\max}$ value cf. Eq. (11) would become nonfeasibly large, a lower boundary condition of $c^t_{z_{\max}-0.5} = c^t_{z_{\max}}$ at a depth well outside the zone of interest (e.g., $z_{\max} = 300$ cm for simulation of a 100 cm soil column) could conveniently be used instead.

To use the SA solution (Eq. (9)), the initial ($c_z^{t=0}$) and boundary ($c^t_{z=0}$ and $c^t_{z=z_{\max}}$) solute concentrations and the values of the solute dispersivity (β) need to be known a priori, and a value of the solute unit mean travel distance (Φ) that does not introduce instability in the calculations must be chosen.

CHOICE OF Φ VALUE

The value of Φ to be used in Eq. (9) is chosen on the basis of the three numerical stability criteria for the MCS model (Moldrup et al. 1992),

$$\Delta t < \frac{\Delta z}{u} \frac{e^{(u/D)\Delta z} - 1}{e^{(u/D)\Delta z} + 1} \tag{12}$$

$$u\frac{\Delta t}{\Delta z} < 0.3 \tag{13}$$

$$\left| \frac{D_{\text{num}}}{D} \right| < 2 \tag{14}$$

Inserting Eqs. (2) and (4) and $\Delta z = 0.5$ cm in Eqs. (12)–(14) and rearranging yields

Criterion 1:

$$\Phi < 0.5 \frac{e^{0.5/\beta} - 1}{e^{0.5/\beta} + 1} \tag{15}$$

Criterion 2:

$$\Phi < 0.15 \tag{16}$$

Criterion 3:

$$-2 < \frac{1}{\beta}\left(0.25 + \frac{0.5}{e^{0.5/\beta} - 1}\right) - \frac{1}{\beta}(0.5\Phi + \beta) < 2 \tag{17}$$

These three criteria must all be observed when using the semi-analytical solution. Criterion 3 will normally be observed except in cases of very small β values ($\ll 1$ cm). This is seen by using the series approximation for the exponential function,

$$e^x = 1 + \frac{x}{1!} + \frac{x^2}{2!} + \frac{x^3}{3!} + \frac{x^4}{4!} \ldots\ldots \tag{18}$$

in Criterion 3 yielding

$$-2 < \frac{0.25}{\beta} + \frac{1}{1 + \frac{(0.5/\beta)^1}{2!} + \frac{(0.5/\beta)^2}{3!} + \frac{(0.5/\beta)^3}{4!} \ldots} - 0.5\,\frac{\Phi}{\beta} - 1 < 2 \tag{19}$$

which will always be fulfilled for small Φ values (we recall that Φ must be <0.15 cm, cf. Criterion 2) and $\beta \geq 0.25$ cm. Hence, only for small β values ($\beta < 0.25$ cm) is it necessary to insure that Criterion 3 is observed.

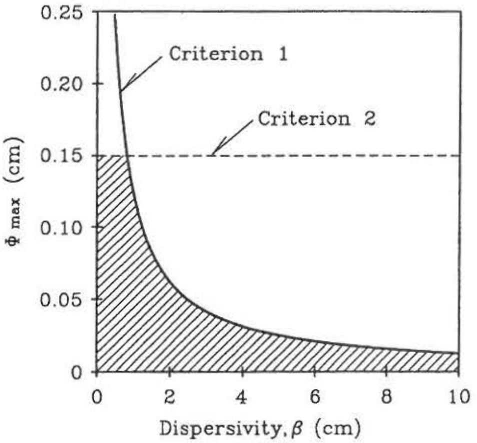

FIG. 1. Maximum allowable value of the solute unit mean travel distance (Φ_{max}) to be used in the semi-analytical solution (Eq. (9)) according to the stability criteria of Eqs. (15) and (16). The shaded area represents Φ values that ensure numerical stability.

Criteria 1 and 2 as functions of β are shown in Fig. 1. Criterion 1 is the stricter criterion for $\beta > 0.8$ cm. However, it is not convenient for each transport experiment and, thus, for each new β value to find the optimal Φ value from Criteria 1 and 2 and then calculate the new values of the six constants K_1–K_6 to be used. Instead, based on Criteria 1 and 2, Table 1 shows recommended values of Φ and K_1–K_6 for different β intervals. For example, if a number of transport experiments are to be simulated and $\beta < 2.5$ cm in all cases, a Φ value of 0.05 cm and

TABLE 1

Recommended values of the solute unit mean travel distance ($\Phi = u\,\Delta t$) and the corresponding values of the constants K_1–K_6 to be used in the semi-analytical solution (Eq. (9)) for different intervals of the solute dispersivity ($\beta = D/u$)

β	Φ	K_1	K_2	K_3	K_4	K_5	K_6
cm	*cm*						
<1[a]	0.12	0.1488	0.48	0.9424	−0.96	−0.0912	0.48
<1.5	0.08	0.0928	0.32	0.9744	−0.64	−0.0672	0.32
<2	0.06	0.0672	0.24	0.9856	−0.48	−0.0528	0.24
<2.5	0.05	0.0550	0.20	0.9900	−0.40	−0.0450	0.20
<3	0.04	0.0432	0.16	0.9936	−0.32	−0.0368	0.16
<4	0.03	0.0318	0.12	0.9964	−0.24	−0.0282	0.12
<6	0.02	0.0208	0.08	0.9984	−0.16	−0.0192	0.08
<12.5	0.01	0.0102	0.04	0.9996	−0.08	−0.0098	0.04

[a] For $\beta < 0.25$ cm, $\Phi = 0.12$ cm can be used only if Eq. (17) is observed. If Eq. (17) is not observed, a Φ value < 0.12 that observes Eq. (17) must be used instead.

the corresponding values of K_1–K_6 can conveniently be used for all calculations.

TEST OF SA SOLUTION AT CONSTANT CONCENTRATION BOUNDARY CONDITION

The semi-analytical solution was tested against the analytical solution to the CDM of solute transport by Lapidus and Amundson (1952; also cf. Eq. (3) of Yamaguchi et al. 1989) for the initial and boundary conditions,

$$c_z^{t=0} = 0;\ c_{z=0}^t = 200 \text{ mg L}^{-1};\ c_{z=z_{\max}}^t = 0 \qquad (20)$$

Excellent agreement between the SA solution (Eq. (9)) with $S_z{}^t = 0$ and the solution of Lapidus and Amundson (1952) was obtained for a wide range of parameter values. Figure 2 shows an example of one test using $\Phi = 0.05$ cm for two different β values <2.5 cm (choice of Φ value cf. Table 1).

For the same boundary conditions (Eq. (20)) and with various values of the first order reaction rate coefficient (k_1), the semi-analytical solution with $k_0 = 0$ and $\mu_{\max} = 0$ in Eq. (10) was tested against the analytical solution of van Genuchten (1985; also cf. Eq. (5) of Yamaguchi et al. 1992). Also in this case, excellent agreement was obtained for a wide range of k_1 values (not shown).

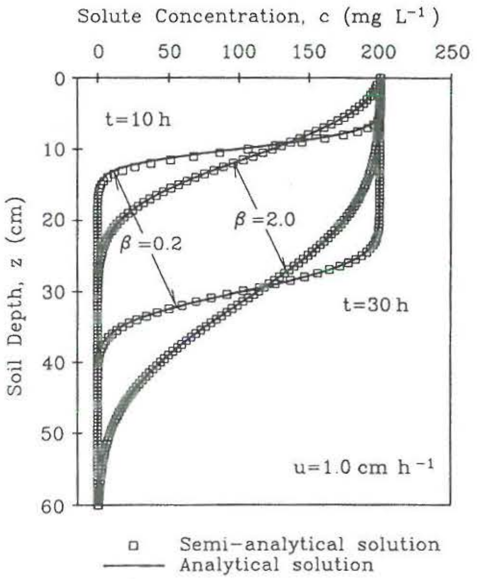

FIG. 2. Test of the semi-analytical solution (Eq. (9) with $\Phi = 0.05$ cm) against an analytical solution. Test conditions: Constant upper boundary condition (cf. Eq. (20)).

TEST OF SA SOLUTION AT VARIABLE CONCENTRATION BOUNDARY CONDITION

To illustrate the use of the semi-analytical solution and, also, test it for variable upper boundary conditions, the solution with $S_z{}^t = 0$ was compared with

1) a data set for chloride transport in an unsaturated, sandy soil from Hiroshima, Japan (packed column, 20 cm in diameter and 50 cm in length, temperature $T = 10$°C) used in the study of Yamaguchi et al. (1994, manuscript submitted);
2) data for chloride transport in an unsaturated, sandy soil from Jyndevad (Southern Jutland), Denmark (packed columns, 6.75 cm in diameter and 50 cm in length, temperature $T = 30$°C) measured during this study;
3) the analytical solution of Lapidus and Amundson (1952) modified for a quasi-stationary input function corresponding to the upper boundary condition of the column experiments (cf. Eqs. (21) and (22)).

The experimental conditions and the physical and chemical properties of the Hiroshima coarse sand (texture: <0.1% organic matter, 0.8% clay and silt, and 99.2% sand) were given by Yamaguchi et al. (1990, 1994). The soil-water content during steady-state flow was 0.31 cm^3 cm^{-3}. The pore-water velocity (u = 3.2 cm h^{-1}) and the dispersion coefficient (D = 3.1 cm^2 h^{-1}) were simultaneously estimated from the solute breakthrough curve (for z = 50 cm and t < 30 h) by the method of Yamaguchi et al. (1989). Hence, the solute dispersivity $\beta = D/u = 0.97$ cm. The experiment was performed under the initial and boundary conditions

$$\begin{aligned} &c_z^{t=0}=0 \\ &c_{z=0}^t=c_s=400\,\text{mg chloride L}^{-1} \quad && t\le 43\,\text{h} \\ &c_{z=0}^t=0 && t>43\,\text{h} \\ &c_{z=z_{\max}}^t=0 \end{aligned} \qquad (21)$$

Three replicate, rapid infiltration experiments with the Jyndevad sand (packed homogeneously to a bulk density of 1.4 g cm^{-3}) were carried out according to the procedure described by van Genuchten and Wierenga (1986). The Jyndevad sand (texture: 4% organic matter, 8%

clay and silt, and 88% sand) was the same as used in the soil-water sorptivity study of Moldrup et al. (1994). The soil-water content during steady-state flow was 0.30 cm^3 cm^{-3}. The pore-water velocity (u = 7.5 cm h^{-1}) and the dispersivity (β = 0.8 cm) were obtained by fitting the semi-analytical solution (Eq. (9)) to the first of the three measured solute breakthrough curves (i.e., for z = 50 cm and t < 12 h; Column no. 1 in Fig. 4) by conventional least mean squares technique. The three experiments were performed under the initial and boundary conditions

$$\begin{aligned} &c_z^{t=0}=0 \\ &c_{z=0}^{t}=c_S=700\,\text{mg chloride L}^{-1} && t\leq 9.17\,\text{h} \\ &c_{z=0}^{t}=0 && t>9.17\,\text{h} \\ &c_{z=z_{\max}}^{t}=0 \end{aligned} \qquad (22)$$

As can be seen from Fig. 3 (Hiroshima sandy soil) and Fig. 4 (Jyndevad sandy soil), good agreement was obtained between the measured data and the semi-analytical solution (Eq. (9) with Φ = 0.12 equal to the recommended Φ value in Table 1 for β < 1 cm). The CDM is not able to simulate the tailing of the solute "breakdown curves," most pronounced for the Hiroshima sandy soil (t > 60 h). The discrepancies are probably due to a small amount of immobile water that can be present even in a sandy soil (Wierenga and van Genuchten 1989). The SA solution and the modified analytical solution of Lapidus and Amundson (1952) are in practice identical (cf. Figs. (3) and (4)).

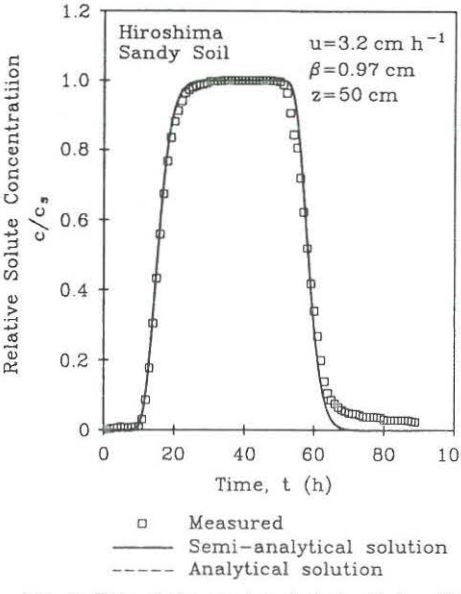

FIG. 3. Test of the semi-analytical solution (Eq. (9) with Φ = 0.12 cm) against an analytical solution and measured data for solute transport in a coarse sandy soil. Test conditions: Variable upper boundary condition (cf. Eq. (21)).

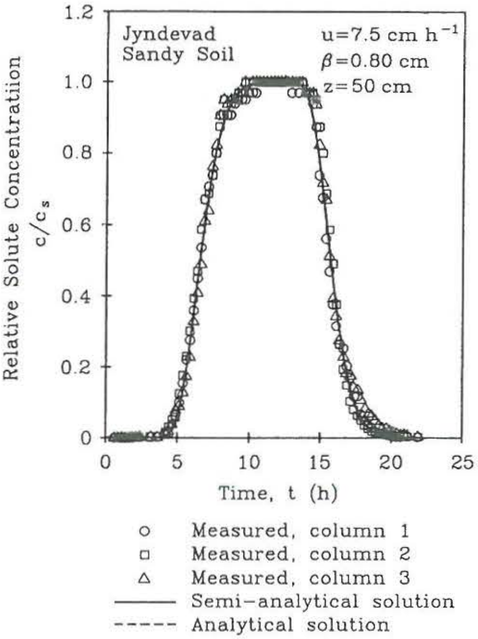

FIG. 4. Test of the semi-analytical solution (Eq. (9) with Φ = 0.12 cm) against an analytical solution and measured data for solute transport in a sandy soil. Test conditions: Variable upper boundary condition (cf. Eq. (22)).

EXAMPLE OF MODEL USE: SIMULTANEOUS TRANSPORT AND REDUCTION OF NITRATE IN POROUS MEDIA COLUMNS

The SA solution was used to describe data for rapid, continuous leaching of nitrate through water-saturated porous media columns at steady water flow, presented in Yamaguchi et al. (1990). The purpose of this example is to illustrate the possible application of the SA solution for a transport problem where an ordinary analytical solution is not available. It was therefore assumed that the nitrate reduction (denitrification) in the columns could be described by nonlinear, Michaelis-Menten kinetics corresponding to using Eq. (10), with k_0 and k_1 both equal to zero.

The column set-up and materials and methods for the experiments were described in detail by Yamaguchi et al. (1990) and will only briefly be presented here. Two column experiments (packed columns, 20 cm in diameter, 60 cm in length) were considered. The porous media used was 98% Hiroshima weathered granitic rock mixed with 2% finely textured agricultural soil (41% clay and silt). Inlet nitrate concentrations of $c_s = 20$ and 40 mg N L^{-1}, respectively, were applied. The temperature was 10°C for both experiments. The constant u and D values (Fig. 5) were estimated from breakthrough curve experiments using the parameter estimation methods of Yamaguchi et al. (1989). The experiments were carried out under noncarbon-limiting conditions by adding sufficient amounts of methanol (to obtain a C/N ratio >1). Only the measured nitrate profiles in the top half of the columns ($z \leq 30$ cm) were considered in the present study since different reduction kinetics were seen in the top and bottom half of the columns (Yamaguchi et al. 1990).

The data material did not suffice to simultaneously estimate K_m and μ_{max} in the Michaelis-Menten term. Therefore, a tentative K_m value of 168 mg L^{-1} was used equal to the K_m value for a similar type of experiment (fine sand, glucose added) estimated by Bowman and Focht (1974). Assuming $K_m = 168$ mg L^{-1}, the SA solution was fitted to the measured steady-state nitrate profiles using μ_{max} as the only fitting parameter. Initial and boundary conditions were

$$c_z^{t=0} = 0;\ c_{z=0}^{t} = c_S;\ c_{z=z_{max}}^{t} = 0 \qquad (23)$$

Simulated, steady-state profiles were obtained using $N_{max} = 2000$ in Eq. (9) for both columns. Fitted μ_{max} values were $\mu_{max} = 21\ h^{-1}$ for $c_s = 20$ mg N L^{-1} (Fig. 5a) and $\mu_{max} = 4.5\ h^{-1}$ for $c_s = 40$ mg N L^{-1} (Fig. 5b). Figure 5 also shows the effect of varying K_m (Fig. 5a) and μ_{max} (Fig. 5b). Assuming the same K_m value for both experiments, the lower μ_{max} value (4.5 h^{-1}) estimated for the highest inlet N concentration (40 mg L^{-1}) indicates that the high inlet N concentration combined with the very high water application rate (rapid infiltration) resulted in a higher N application than the denitrifying microorganisms were able to use optimally at this low temperature (10°C).

CONCLUSIONS

The proposed semi-analytical solution to the convection-dispersion model of solute transport is able to correctly simulate one-dimensional solute transport during steady water for both constant and variable concentration boundary conditions. Advantages/disadvantages of the SA solution compared to traditional analytical solutions are,

Advantages:

- The SA solution is very simple to program and evaluate (cf. Eqs. (9) and (10)).
- The SA solution allows for highly variable initial and boundary conditions (no restrictions on the variation of c_z^t=0 and

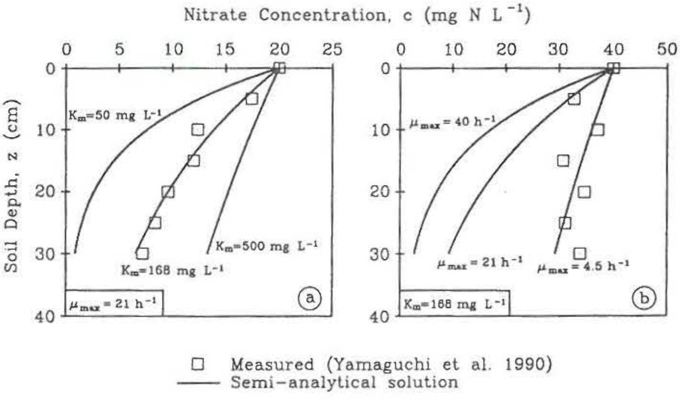

FIG. 5. The semi-analytical solution including a Michaelis-Menten reaction term used on data from two continuous nitrate leaching experiments. Measured, steady-state NO_3-N profiles together with calculated steady-state profiles for different values of the kinetic parameters K_m and μ_{max} are shown. Remaining parameter values: (a) $c_s = 20$ mg NO_3-N L^{-1}, $u = 2.9$ cm h^{-1}, $\beta = 2.41$ cm, and $\Phi = 0.05$ cm; (b) $c_s = 40$ mg NO_3-N L^{-1}, $u = 2.1$ cm h^{-1}, $\beta = 2.0$ cm, and $\Phi = 0.05$ cm.

$c^t_{z=0}$) and linear or nonlinear sink/source terms without making the solution more complex. In the cases of nonlinear reaction terms, i.e., situations where analytical solutions are not available, the simple SA solution represents a convenient alternative to using conventional numerical solutions.

Disadvantages:

- The SA solution often requires more computer time since the summation terms in Eq. (9) must be evaluated from time $t = 0$. However, all tests carried out were performed in less than a minute on a 486 computer. The quick progress within relatively cheaper and more rapid personal computers makes the question about computer time less important compared with just a few years ago.
- An accumulated error of typically 0–1% in solute concentration compared with the traditional analytical solutions is introduced when using the SA solution. However, this is acceptable for most purposes.

Thus, the proposed semi-analytical solution (Eq. (9)) to the CDM in many ways builds a bridge between the traditional analytical and numerical solutions by combining the good qualities of both, i.e. the functional simplicity of an analytical solution with the flexibility of a numerical solution. The SA solution seems a good alternative to existing solutions to the CDM, especially in cases of nonlinear sink/source terms and variable initial and boundary conditions.

ACKNOWLEDGMENTS

A travel grant from the Japanese Ministry of Education (Monbusho International Scientific Research Program: Joint Research, No. 04044127) has greatly enhanced the work and cooperation of the authors and is hereby gratefully acknowledged.

REFERENCES

Bowman, R. A., and D. D. Focht. 1974. The influence of glucose and nitrate concentrations upon denitrification rates in sandy soil. Soil Biol. Biochem. 6:297–301.

Lapidus, L., and N. R. Amundson. 1952. Mathematics of adsorption in beds, VI. The effect of longitudinal diffusion in ion exchange and chromatographic columns. J. Phys. Chem. 56:984–988.

Moldrup, P., D. E. Rolston, and J. Aa. Hansen. 1989. Rapid and numerically stable simulation of one-dimensional transient water flow in unsaturated, layered soils. Soil Sci. 148:219–226.

Moldrup, P., T. Yamaguchi, J. Aa. Hansen, and D. E. Rolston. 1992. An accurate and numerically stable model for one-dimensional solute transport in soils. Soil Sci. 153:261–273.

Moldrup, P., J. Aa. Hansen, D. E. Rolston, and T. Yamaguchi. 1993. Improved simulation of unsaturated soil hydraulic conductivity by the moving mean slope approach. Soil Sci. 155:8–14.

Moldrup, P., T. Yamaguchi, D. E. Rolston, and J. Aa. Hansen. 1994. Estimation of the soil-water sorptivity from infiltration in vertical soil columns. Soil Sci. 157:12–18.

Philip, J. R. 1987. The quasi-linear analysis, the scattering analog, and other aspects of infiltration and seepage. *In* Pre-conference proceedings of the International Conference on Infiltration Development and Application, 6–9 January 1987. Y.-S. Fok (ed.), Water Resources Research Center, University of Hawaii at Manoa, Honolulu, Hawaii, pp 1–27.

Philip, J. R., and J. H. Knight. 1974. On solving the unsaturated flow equation: 3. New quasi-linear technique. Soil Sci. 117:1–13.

van Genuchten, M. Th. 1985. Convective-dispersive transport of solutes involved in sequential first-order decay reactions. Comp. Geosci. 11:129–147.

van Genuchten, M. Th., and P. J. Wierenga. 1986. Solute dispersion coefficients and retardation factors. p. 1025–1054. *In* Method of soil analysis. Part 1. 2nd ed. A. Klute (ed.). Agron. Monogr. 9, ASA and SSSA, Madison, WI.

Wierenga, P. J., and M. Th. van Genuchten. 1989. Solute transport through small and large unsaturated soil columns. Ground Water 27:35–42.

Yamaguchi, T., P. Moldrup, and S. Yokosi. 1989. Using breakthrough curves for parameter estimation in the convection-dispersion model of solute transport. Soil Sci. Soc. Am. J. 53:1635–1641.

Yamaguchi, T., P. Moldrup, S. Teranishi, and D. E. Rolston. 1990. Denitrification in porous media during rapid, continuous leaching of synthetic wastewater at saturated water flow. J. Environ. Qual. 19:676–683.

Yamaguchi, T., P. Moldrup, D. E. Rolston, and J. Aa. Hansen. 1992. A simple, inverse model for estimating nitrogen reaction rates from soil-column leaching experiments at steady water flow. Soil Sci. 154:490–496.

Yamaguchi, T., P. Moldrup, D. E. Rolston, and S. Teranishi. 1994. Nitrification in porous media during rapid, unsaturated leaching of synthetic wastewater (submitted for publication in Water Research).

ISBN 87-90033-07-8
ISSN 0909-6159: The Environmental Engineering Laboratory Ph.D. Dissertation Series